This work is protected by copyright and other intellectual property rights and duplication or sale of all or part is not permitted, except that material may be duplicated by you for research, private study, criticism/review or educational purposes. Electronic or print copies are for your own personal, non-commercial use and shall not be passed to any other individual. No quotation may be published without proper acknowledgement. For any other use, or to quote extensively from the work, permission must be obtained from the copyright holder/s.

THE THERMOCHEMISTRY OF SOME TRANSITION METAL COMPLEXES

by

Janice L. McNaughton, M.A.(Oxon.)

A thesis submitted to the University of Keele
in partial fulfilment of the requirements
for the degree of Doctor of Philosophy.

Chemistry Department,
University of Keele.
March, 1974.

BRITISH LIBRARY

IMAGING SERVICES NORTH

Boston Spa, Wetherby
West Yorkshire, LS23 7BQ
www.bl.uk

PUBLICATIONS AT THE END OF THESIS NOT SCANNED AT REQUEST OF UNIVERSITY

ACKNOWLEDGEMENTS

In presenting this thesis, I would like to acknowledge the contributions of the following people:-

Dr. Colin Mortimer for his valuable guidance and advice throughout this work.

Professor H.D.Springall for providing the laboratory facilities for this research.

My former colleague, Dr. D.S.Barnes, now Research Fellow at the University of Manchester, for his constant help and encouragement.

My husband, David, who was the reason for this thesis being written, for viewing the entire enterprise philosophically throughout.

Mrs. Linda Battersby for the loan, yet again, of a typewriter.

Lastly, my Mum and Dad, to whom this thesis is dedicated, for providing every opportunity and encouragement at all times during my school and university career.

All the research reported in this thesis, with the exception of some preparative work described in Chapter 4, has been carried out by the author, under the supervision of Dr. Colin Mortimer.

ABSTRACT

In this thesis, thermochemical data for two different groups of transition-metal complex are reported.

The first group of complexes is of the type MX_2L_n, where M is a first-row transition-metal or Cd, X is a halogen and L is a heterocyclic ligand. The heterocyclic ligands are as follows: thiazole, benzothiazole and their methyl-derivatives; benzoxazole and substituted benzoxazoles; 3-methylpyrazole and the 2- and 3-halogenopyridines. These MX_2L_n complexes decompose, as indicated below, on raising the temperature. The enthalpies of decomposition

$$MX_2L_n\ (c) \longrightarrow MX_2\ (c) + nL\ (g)$$

of about fifty of these complexes were determined by use of a differential scanning calorimeter. Molar heat capacities for about thirty of the complexes were also evaluated by this technique. Heats of sublimation of nineteen of the complexes, mainly of the stoichiometry CoX_2L_2, were determined by a thermogravimetric method. With these data, the enthalpies of the gas-phase dissociation reaction, indicated below, have been calculated and values of the

$$MX_2L_n\ (g) \xrightarrow[nD(M\text{-}L)]{} MX_2\ (g) + nL\ (g)$$

mean bond dissociation energies, $\bar{D}(M - L)$ have been obtained. Estimates of the values, $\bar{D}(M$ - pyridine), for the analogous complexes, $MX_2(pyridine)_2$, have also been made. It has been found that, for the complexes studied, the $\bar{D}(M - L)$ values were very similar to the corresponding $\bar{D}(M$ - pyridine) values. This is

attributed to a compensation of the poorer σ-bonding ability of the heterocyclic ligands, L, compared with pyridine, by a higher degree of metal to ligand π-bonding.

The second group of complexes studied was of the type $MXYZ_2.L$, where M is Ir(I) or Pt(II); X is a halogen; Y is CO, Z is PPh_3 (for the iridium complexes), and Y is CH_3 and Z is either $AsMe_3$ or $AsMe_2Ph$ (for the platinum complexes). The ligand L is C_2F_4, C_4F_6 or (for the iridium complexes only) $CH_2CH(CN)$. These complexes decompose as shown below. The enthalpies of decomposition were

$$MXYZ_2.L\ (c) \longrightarrow MXYZ_2\ (c) + L\ (g)$$

determined by differential scanning calorimetry. The DSC data have been interpreted in terms of the stability of the complexes. The C_4F_6 complexes of iridium and platinum were found to be more stable than the C_2F_4 complexes. It is proposed that this is due to the fine balance between the σ and π-bonding contributions to the metal-C_4F_6 or metal-C_2F_4 bond strengths.

INDEX

INDEX (cont.)

INDEX (cont.)

INDEX (cont.)

INDEX (cont.)

INDEX (cont.)

1 INTRODUCTION

When a chemical reaction takes place, some bonds are broken and others formed and the heat of the reaction is a measure of the difference between the strengths of these bonds. A number of crystalline transition-metal complexes of the types MX_2L_n, and $MXYZ_2.L$ undergo simple decomposition reactions in which only the metal-ligand bond, M - L, is broken. These reactions can be

$$MX_2L_n\ (c) \longrightarrow MX_2\ (c) + nL\ (g)$$

or

$$MXYZ_2.L\ (c) \longrightarrow MXYZ_2\ (c) + L\ (g)$$

initiated simply by raising the temperature, and the heat of the reaction can be measured by use of a differential scanning calorimeter.

This thesis reports the measurement of the heats of thermal decomposition of a number of transition-metal complexes of these two main types. The complexes studied are described briefly below.

(a) MX_2L_n

where M = Mn, Co, Ni, Cu, Zn or Cd;

X = Cl, Br,

L = heterocyclic ligand

Figure 1.1 shows the heterocyclic ligands used in the preparation of this type of complex. This category of complex will hereafter be loosely referred to as the "heterocyclic metal complexes". Such complexes are of particular interest because of the relationship of the heterocyclic ligands to the imidazole

Figure 1.1 Heterocyclic ligands in the complexes MX_2L_n

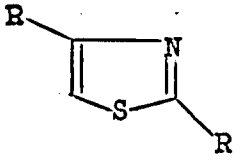

R = H thiazole

R = Me 2,4-dimethylthiazole

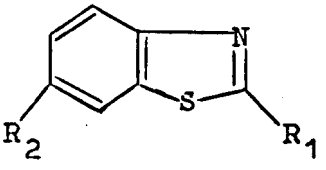

$R_1 = R_2 = H$ benzothiazole

R_1 = Me; R_2 = H 2-methylbenzothiazole

$R_1 = R_2$ = Me 2,6-dimethylbenzothiazole

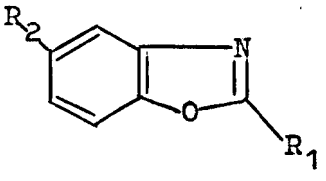

$R_1 = R_2 = H$ benzoxazole

R_1 = Me; R_2 = H 2-methylbenzoxazole

$R_1 = R_2$ = Me 2,5-dimethylbenzoxazole

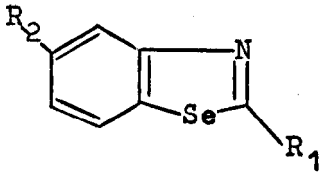

R_1 = Me; R_2 = MeO 2-methyl-5methoxy-benzoselenazole

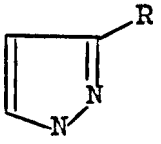

R = Me 3-methylpyrazole

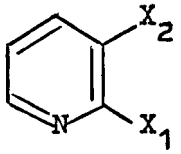

X_1 = Cl; X_2 = H 2-chloropyridine

X_1 = Br; X_2 = H 2-bromopyridine

X_1 = H; X_2 = Cl 3-chloropyridine

X_1 = H; X_2 = Br 3-bromopyridine

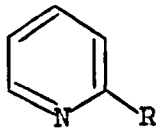

R = MeO 2-methoxypyridine

R = Et 2-ethylpyridine

nucleus. The latter, and its derivatives, are known to play

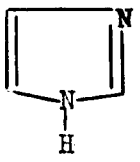

Imidazole

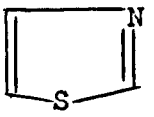

Thiazole

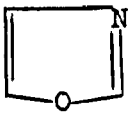

Oxazole

very crucial roles in the structures and behaviour of a number of biologically important molecules, generally by virtue of their being coordinated to metal ions. There is evidence that in proteins containing heme as a prosthetic group, for example in hemoglobin and myoglobin, imidazole nitrogen atoms, probably in histidine residues of the proteins, are coordinated to the iron atoms. The

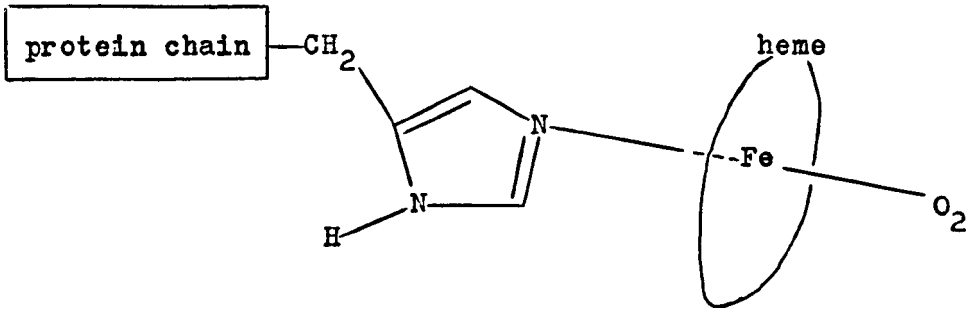

activities of many enzymes are also known to be dependent on the interaction of a thiazole group with a metal ion. It is, therefore, of particular use to study the coordinating ability of these heterocyclic ligands in transition-metal complexes and to gain information on the strength and nature of the metal-heterocyclic ligand bond.

The second main group of complexes studied is as follows.

(b) $MXYZ_2.L$

where M = Ir;

X = F, Cl, Br or I;

Y = CO;

Z = PPh_3;

L = C_2F_4, C_4F_6 or $CH_2CH(CN)$

or

where M = Pt;

X = Cl or Br;

Y = Me;

Z = $AsMe_3$ or $AsMe_2Ph$;

L = C_2F_4 or C_4F_6

These complexes will be referred to as the "olefinic or acetylenic complexes."

A great deal of research has been carried out on the reactions of the d^8 complex $IrCl(CO)(PPh_3)_2$. It is a property of d^8 low-spin transition-metal ions that they will undergo oxidative addition reactions whereby the original four-coordinate planar complex is converted to a six-coordinate octahedral complex. The occurrence of oxidative addition reactions reflects the "eighteen-electron rule".[1] The compound $IrCl(CO)(PPh_3)_2$ undergoes a variety of reactions[2] in which a molecule AB is coordinated, with dissociation of the A - B bond. It is also involved in oxidative addition

reactions where the addendum, AB, does not dissociate on coordination.

$$IrCl(CO)(PPh_3)_2 + A - B \longrightarrow IrCl(CO)(PPh_3)_2(A)(B)$$

e.g. A - B = H_2, RCl or Cl_2

$$IrCl(CO)(PPh_3)_2 + A - B \longrightarrow IrCl(CO)(PPh_3)_2(A - B)$$

e.g. A - B = C_2F_4, O_2 or $C_2(CN)_4$

These oxidative addition reactions are of importance for two main reasons. The ability of complexes like $IrCl(CO)(PPh_3)_2$ to dissociate molecular hydrogen by a reaction of this type has resulted in the use of such complexes as catalysts in the hydrogenation of olefins. The structures of compounds formed by the coordination of simple molecules, such as oxygen[3-5] and tetracyanoethylene,[6] to $IrX(CO)(PPh_3)_2$ show that the geometry of the simple molecule has been drastically altered on coordination. The extent of this ligand distortion is of importance in explaining the bonding in such complexes and the latter, it is hoped, may throw some light on the factors determining the strength of coordination of simple molecules to transition-metals. This has bearing on the transport of oxygen by hemoglobin and myoglobin.

Most of the previous work on the oxidative addition processes of the complexes $IrX(CO)(PPh_3)_2$ has referred to reactions in solution. The only previous solid-state work has been on the decomposition of the sulphur dioxide adducts of $RhCl(CO)(PPh_3)_2$[7] and $IrCl(CO)(PPh_3)_2$,[8] also studied by the differential scanning calorimetry technique, and very recent work on the dehydrochlorination of cis and trans $Ir(H)Cl_2(CO)(PPh_3)_2$.[9]

The platinum(II) complexes studied in this thesis, which are

also d^8, may be considered as oxidative adducts analogous to those formed by $IrCl(CO)(PPh_3)_2$.

The heats of sublimation of a number of the heterocyclic metal complexes, MX_2L_n, have been obtained by the application of a thermogravimetric method, in order to calculate metal-ligand mean bond dissociation energies.

The heat capacities of some of the heterocyclic metal complexes, MX_2L_n, have also been measured, by the use of the differential scanning calorimeter, so that the enthalpies of decomposition of these complexes might be corrected to a common temperature, when heat capacity data for the heterocyclic ligands become available.

The differential scanning calorimetry thermograms for the decomposition reactions of many complexes of both main types have been used to derive kinetic parameters for these decompositions. All details of this kind of work and of the parameters measured are to be found in Chapter 9.

The remainder of this introduction is taken up with brief definitions of the thermochemical quantities referred to in this thesis i.e. the heat of reaction, heat capacity, heat of sublimation and mean bond dissociation energy.

1.1 The heat content, or enthalpy

According to the first law of thermodynamics, the net energy change of a closed system on passing from a state (A) to a state (B) must depend only on the initial and final states and is independent of the path followed. We may write

$$\Delta E = E_B - E_A$$

where E is the internal, or intrinsic energy. If this closed system only interacts with its surroundings by the transfer of heat, q, to the system, or the performance of work, w, on the system, we may write

$$\Delta E = q + w$$

and $$dE = dq + dw$$

The energy function is undetermined, to the extent of an arbitrary additive constant, since it is defined only in terms of the difference in energy between two states. Provided only pressure/volume work is permitted, we may write

$$dw = -PdV$$

It is seen then, that for a process carried out at constant volume as, for example, during combustion in a bomb calorimeter, the increase in energy is equal to the heat absorbed.

$$\Delta E = q_V$$

However, if the pressure is held constant, as in experiments carried out under atmospheric pressure, and no work is done except pressure/volume work, we may write

$$\Delta E = E_B - E_A = q + w = q - P(V_B - V_A)$$

$$q_P = (E_B + PV_B) - (E_A + PV_A)$$

If the new function, called the "enthalpy" or "heat content", is defined as follows

$$H = E + PV$$

then $\Delta H = H_B - H_A = q_P$

The increase in enthalpy equals the heat absorbed at constant pressure. The enthalpy, H, is a function of the state of the system alone and is independent of the path by which that state is reached. This follows from the above since E, P and V are all state functions.

The enthalpy change at constant pressure is the quantity most commonly quoted in thermochemical work. The differential scanning calorimetry data for the heats absorbed by the various transition-metal complexes on decomposition were obtained at atmospheric pressure. Hence, the heats of decomposition measured are the enthalpies of decomposition. For bomb calorimetric work it is necessary to calculate ΔH from the measured ΔE,

$$\Delta H = \Delta E + \Delta(PV)$$

When gases are involved in the reaction under study, $\Delta(PV)$ depends on the change in the number of molecules of gas, Δn, as a result of the reaction.

$$\Delta H = \Delta E + \Delta n.RT$$

To specify the enthalpy of a reaction, it is necessary to write the exact, chemical equation for the reaction and to specify the

states (gas, liquid or solid) of all the reactants and products, noting the constant temperature at which measurement is made. The "Law of Constant Heat Summation" embodies the fact that the enthalpy is a state function. The heat of a reaction at a particular constant pressure may be calculated from the heats of other reactions (at the same constant pressure) if these reactions combine to yield the required reaction. The "standard states" to which tabulated enthalpies of reaction generally refer are defined[10] below.

(a) For a gas, the standard state is that of the hypothetical "ideal" gas at one atmosphere pressure. In such a state, the heat content is the same as that of the "real" gas at the same temperature and zero pressure.

(b) For a liquid, the standard state is the pure substance under one atmosphere pressure.

(c) For a solid, the standard state is the pure, crystalline solid under one atmosphere pressure.

Standard enthalpies of reactions are denoted by the symbol ΔH°. It is noted that temperature is not part of the definitions of standard states and must be quoted separately as a subscript i.e. ΔH°_{298} refers to the standard enthalpy at a temperature of $298^{\circ}K$. By convention, the enthalpies of the chemical elements in their standard states are set equal to zero. The standard enthalpy of formation, ΔH°_{f}, of any compound is then the heat of the reaction by which it is formed from its elements, the reactants and products all being in their standard states and at a specified temperature. The standard heat of any reaction at a specified temperature is then readily found as the difference between the standard heats of formation of the products and reactants at that temperature.

1.2 Heat capacity

The last section has shown that a method of converting enthalpy changes at one temperature to another may need to be used. This can be done through the application of the Kirchoff equation. The "heat capacity" of a system is defined as the quantity of heat required to raise the temperature by one degree. Thus, the dimensions of the heat capacity are (energy) (temperature)$^{-1}$ and it is an extensive property. The "specific heat" is the heat capacity per unit mass.

Since the heat capacity, C, is a function of temperature, it should be precisely defined in terms of a differential heat flow, dq, and a differential temperature change, dT.

$$C = \frac{dq}{dT}$$

Heat capacities may be measured at constant volume or constant pressure. At constant volume we may write

$$C_V = \frac{dq_V}{dT} = \left[\frac{dE}{dT}\right]_V$$

and at constant pressure

$$C_P = \frac{dq_P}{dT} = \left[\frac{dH}{dT}\right]_P$$

The enthalpy change of a reaction at a temperature T_1 is related to that at a higher temperature T_2 by the following equation.

$$\Delta H_{T_2} - \Delta H_{T_1} = \int_{T_1}^{T_2} C_P \, dT$$

If it is assumed that the heat capacities of all the products and reactants are constant over the temperature range T_1 to T_2, then we may write

$$\Delta H_{T_2} - \Delta H_{T_1} = \Delta C_P (T_2 - T_1)$$

where ΔC_P is the difference between the heat capacities of the products and reactants. In the limit we may write

$$\frac{d\Delta H}{dT} = \Delta C_P$$

In fact, heat capacities do vary with temperature, although it is often sufficiently accurate to use the average value of the heat capacity over the range of temperature considered. More precisely, the heat capacity per mole, $\bar{C}$, can be expressed as a power series

$$\bar{C}_P = a + bT + cT^2 + ...$$

and the integration carried out analytically.

There can be considerable confusion over the terms (molar) heat capacity and specific heat. The molar heat capacity is an intensive property and is strictly a "specific heat", but the latter is usually limited to units of mass other than one mole. The term "heat capacity" can be applied to any system, for example a calorimeter, although the terms "heat capacity" and "specific heat" are frequently used interchangeably.

1.3 Heats of sublimation

The term "heat of sublimation" describes the heat required to transfer unit mass from the solid to the vapour phase. As long as both solid and vapour are present, this added heat does not change the temperature of the system. Since the process occurs under a constant pressure, the heat absorbed is the enthalpy of sublimation. The sublimation process is endothermic and reversible, when carried out under equilibrium conditions. Hence, we may write

$\Delta G^{o} = 0$

$\Delta H^{o} = T\Delta S^{o}$

ΔS^{o} is positive

The entropy of a solid is usually low, since the thermal energy is stored mainly as vibration. Hence, when a solid sublimes to the gaseous product, the large increase in entropy is due to the new and closely-spaced rotational and translational energy levels in the product, over which the thermal energy can be spread. Heats of sublimation can be used to convert thermochemical quantities for the condensed phase to those of the gas phase where, it is assumed, there are no intermolecular attractions.

1.4 The enthalpy change as a measure of bond strength

The enthalpy change may be regarded as a measure of the difference between products and reactants in respect of total bond strength.[11] Thus, an exothermic reaction is one in which the bonds in the products are collectively "stronger" than those in the

reactants. For reactions involving solids, liquids and solutions, the view of the enthalpy change as a measure of the bond strength difference is only valid as long as the term "bond" is taken to include all intermolecular and intramolecular interactions.

"Bond strength" may be interpreted in the following ways.

(a) It can be viewed as the energy required to break a chemical bond; the bond dissociation energy.

(b) It can be regarded as a "bond energy term" characteristic of each bond, which when summed over all the bonds in the molecule gives the heat of formation of the molecule from the atoms.

(c) It can be related to molecular physics and geometry in two ways; to bond lengths and, by various theoretically calculated parameters defining the bond properties, to force constants.

The bond dissociation energy of a bond, D(A - B), is a quantity that can, in principle, be measured experimentally. It refers to the internal energy change of the reaction $AB \rightarrow A + B$ in the ideal gas state at $0^{\circ}K$, where the reactant molecules and product atoms are in their ground states.[12] The difference in internal energy is then dependent only on the electrostatic interactions which distinguish the AB molecule from the component atoms, since a correction for the residual zero-point vibrational energy in AB at $0^{\circ}K$ can be made.

For polyatomics, AB_n, there will be more than one bond dissociation energy, as the following example[11] shows.

$$NH_3\ (g) \longrightarrow NH_2\ (g) + H\ (g) \qquad \Delta E_o = D_1 = 107.2 \text{ kcal mol}^{-1}$$

$$NH_2\ (g) \longrightarrow NH\ (g) + H\ (g) \qquad \Delta E_o = D_2 = 88.0 \text{ kcal mol}^{-1}$$

$$NH\ (g) \longrightarrow N\ (g) + H\ (g) \qquad \Delta E_o = D_3 = 85.2 \text{ kcal mol}^{-1}$$

Hence, the bond dissociation energy of a bond between two specified atoms, nitrogen and hydrogen in the above, is not a constant quantity and its value will depend on the molecular environment of the atoms considered. Therefore, the bond involved must be specified. Sometimes, the bond dissociation energy is taken as the enthalpy change at 298°K, ΔH_{298}, since the difference between the internal energy at 0°K and the enthalpy at 298°K is small.

However, it is convenient to have a measure of the average value of the energy of a particular bond. For a molecule AB_n, the "mean bond energy" of the A - B bond in the gaseous state, $\bar{E}(A - B)$, is defined by the expression given below,[12] where ΔH_f^a is the heat

$$\bar{E}(A - B) = -\frac{1}{n}\left[\Delta H_f^a\ AB_n\ (g)\right]$$

of formation of the compound from the atoms in their ground states.

$$\Delta H_f^a = \Delta H_f^o - \sum \Delta H_f^o\ (\text{atoms})$$

For this restricted case of the compound AB_n, which contains only one type of bond, A - B, the bond energy, as defined above, is identical with the mean bond dissociation energy. Hence, using the figures already given, we may write for the nitrogen-hydrogen bond

$$\bar{E} = \bar{D} = 93.5 \text{ kcal mol}^{-1}$$

If the assumption is made that for a given bond, the bond energy is constant from one molecule to another, the bond energy for a given bond in a molecule may be calculated, provided that the value of the heat of atomisation of the molecule and all the other bond energies are known. There is no experimental method of verifying that the bond energy ascribed to a particular bond is correct, except in the restricted case of a molecule containing only one type of bond. The energy of a particular bond will always depend, to some degree, on its environment and the assumption of constancy from molecule to molecule introduces an element of uncertainty. Although there is no simple way of making energetic corrections for the molecular environment of a bond, it is possible to recognise circumstances when departures from constancy are likely to be most marked.

1.5 Units

All thermochemical quantities in this thesis have been reported in kilocalories. All temperature data have been given in degrees Kelvin, ^{o}K.

1 calorie $\equiv$ 4.184 joules

2 DIFFERENTIAL SCANNING CALORIMETRY

The two main types of complexes studied in this work, MX_2L_n and $MXYZ_2.L$, decompose on heating. The enthalpies of decomposition have been measured by the use of a Perkin-Elmer differential scanning calorimeter. The calorimeter has also been used to calculate the (molar) heat capacities of some of the heterocyclic metal complexes, MX_2L_n. A description of the theory and operation of the calorimeter is given below.

2.1 Theory of differential scanning calorimetry (DSC)

Differential scanning calorimeters are designed to measure the enthalpies of physical or chemical processes by measurement of the differential heat flow required to maintain a sample of the material and an inert reference at the same temperature. This temperature is usually programmed to scan a temperature range by increasing linearly at a predetermined rate. The theory and design of differential scanning calorimeters has been given by Watson et al.[13] and by O'Neill.[14] In using a "null-balance" principle, DSC instrumentation is fundamentally different from that of DTA systems, since the sample and reference holders are thermally well insulated from each other and are each provided with individual heaters. Figure 2.1 gives a schematic representation of the DSC sample holder assembly.

It is convenient to think of the DSC system as being divided into two control loops, shown schematically in Figure 2.2. One

Figure 2.1 Schematic representation of the DSC sample holder assembly

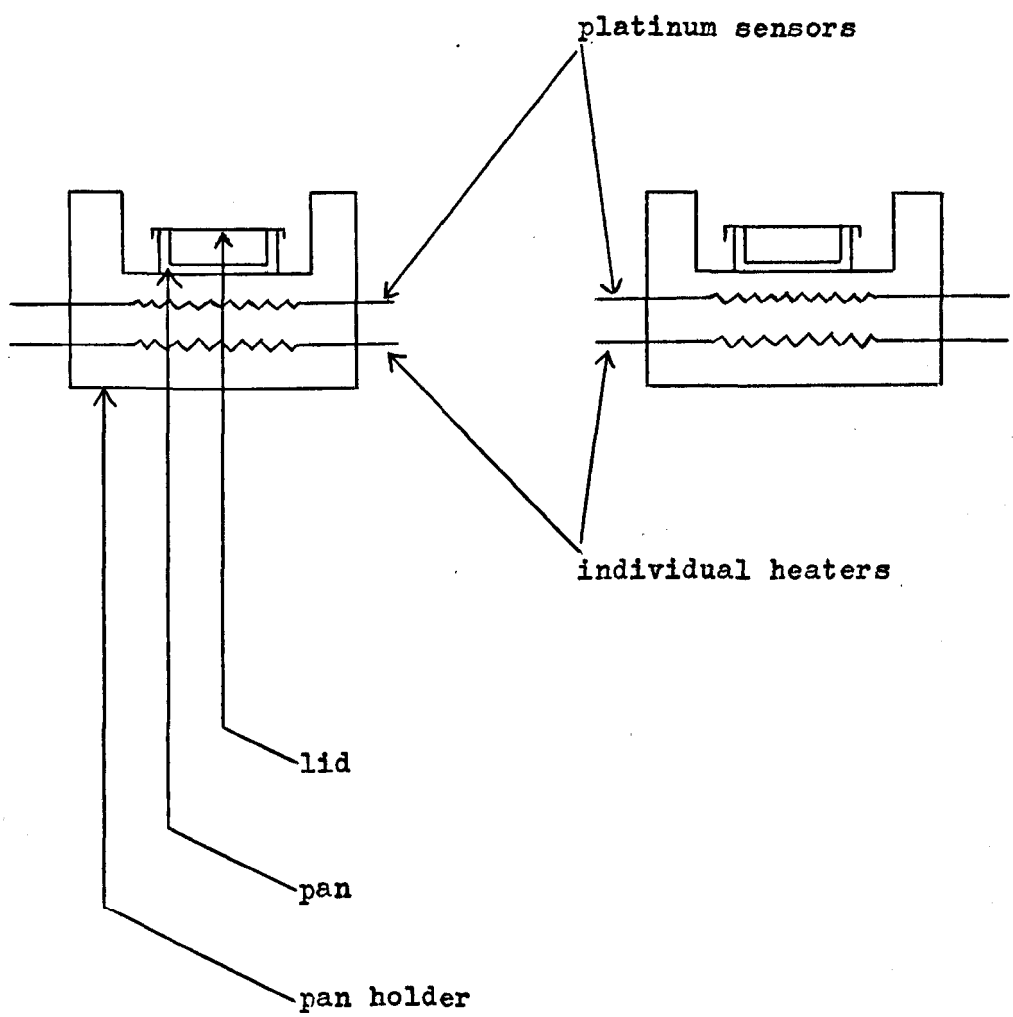

Figure 2.2 Schematic representation of the DSC control loops

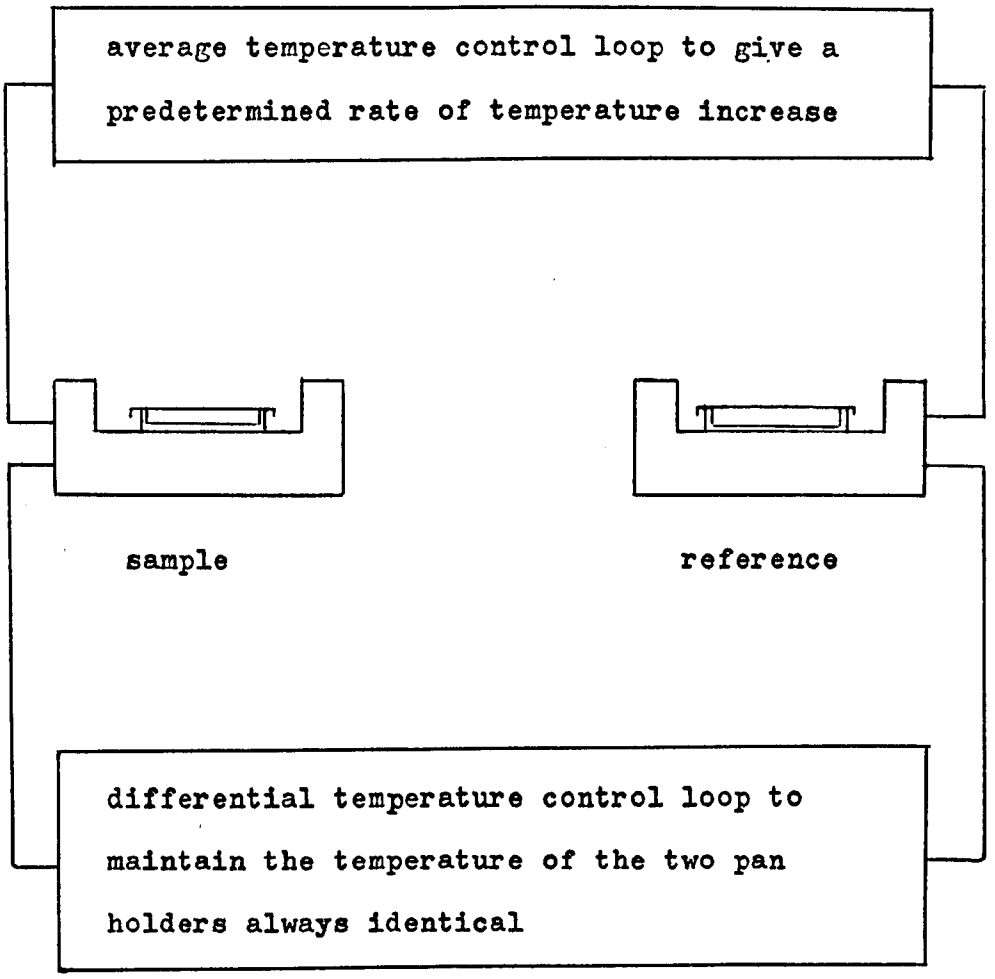

loop is for the average temperature control, so that the average, programmed temperature, T_{prog}, of the sample and reference may be increased at the preselected scanning speed, which is recorded. The second loop controls the differential temperature, in that it ensures that if a temperature difference develops between the sample and reference (because of exothermic or endothermic reaction in the sample itself), the power input is adjusted to remove this difference. Thus, the temperature of the sample holder is always kept the same as that of the reference holder by the continuous and automatic adjustment of the heater power. A signal, which is directly proportional to the differential power input to the sample and reference heaters, is fed into a recorder. This differential power input is also directly proportional to the differential heat flow to the sample and reference pan holders, dH/dt.

In practice, the recorder is also used to register the average, programmed temperature, T_{prog}, of the sample and reference. Figure 2.3 shows an idealised thermogram; the record of the differential heat flow, dH/dt, against the temperature, T, (or time, t, on the same axis.)

The temperature equality of the sample and reference holders can be maintained by the selective addition of power to one holder or to the other. In fact, the differential power is split between the two, so that there is always a biasing amount of power provided to one pan holder in the differential power control system.[15] The temperature sensors and electrical heaters, both of which are embedded in the base of the pan holders, are shared by the average and differential control systems. Even though these two control loops are separate in time, the switching rate

Figure 2.3 Idealised DSC thermogram

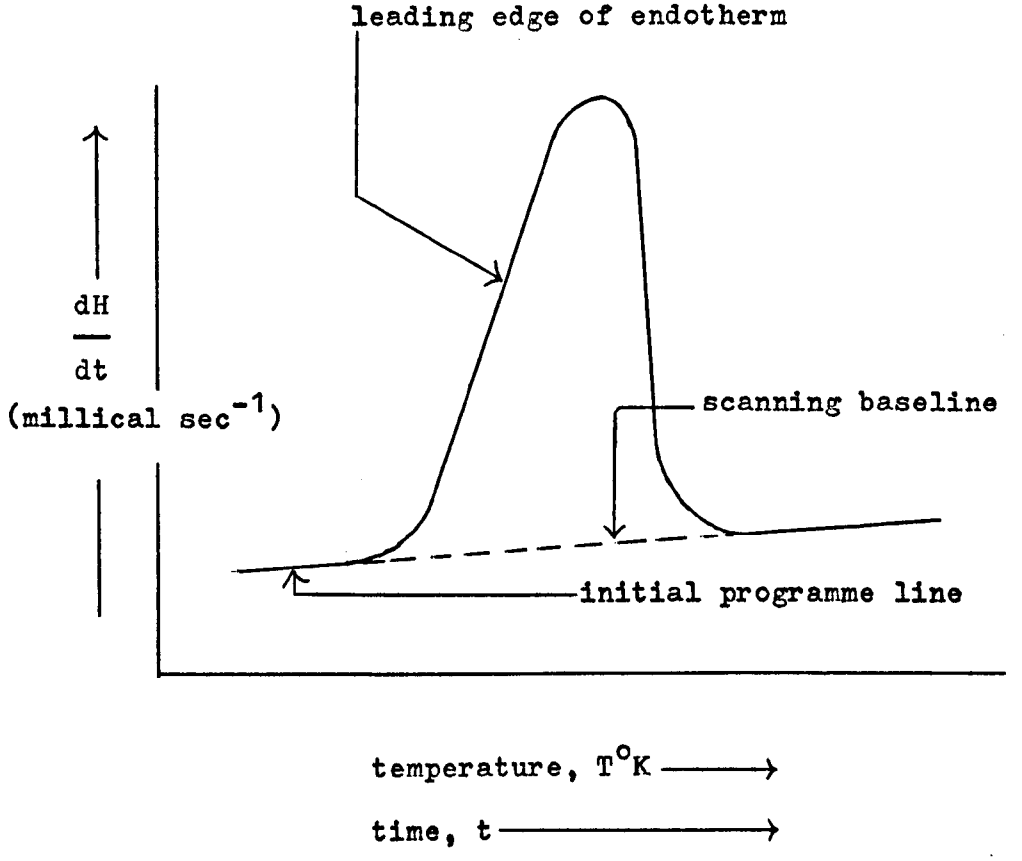

between the two is so much faster than any conceivable thermal change in the system that the effects of the two loops can be considered to be essentially superimposed.

In the DSC technique, the thermal mass of the sample and reference pan holders is minimised and the thermal resistances in the system reduced as much as possible. These measures, along with the use of a high "loop gain" in the closed loop of the differential power control circuit, ensure that the response of the system is short. Consequently, the assumption that the sample and reference holders are always at the same temperature, T_{prog}, is valid. The response of the system depends on the thermal resistances in the system. (See Figure 2.4.) For the case of a small, evenly distributed sample in a tightly-enclosed aluminium sample pan, the thermal resistance of the pan and sample is small at moderate scanning speeds. This thermal resistance, along with the thermal resistance of the power control circuitry, may be neglected, relative to the thermal resistance between the base of the sample pan and the sample holder, R_o. In practice, the response of the system can be made as fast as possible, if the following simple precautions are observed.

(a) The surfaces of the pan holders should be free from contamination.

(b) The base of the sample pans should be clean and flat.

(c) The sample should be of small weight, be finely divided and spread out over the entire area of the sample pan base.

(d) Scanning speeds should be low.

Figure 2.4 Thermal resistances in the DSC system

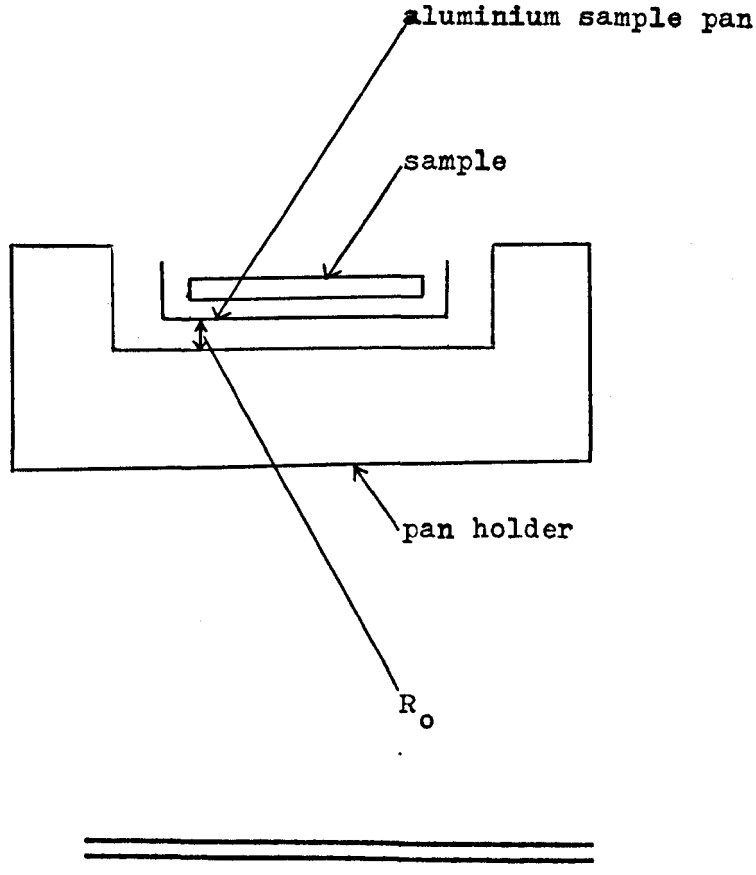

Although variations in the magnitude of R_o will affect the response of the system, and hence the peak shape, the area of the peak is unchanged. A rapid response is important for kinetic studies, but of less importance for the measurement of heats of reaction. An infinitely sharp peak would be obtained for the case when R_o is zero.

Brennan[16] has derived the mathematical equations for the output from a differential scanning calorimeter and has shown that, for a sample undergoing an endothermic transition, the signal displacement is made up of three terms. The equation, from which this is deduced, is given below.

$$\left[\frac{dq_S}{dt} - \frac{dq_R}{dt}\right] = (C_S - C_R)\frac{dT_{prog}}{dt} + \frac{dh}{dt} - R_S \cdot C_S \cdot \frac{d^2 q_S}{dt^2}$$

Term [A] Term [B] Term [C]

where dq_S/dt is the heat flow between the pan holder and the sample, along a path of total thermal resistance, R_S, which, in practice, is usually the thermal resistance, R_o; C_S is the total heat capacity of the sample and container; dT_{prog}/dt is the scanning speed, i.e. the rate of change of temperature of the pan holders and dh/dt is the rate of enthalpy change of the sample due to an endothermic transition. The quantities dq_R/dt and C_R refer to the reference side. Term [A] is the baseline displacement due to the difference in total heat capacity of the sample and reference. Term [B] is a signal displacement due to the rate of enthalpy change of the sample. Term [C] is a correction term for the thermal lag of the sample. Terms [A], [B] and [C] are illustrated schematically in Figure 2.5.

Figure 2.5 Schematic illustration of the terms [A], [B] and [C] of the Brennan[16] equation

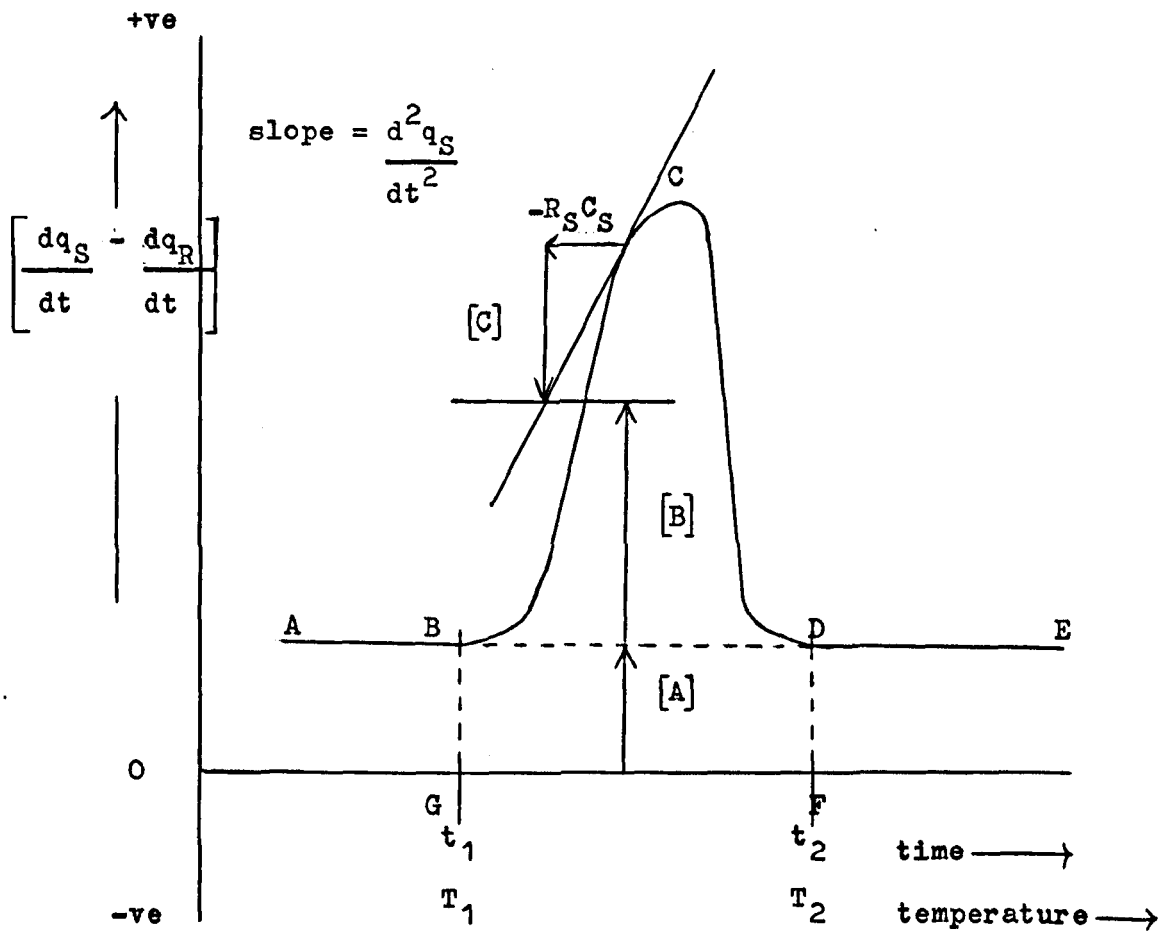

The equation given on the last page can be integrated over the time interval of the thermal event, t_1 to t_2, corresponding to the temperatures T_1 and T_2. If the assumption is made that C_S is constant over this temperature range, the following expression is obtained.

$$\int_{t_1}^{t_2} \left[\frac{dq_S}{dt} - \frac{dq_R}{dt} \right] = (C_S - C_R) (T_2 - T_1) + \Delta h$$

This clearly shows that the area under the DSC trace is equal to the sum of two terms. These terms are the difference in heat needed to raise the sample temperature from temperature T_1 to T_2 from that needed for the reference, which is area BDFGB in Figure 2.5, and the total enthalpy change of the thermal event, which is area BCDB in Figure 2.5.

Hence, differential scanning calorimetry can be used to measure directly the enthalpies of transition that occur in the sample as it is heated (or cooled). These enthalpies are not dependent on any thermal resistance, but only on the electrical characteristics of the instrumentation. Measurement of the differential electric power is equivalent to measuring the differential heat flow, $(dq_S/dt - dq_R/dt)$, as defined above. The electrical conversion constant is invariant with temperature and has been assumed to be unity in the above equations. Hence, a single point calibration to obtain a calibration constant in terms of calories $(\text{unit area})^{-1}$ is, in principle, all that is required in the DSC technique.

Since the decomposition peaks we have obtained for the complexes, MX_2L_n and $MXYZ_2.L$, extend over a considerable temperature range, we

must define the temperature to which the measured enthalpies refer. The record of a typical decomposition of the type indicated below

$$A\ (c) \longrightarrow B\ (c) \ +\ C\ (g)$$

is shown in Figure 2.6. In the following, ΔH_{T_i} is the heat of reaction at a temperature T_i, which signifies the start of the reaction. Similarly, ΔH_{T_m} is the heat of reaction at a temperature T_m, which is midway between T_i and T_f, where T_f signifies the end of the decomposition. The terms $C_{P,A}$, $C_{P,B}$ and $C_{P,C}$ are the heat capacities (mass in grams times the specific heat in calories $gram^{-1}$ $degree^{-1}$) for A, B and C respectively. In Figure 2.6 the whole area, (a + b + c), represents the heat required to carry out the decomposition in which the gas C is continually evolved. If the evolution of C is symmetrical about T_m, that is as much of the gas C is evolved before T_m as after T_m, then the process may be simplified to one having the same enthalpy change but simpler steps, as indicated below.

(1) A is isothermally decomposed at T_i. ΔH_{T_i}
(2) B is heated from T_i to T_f. $C_{P,B}(T_f - T_i)$ = c
(3) C is heated from T_i to T_m. $C_{P,C}(T_m - T_i)$

The total enthalpy change may then be written as

$$(a + b + c) = \Delta H_{T_i} + C_{P,C} (T_m - T_i) + c$$

$$(a + b) = \Delta H_{T_i} + C_{P,C} (T_m - T_i)$$

If we take the heat capacities to be independent of temperature, as indicated in Figure 2.6, then we may further write

Figure 2.6

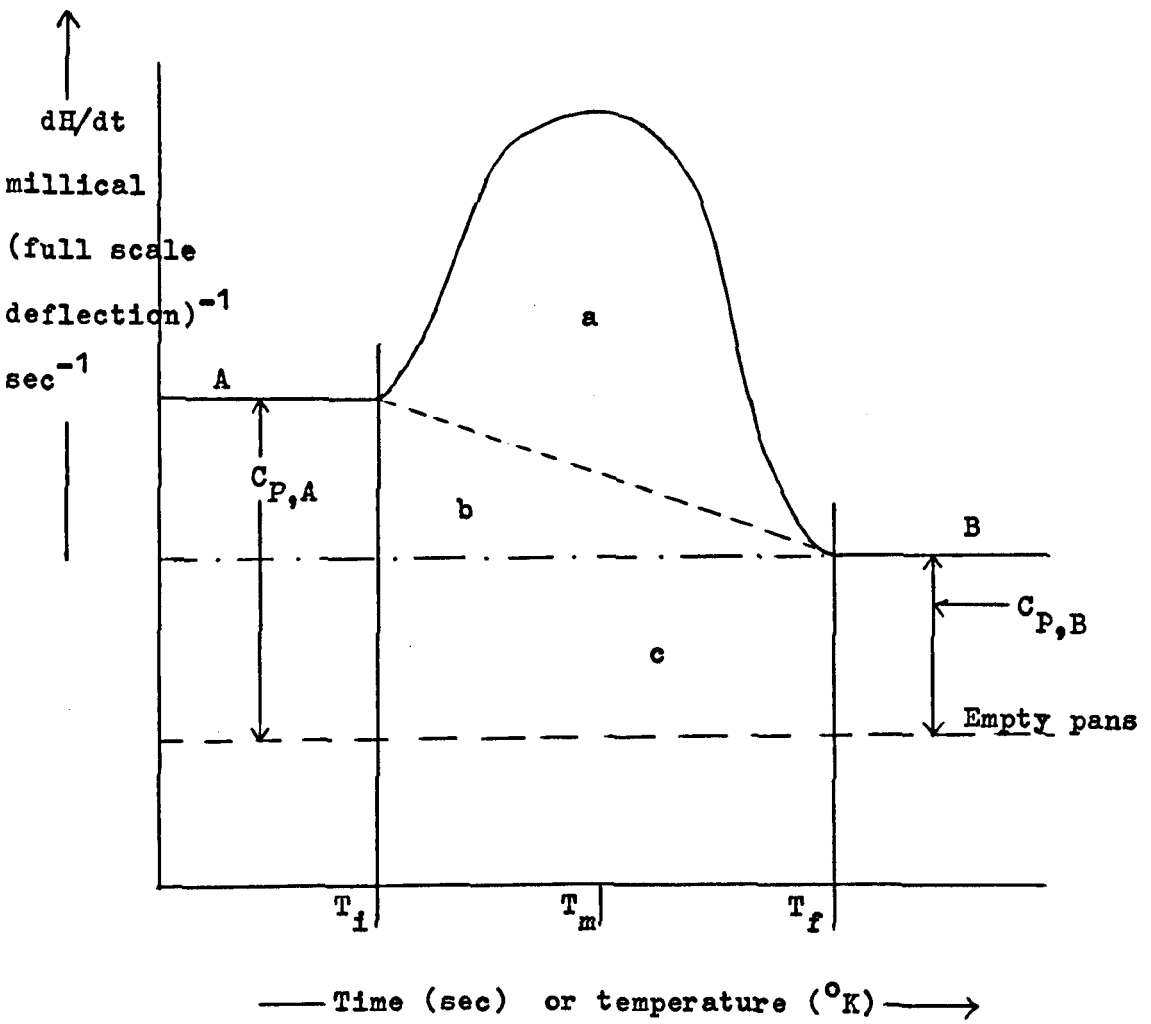
dH/dt
millical
(full scale
deflection)$^{-1}$
sec^{-1}
A
a
b
B
$C_{P,A}$
$C_{P,B}$
c
Empty pans
T_i
T_m
T_f
Time (sec) or temperature (^oK)

$$b = \frac{1}{2}\left[(C_{P,A} - C_{P,B}) (T_f - T_i) \right]$$

$$= (C_{P,A} - C_{P,B}) (T_m - T_i)$$

and

$$a = \Delta H_{T_i} + (T_m - T_i) (C_{P,C} + C_{P,B} - C_{P,A})$$

$$= \Delta H_{T_i} + (T_m - T_i) \Delta C_P$$

$$= \Delta H_{T_m}$$

where ΔC_p is the difference in heat capacities between the products and reactant. Hence, we have shown that the measured enthalpy refers to a temperature T_m, for this particular case. In this example, T_m coincides with the peak temperature, T_p. However, for the more general case when the evolution of C is not symmetrical but is more or less linear, an additional term must be incorporated, since half of C will not be evolved until some temperature T_x, which is higher than T_m. Hence, the last equation may be rewritten as

$$a = \Delta H_{T_m} + C_{P,C} (T_x - T_m)$$

At some temperature T_y, where $T_y > T_x > T_m$, we may write

$$\Delta H_{T_y} = \Delta H_{T_m} + \Delta C_P (T_y - T_m)$$

when $a = \Delta H_{T_y}$;

$$C_{P,C} (T_x - T_m) = \Delta C_P (T_y - T_m)$$

$$T_y = \frac{C_{P,C}}{\Delta C_P} (T_x - T_m) + T_m$$

Therefore, in general the measured area, a, represents the heat of reaction at some temperature slightly above T_m. The exact calculation of T_y requires not only the form of the equation representing the rate of gas evolution but also $C_{P,C}$ and ΔC_p. Strictly, these heat capacity terms are also temperature dependent so that the above derivation should contain integration terms rather than the simple ΔC_p term.

The most characteristic temperature parameters of the DSC thermogram are, therefore, the values T_i and T_f, which denote the beginning and end of the decomposition, and T_p, which is the peak temperature where the rate of gas evolution, and hence of reaction, is a maximum. In this thesis, no attempt has been made to calculate T_y, which will lie between T_m and T_p. All the enthalpies have been taken to refer to the peak temperature, T_p. This would cause an error in the calculation of the Kirchoff corrections to refer the heats of reaction to 298°K, but, since most of the decompositions studied occur at relatively high temperatures, this would be very small.

For the case of a decomposition which occurs in several stages, the overall enthalpy of decomposition has been taken to refer to an approximate mean of the individual peak temperatures, denoted by T_{mp}. It was found for the complexes MX_2L_n, that the T_{mp} values for complexes of a given ligand L usually fell into a relatively narrow temperature interval of about 50°. Hence, the Kirchoff corrections to obtain the enthalpies of decomposition at 298°K would be similar for complexes MX_2L_n of the same ligand L.

2.2 Operation

The differential scanning calorimeter used in this work was the Perkin-Elmer DSC-1. Scanning speeds of 0.5, 1, 2, 4, 8, 16, 32 and 64°min^{-1} are available with this instrument. The sensitivity can be selected from values of 2, 4, 8, 16 and 32 millicalories $(full\ scale\ deflection)^{-1}\ sec^{-1}$. Figure 2.7 is a plate of the analyser, recorder and control unit, from left to right, for the DSC-1. A close-up of the sample holder assembly is shown in Figure 2.8. The pen-recorder used was a Texas Instruments Inc. 5ma recorder, with chart speeds of 0.75, 1.5, 3.0, 6.0 and 12.0 in min^{-1}.

2.2.1 Sampling technique

The most common encapsulation method (and the one used exclusively in this work) is the use of an aluminium pan with a domed lid, which may, if required, be crimped in position. The qualitative appearance of a thermogram will be affected by the sample configuration, since this will slightly alter the thermal resistance, but the peak area will be unaffected. For the maximum peak sharpness and resolution, the solid samples were ground to a fine powder.

The sample weights were normally between five and ten milligrams and were weighed on a Cahn Gram Electrobalance (Ventron Instruments Corp.) to an accuracy within 0.01%. The weight loss percentages of the sample after each intermediate decomposition step and over the entire decomposition were noted, so that the progress of the decomposition could be ascertained. The percentage weight losses,


DETECTOR
POLARITY
TEMPERATURE CALIBRATION

Figure 2.7.

The DSC-1 analyser,

recorder and control unit

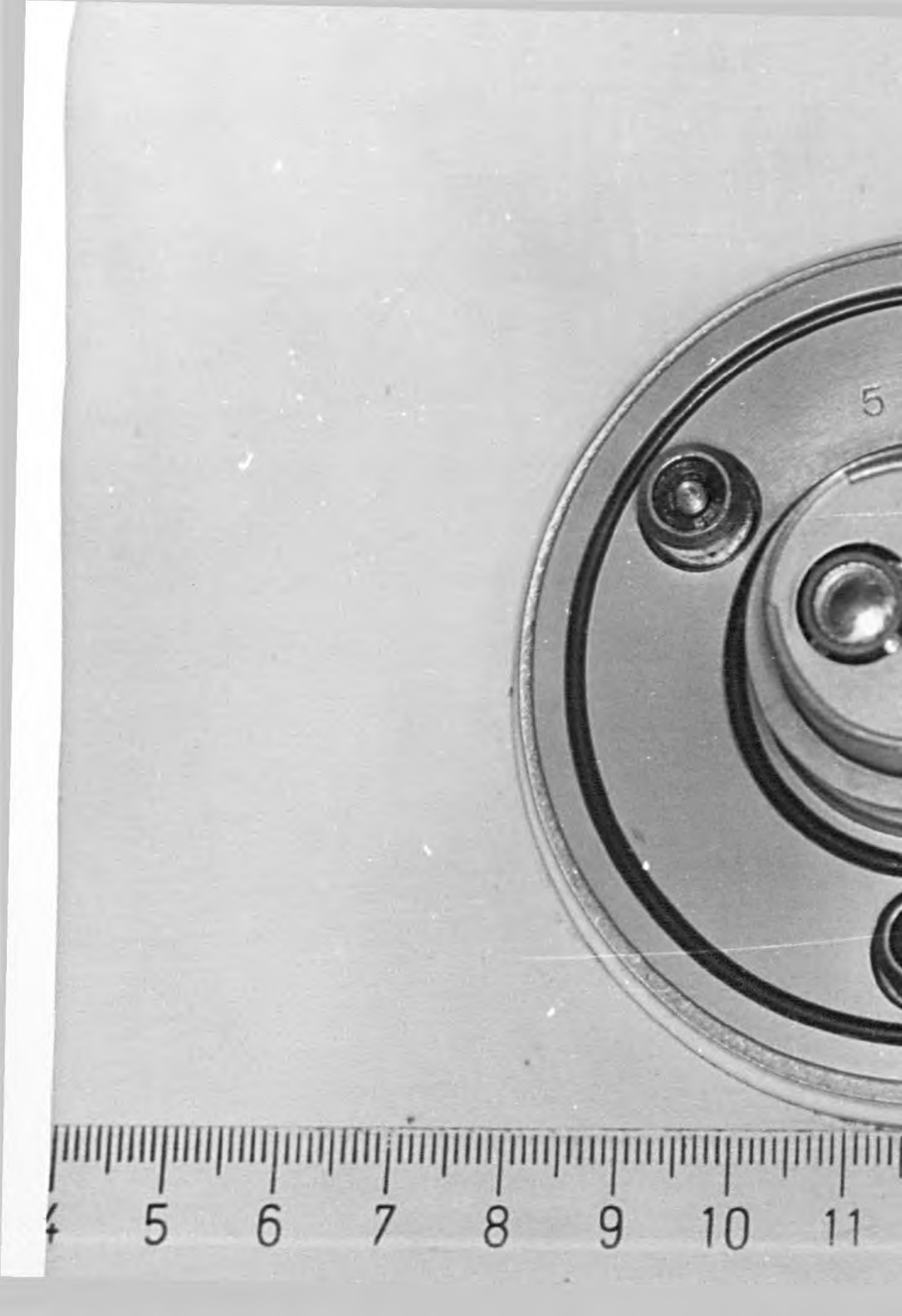
5
5
6
7
8
9
10
11

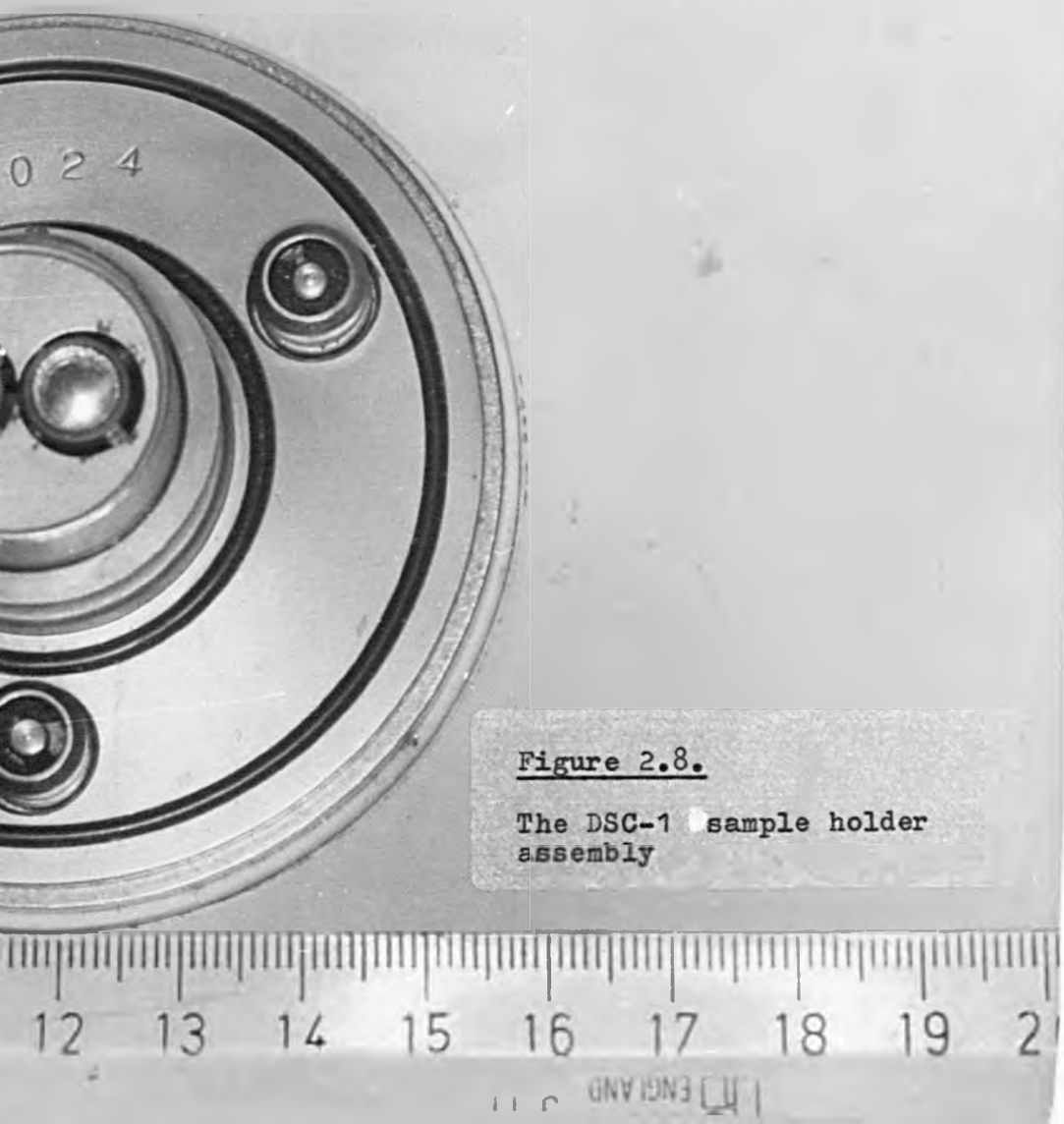

Figure 2.8.

The DSC-1 sample holder assembly

reported with the decomposition enthalpy data in this thesis, are the mean of at least three determinations and the associated error is the standard deviation of the mean. All the decompositions were carried out in an atmosphere of nitrogen, which passed through the sample holder enclosure at a rate of about 20 ml min^{-1}.

2.2.2 Calibration and measurement of decomposition enthalpies

In calibrating the calorimeter, high purity metals with accurately known heats of fusion are commonly used as standards. The one used here was indium of 99.999% purity, (available from Koch-Light Laboratories Ltd.), with an enthalpy of fusion of 0.780[17] kcal $(gram\ atom)^{-1}$, m.p. 429°K. The instrumental conditions for the calibration were as follows.

(a) Calorimeter sensitivity (or "range") of 4 millical (full scale deflection)$^{-1}$ $(sec)^{-1}$.

(b) Calorimeter temperature programming speed of 16° min^{-1}.

(c) Recorder chart speed of 3 in min^{-1}.

A thermogram of the melting peak was obtained. This procedure was repeated several times for the same sample. The "scanning baseline" (Figure 2.3) was drawn in from the point at which the trace begins to depart from the initial programme line and the point at which the trace returns to the programme line. The area between the interpolated baseline and the peak was integrated by a planimeter (Allbritt). This measuring device gives a reproducibility on the area measurements of about ± 1%, so that as DSC instrumentation becomes more sophisticated, more precise integrating techniques should be used.[18] The area values for the

repeated melting endotherms were averaged to give a final value for the calibration peak area. The calibration constant, k, in cal (unit area)$^{-1}$ was calculated from the relationship

$$k = \frac{\Delta h_{In(fusion)} \cdot m_{In}}{A_{In}} \quad \text{cal (unit area)}^{-1}$$

where $\Delta h_{In(fusion)}$ is the enthalpy of fusion of indium in cal milligram^{-1}; m_{In} is the mass of indium in milligrams and A_{In} is the average peak area of the thermogram. The value of k can be subsequently used to find the enthalpies of decomposition of the metal complexes, MX_2L_n and $MXYZ_2.L$, by application of the expression

$$\Delta H_S = k \cdot \frac{[CS]_{In}}{[CS]_S} \cdot \frac{[S]_S}{[S]_{In}} \cdot \frac{M_S}{m_S} \cdot A_S \quad \text{kcal mol}^{-1}$$

where the use of the square brackets ([ ]) denotes a particular instrumental setting; $[CS]_S$ and $[CS]_{In}$ are the recorder chart speeds for the sample and indium calibrant respectively; $[S]_S$ and $[S]_{In}$ are the sensitivity settings for sample and indium; M_S is the molecular weight of the sample; m_S is the sample mass in milligrams and A_S is the peak area of the sample endotherm. The heating rate, T_{prog}, does not appear in the above equation. However, the heating rate used for the indium calibration was the same as that used for the decomposition reactions, 16^{o}min^{-1}, thereby ensuring that the thermal resistance between pan holders and pans, R_o, was constant. The instrumental conditions for the measurement of the decomposition enthalpies were as follows

(a) Calorimeter sensitivity (or "range") of 2, 4 or 8 millical (full scale deflection)$^{-1}$ sec^{-1}.

(b) Calorimeter temperature programming speed of 16°min^{-1}.

(c) Recorder chart speed of 0.75 in min^{-1}.

A much slower value of the recorder chart speed was required for the decomposition reactions (0.75 in min^{-1}) than for the calibration melting endotherm (3.0 in min^{-1}). This was necessitated by the relatively large temperature interval over which decompositions occurred.

The last equation for the calculation of the heats of decomposition requires the values of sensitivity (range) and chart speed for both the indium calibrant and the sample. The data in Table 2.1 show that the slower chart speed, used in the decomposition reactions, is more correctly denoted as 0.749 in min^{-1}, and the chart speed used for the calibration is more correctly denoted as 2.99 in min^{-1}.

A check was also made on the values of the sensitivity settings. Table 2.2 shows that data for the calibration constant, k, obtained at various sensitivity settings lead to experimental values for the ratio of the sensitivity settings. The mean value for the experimental ratio of sensitivities of 2.00 ± 0.01 : 4.00 : 8.00 ± 0.03 is in good agreement with the denoted sensitivity settings of 2 : 4 : 8.

Hence, the heats of decomposition were calculated from the slightly amended equation, shown on page 35.

Table 2.1 The DSC chart speeds used for the calibration and decomposition reactions

baseline length / inches	time / min	baseline length / inches min^{-1}
(a) Calibration chart speed, "3.0" in min^{-1}		
4.78	1.600	2.99
5.02	1.690	2.97
5.68	1.893	3.00
6.28	2.098	2.99
4.25	1.421	2.99
5.39	1.801	2.99
9.30	3.108	2.99
average baseline length = 2.99 in min^{-1} = chart speed		
(b) Decomposition reaction chart speed, "0.75" in min^{-1}		
4.11	5.488	0.749
4.31	5.760	0.748
4.54	6.064	0.749
5.02	6.700	0.749
5.42	7.240	0.749
6.04	8.050	0.750
6.79	9.054	0.750
average baseline length = 0.749 in min^{-1} = chart speed		

Table 2.2 The DSC sensitivity settings used in the calibration and decomposition reactions

Calibration constant cal (unit area)$^{-1}$ at [S] = 2*	at [S] = 4*	at [S] = 8*	Experimental ratio of sensitivities
0.188	0.377	0.755	2.00 : 4.00 : 8.02
0.186	0.375	0.747	1.99 : 4.00 : 7.97
0.190	0.373	0.754	2.03 : 4.00 : 8.07
0.186	0.378	-----	1.97 : 4.00 : ----
-----	0.400**	0.795**	---- : 4.00 : 7.95

average experimental ratio of sensitivities:

2.00 ± 0.01 : 4.00 : 8.00 ± 0.03

* [S] = sensitivity or "range" setting for the DSC. The values of sensitivity used were 2, 4 or 8 millical (full scale deflection)$^{-1}$ sec^{-1}.

** These calibration constant values were obtained at different settings of the differential temperature control from those used to determine the other calibration constants given above.

$$\Delta H_S = k \cdot \frac{2.99}{0.749} \cdot \frac{[S]_S}{[S]_{In}} \cdot \frac{M_S}{m_S} \cdot A_S \quad \text{kcal mol}^{-1}$$

hence

$$\Delta H_S = k \cdot 3.99 \cdot \frac{[S]_S}{[S]_{In}} \cdot \frac{M_S}{m_S} \cdot A_S \quad \text{kcal mol}^{-1}$$

It has been suggested that the calibration constant is dependent, to some extent, on the temperature for the DSC-1 instrument and that the constant should be determined at several temperatures by using various calibrating substances. Barrall and Johnson[19] have proposed that the calibration constant at 603°K may be $\simeq$20% greater than that at 333°K. However, this pessimistic conclusion is not in agreement with that of Schwenker and Whitwell,[20] who suggest a calibration coefficient that varies by only $\simeq$ 4% over the temperature range 429°K to 693°K. In this thesis, an indication of whether a multipoint calibration was required was obtained by checking the enthalpy values for certain well-documented reactions occurring at temperatures far removed from the indium calibration temperature. The results are described below and in Table 2.3. In all cases good agreement was found with the literature values. All the enthalpy data recorded in this thesis are the mean of at least five determinations. The associated error is the standard deviation of the mean, s, which may be calculated from

$$s = \sqrt{\sum_{i}^{n} (x_i - x)^2 \Big/ n(n-1)}$$

where x_i is the value of the i^{th} measurement; x is the average value from n measurements and n is the total number of measurements.

(a) The fusion of lead

The enthalpy, corresponding to the fusion of lead, was measured as 1.14 ± 0.01 kcal mol^{-1}. This value is in excellent

$$Pb\ (c) \longrightarrow Pb\ (liq) \quad \ldots\ldots\ldots\ldots\ldots\ldots\ldots\ldots (1)$$

agreement with the value quoted by Stull and Sinke,[17] also of 1.14 kcal mol^{-1}. Both values refer to the heat of fusion at the melting point of lead. The lead foil used was of "Analar" quality. The recorder chart speed used here was 2.99 in min^{-1}, since a melting process, like the indium calibration, was being measured.

(b) The decomposition of copper sulphate pentahydrate

This compound decomposed in two stages yielding the monohydrate initially and then the anhydrous salt. The enthalpy changes for

$$CuSO_4.5H_2O\ (c) \longrightarrow CuSO_4.H_2O\ (c) + 4H_2O\ (g) \quad \ldots\ldots (2)$$

$$CuSO_4.H_2O\ (c) \longrightarrow CuSO_4\ (c) + H_2O\ (g) \quad \ldots\ldots (3)$$

these stages were found to be 51.7 ± 0.5 and 16.5 ± 0.6 kcal mol^{-1} at peak temperatures of 375°K and 500°K, respectively. The Kirchoff corrections to convert these data to 298°K are + 0.2 and + 0.02 kcal mol^{-1}, using literature values[21,22] for the specific heats at 298°K. Therefore, the enthalpies at 298°K are obtained as 51.9 ± 0.5 and 16.5 ± 0.6 kcal mol^{-1}. The literature values[21,22] for these reactions at 298°K are 54.2 and 17.3 kcal mol^{-1} respectively. The copper sulphate pentahydrate used was of "Analar" quality.

(c) The decomposition of sodium bicarbonate

On heating, this compound decomposes to give the carbonate and gaseous products. An enthalpy value of 15.8 ± 0.07 kcal mol^{-1} was

$$NaHCO_3\ (c) \longrightarrow \tfrac{1}{2}Na_2CO_3\ (c) + \tfrac{1}{2}CO_2\ (g) + \tfrac{1}{2}H_2O\ (g) \quad . \ . \ . \ (4)$$

found for the decomposition at a peak temperature of 425°K. Applying a Kirchoff correction[21,23] of - 0.09 kcal mol^{-1} yields the value 15.7 ± 0.07 kcal mol^{-1} at 298°K. The literature value[21,23] is 15.4 kcal mol^{-1} at 298°K. The sodium bicarbonate was of "Analar" quality.

(d) The decomposition of the tetrahedral, blue form of dichlorodipyridine cobalt (II)

The violet complex, $\alpha - CoCl_2(py)_2$, where (py) denotes the pyridine molecule, was made by the general method of preparation for the complexes MX_2L_n, as described in Chapter 4. A satisfactory microanalysis was obtained. (See Table 4.2.) The decomposition of this complex was then studied by use of the calorimeter. The first peak, $T_p \simeq 380°K$, corresponds to the conversion of the α to the β-complex. The enthalpy of this conversion has already been obtained by other workers.[24,25] The decomposition of $\beta - CoCl_2(py)_2$ was investigated, since the complex may be considered as typical of the heterocyclic metal complexes, MX_2L_n, studied in this thesis. The complex decomposed in three stages, as shown overleaf. The stoichiometry of this decomposition scheme is in agreement with that proposed by Allan et al.,[26] who tentatively suggested that some of

the stages might involve intermediate, liquid phases. This was not found to be the case.

$$\beta - CoCl_2(py)_2\ (c) \longrightarrow CoCl_2(py)\ (c) + (py)\ (g) \quad \ldots\ldots (5)$$

$$CoCl_2(py)\ (c) \longrightarrow CoCl_2(py)_{\frac{2}{3}}\ (c) + \tfrac{1}{3}(py)\ (g) \quad \ldots\ldots (6)$$

$$CoCl_2(py)_{\frac{2}{3}}\ (c) \longrightarrow CoCl_2\ (c) + \tfrac{2}{3}(py)\ (g) \quad \ldots\ldots (7)$$

The enthalpy values for the decomposition stages were found to be 9.25 ± 0.19, 5.82 ± 0.09 and 13.22 ± 0.17 kcal mol^{-1} at peak temperatures of 465, 525 and 600°K respectively. Summation of these values gave the enthalpy of overall decomposition, which may be represented by the equation given below. The value obtained was

$$\beta - CoCl_2(py)_2\ (c) \longrightarrow CoCl_2\ (c) + 2(py)\ (g) \quad \ldots\ldots (8)$$

28.3 ± 0.5 kcal mol^{-1}, at a temperature of approximately 530°K. This is in excellent agreement with an earlier DSC result[25] of 28.6 ± 0.5 kcal mol^{-1} at a temperature of 510°K. The latter work, however, did not apportion enthalpy data to the various decomposition stages.

It would appear that these DSC enthalpy data are in agreement with the literature values to within about 1 to 2%. This error is relatively large compared to that associated with enthalpy data from solution calorimetry. However, in this thesis, we have been concerned mainly with the relative magnitudes of the decomposition enthalpies of MX_2L_n and $MXYZ_2.L$ as the ligands in these complexes are varied. In some cases, reference is made to earlier DSC data, which are also subject to a similar error.

Table 2.3 Enthalpy data for reactions used to check the calibration

Reaction	$\triangle H$ kcal mol^{-1}	T_i^*	T_p^*	T_f^* (^oK)	Weight loss % obs.	calc.
(a) Fusion of lead						
1	1.14 ± 0.01	593	595	597	- - -	- - -
(b) Decomposition of copper sulphate pentahydrate						
2	51.7 ± 0.5	340	375	390	27.6 ± 1.3	28.9
3	16.5 ± 0.6	455	500	550	36.1 ± 1.4	36.1
(c) Decomposition of sodium bicarbonate						
4	15.8 ± 0.07	380	425	460	35.9 ± 0.9	36.9
(d) Decomposition of β-dichloro-dipyridine cobalt(II)						
5	9.25 ± 0.19	400	465	475	32.6 ± 0.1	37.5
6	5.82 ± 0.09	480	525	540	37.9 ± 0.3	36.6
7	13.2 ± 0.17	540	600	610	55.7 ± 0.7	54.9

* T_i, T_p and T_f are the temperatures of initial pen displacement from the programme line, maximum (peak) displacement and pen return to the programme line.

2.2.3 Temperature correction

To fix the temperature scale, the average temperature control setting on the DSC-1 was adjusted until the vertex of the melting endotherm for the indium calibration peak occurred at a programme temperature of 429°K. To calibrate the temperature scale more accurately, (to within ± 0.2°K), two major corrections are necessary. Firstly, the vertex temperature of the melting endotherm is not strictly the transition temperature and it must be corrected for the thermal lag[27,28] between the pan holder and the sample and pan. Secondly, for samples which undergo transitions at temperatures significantly above or below 429°K, the temperature indicated on the instrument dial may be inaccurate. Hence, a correction curve[28] to the indicated temperature should be constructed. Pella and Nebuloni[29] have discussed in detail the further corrections that are needed to give an accuracy of ± 0.1°K for temperature data. However, since in this thesis we are concerned mainly with enthalpy values which refer to only an approximate temperature value, taken to be the peak temperature, the many corrections to obtain accurate temperature data have not been applied. An indication of the error on the temperatures quoted in this thesis is found in the work on the heat of fusion of lead. The data in Table 2.3 show that the observed peak temperature for the lead melting endotherm was 595°K. This is 5° below the expected melting point. It would appear, then, that the simple temperature calibration at the indium melting point results in an error of - 5° in the indicated temperature data for transitions occurring around 600°K.

Table 2.4 Temperature data for the reaction:-

$$\beta\text{-}CoCl_2(py)_2\ (c) \longrightarrow CoCl_2(py)\ (c) + (py)\ (g)$$

weight of complex milligrams	T_i	T_p °K	T_f
3.984	396	458	464
4.124	399	457	468
4.746	402	460	471
6.586	399	465	479
6.840	400	467	478
6.960	401	463	474

Span of temperature values for T_i, T_p and T_f = 6°K, 10°K and 14°K, respectively.

It was also observed that the temperature parameters, T_i, T_p and T_f seemed to be slightly dependent on the weight of sample used. The data for the first stage in the decomposition of β - dichlorodipyridine cobalt (11), which led to this conclusion are given in Table 2.4. Hence, the T_i, T_p and T_f data associated with the enthalpy values recorded in this thesis are only quoted to the nearest multiple of 5°.

2.2.4 Measurement of specific heats

When a sample material is subjected to a linear temperature increase, the rate of heat flow into the sample is proportional to the instantaneous specific heat. By recording this rate of heat flow, as a function of temperature, and comparing it with a standard material under the same conditions, the specific heat, as a function of temperature, may be obtained. The procedure adopted for the determination of specific heats by use of the Perkin-Elmer differential scanning calorimeter has been described in detail elsewhere.[19,30,31] O'Neill[30] claims a precision of specific heat data, obtained by this method, of ± 0.3% or better. Excellent agreement of specific heat data from this DSC method with data from classical techniques has been found.[30] In this thesis, the measurement, by the DSC method, of the molar heat capacities of several heterocyclic metal complexes, MX_2L_n, is reported.

It is important that, when neither sample nor reference material is present in the calorimeter, the "no-sample" trace and the interpolated scanning baseline are reproducible. (See Figure 2.9 overleaf.) This is necessary, since the determination of the

Figure 2.9 The measurement of specific heats

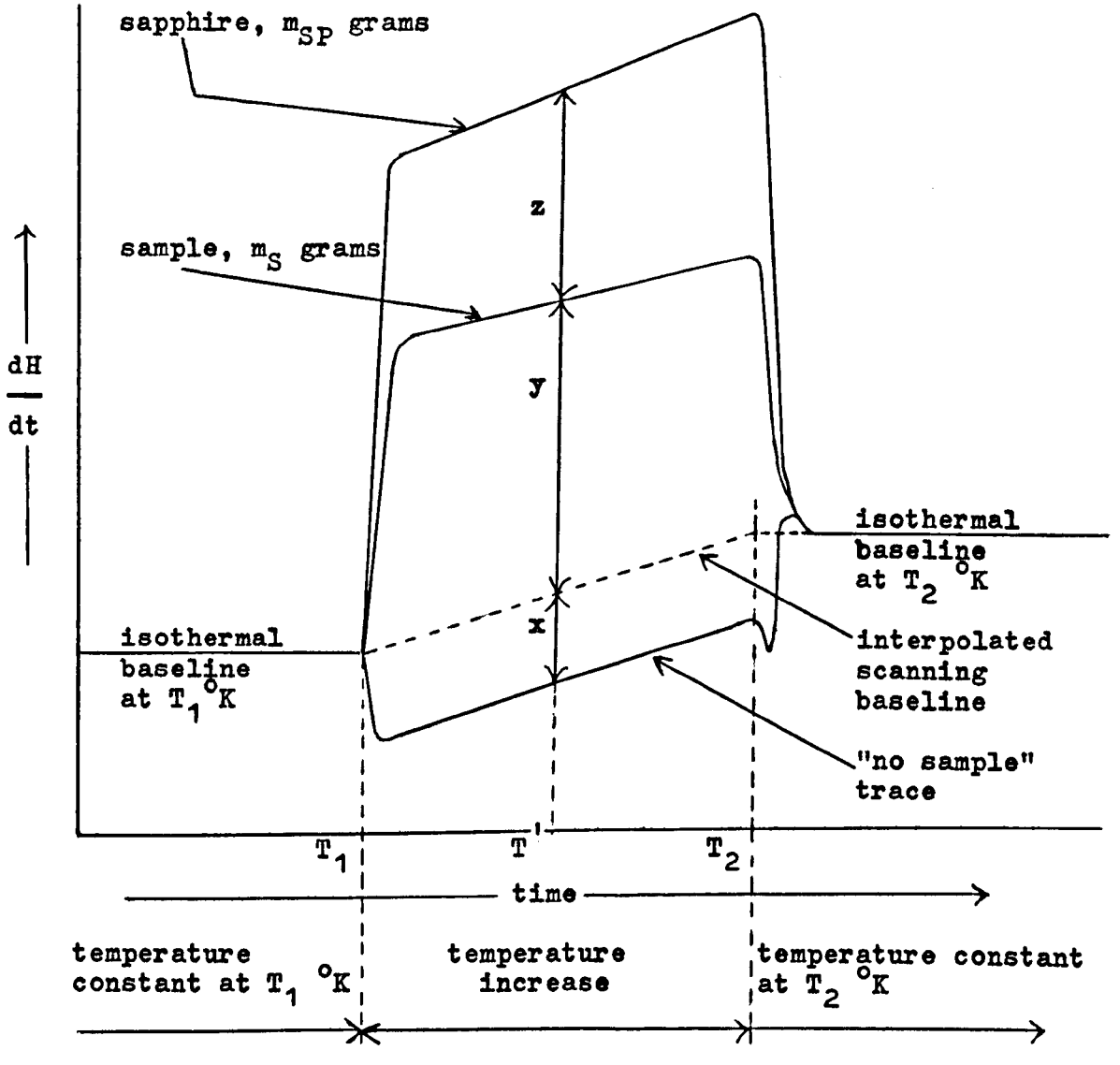

at the temperature T', $\frac{\bar{C}'_{P,S}}{\bar{C}'_{P,SP}} = \frac{m_{SP} \cdot (x + y)}{m_S \cdot (x + y + z)}$

where $\bar{C}'_{P,S}$ and $\bar{C}'_{P,SP}$ are the specific heats of the sample and sapphire, respectively, in cals $gram^{-1}$ deg^{-1}.

specific heat of a sample depends on the magnitude of the pen deflection from the "no-sample" trace. Therefore, the differential thermal losses between the holders of the sample and reference pans must be reproducible and independent of the contents of these holders. The differential power readout, at isothermal equilibrium, depends only upon these differential heat losses and serves as a check on their reproducibility.[31] The calorimeter is equipped with a "slope" control, which balances this thermal mismatch between the holders in the temperature range studied. The slope control operates by providing the required difference in heater power during that half of the control cycle when the average temperature "loop" is in operation. This reduces the burden from the other half of the control cycle, when the differential temperature "loop" operates. Hence, the slope control reduces baseline drift, which can become excessive at high temperatures, when the pan holders are poorly matched.

The procedure adopted for the measurement of heat capacities was as follows. Empty aluminium sample pans and lids were placed in the pan holders and an isothermal baseline recorded at a temperature, T_1, for a few minutes. (See Figure 2.9.) The temperature was programmed to increase over a range so that the "no-sample" trace was obtained. An isothermal baseline was then recorded at the upper temperature, T_2, for a few minutes. The two isothermal baselines, at temperatures T_1 and T_2, were used to interpolate a baseline over the temperature scanning section. This was done by extrapolating the isothermal baseline at the higher temperature, T_2, back to the time at which temperature scanning was stopped and a baseline drawn between this point and the point on the low temperature, T_1, isothermal baseline where scanning commenced.

The difference in position between the isothermal baselines at T_1 and T_2 was minimised by adjustment of the slope control. This ensured that the differential heat losses between sample and reference pan holders did not vary greatly with temperature. To further ensure that the position of the isothermal baseline at the higher temperature was as near as possible to that at the lower temperature, the scanning interval, $T_2 - T_1$, was limited to 60°. The small pen displacement from the interpolated baseline, denoted by x in Figure 2.9, is then a measure of the difference between the thermal capacities of the pan holders.

The procedure was repeated with a known mass of sample in the sample pan. A pen displacement was noted due to the absorption of heat by the sample and we may write

$$\frac{dH}{dt} = m \cdot \bar{C}_P' \cdot \frac{dT_{prog}}{dt}$$

where m is the mass of sample in grms; $\bar{C}_P'$ is the specific heat of the sample in cal $gram^{-1}$ $degree^{-1}$; dT_{prog}/dt is the programmed rate of temperature increase and dH/dt is the total ordinate deflection from the "no-sample" trace.

The above equation could be used to obtain values of the specific heat directly, but any errors in the ordinate readout, dH/dt, and in programming rate, dT_{prog}/dt, would reduce the accuracy. To minimise these errors, the procedure was repeated with a known mass of sapphire, of well established specific heat[32], in the sample pan. Thus, measurement of the total ordinate deflections at the same temperature, (x + y) and (x + y + z) of Figure 2.9, enables a value for the ratio of the specific heats for

sample and sapphire to be calculated for that temperature. Hence, the specific heat of the sample was obtained over a temperature range up to a temperature just below the onset of decomposition, T_i. Since the method involves the measurement of small changes in heat content, the traces were all run at the most sensitive setting of 2 millical (full scale deflection)$^{-1}$ sec^{-1} and a scanning speed of 16^{o} min^{-1}.

To eliminate possible errors due to the weight variation of the aluminium sample pans,[19] the same empty pan was used on the reference pan holder throughout the experimental work and the same pan was used to contain all the samples and the sapphire standard. The slope control setting was kept the same throughout the specific heat determinations.

Most of the literature[30,31] on the measurement of specific heats by DSC recommends the use of tightly-fitting metal covers that fit over each pan holder, pan and lid. These covers should be located in the same relative position and have been found to reduce the thermal mismatch between sample and reference sides. However, it was found, in the work reported in this thesis, that these covers were not necessary. Better traces were obtained without the use of the covers. Because this was a departure from the usual method, the validity of the modified experimental procedure was checked by measuring the specific heat of indium, which is well documented.[17,33] The reproducibility of the interpolated baseline, of which the deflection x in Figure 2.9 is a measure, was checked each day to ensure that the previously obtained data for x, as a function of temperature, were still valid.

The specific heat determinations for some of the heterocyclic metal complexes, MX_2L_n, were carried out in two major "blocks". These two sets of results differed in minor detail. For one set, the ordinate deflections were measured in centimetres by ruler; values taken for the deflections x, x + y and x + y + z, of Figure 2.9 were the mean of four determinations. The specific heat values, and hence the molar heat capacities, were calculated. A "least squares" analysis of the molar heat capacity data as a function of temperature was carried out by use of a simple computer programme. The molar heat capacity, $\bar{C}_p$, can be written as a power series, $\bar{C}_p = a + bT + cT^2 + \ldots\ldots$ It was assumed that terms dependent on the square and higher powers of temperature were negligible. The least squares analysis yielded "best" values for the coefficients a and b, in the relationship $\bar{C}_p = a + bT$.

For the other set of heat capacity results, the deflections x, x + y and x + y + z were measured in inches by a Leytool Microdivider Setter, British Patent No. 685106, reading to within one thousandth of an inch. The Setter can only be used, however, to measure deflections greater than 0.25 inches. The values of the deflections used were the mean of three determinations and the same least squares analysis was applied to the resulting heat capacity data. An estimation of the error associated with the simple ruler measurement of ordinate deflections, compared with that associated with measurement by the Microdivider Setter, was necessary for the evaluation of kinetic data from DSC traces. This comparison is given in Chapter 9, Table 9.1, which shows that the error in the direct ruler measurement is only about ± 1% and is removed by repetition of the traces.

Table 2.5 Molar heat capacities for solid indium

$\bar{C}_P = a + bT$ cal deg^{-1} mol^{-1}

a	b x 10^3	Temperature range ^oK	Reference
4.47	6.75	320 - 420	this work
4.61	5.45	330 - 420	this work
4.18	6.80	330 - 425	34*
5.81	2.50	298 - 429	33
4.90	5.00	298 - 400	17

* Also obtained by the DSC method.

Table 2.6 Point by point comparison of the indium molar heat capacity data

$\bar{C}_{P_{298}}$	$\bar{C}_{P_{400}}$	Reference
←cal deg^{-1} mol^{-1}→		
6.48	7.17	this work
6.23	6.79	this work
6.21	6.90	34
6.55	6.81	33
6.39	6.90	17

The validity of the experimental procedure for the measurement of heat capacity for both sets of results is upheld by the good agreement of the measured molar heat capacity, $\bar{C}_p$, of solid indium with the literature values.[17,33] Table 2.5 gives the literature data for $\bar{C}_p$ of indium and the data obtained in this work. A point by point comparison, Table 2.6, shows that the error on the two experimental results obtained here, for the two methods of treatment of data, was about ± 3% in both cases.

The DSC calorimeter would seem, therefore, to give heat capacity data which are adequate for the calculation of Kirchoff corrections. Unfortunately, the specific heats of the gaseous azole and halogenopyridine ligands have not been documented.

2.2.5 Baseline correction in enthalpy measurements

In the DSC work reported in this thesis, the simple drawing in of the scanning baseline for the endothermic decomposition peaks has been adopted, as indicated in Figure 2.3. However, Brennan et al.[35] have shown that this procedure can give an error of ± 0.5% on the enthalpy values for decompositions where there is a moderate change in heat capacity. They point out that, ideally, the scanning baseline should be drawn in so as to allow for the change in heat capacity of the sample during decomposition. For the most recent DSC-2 instrument, [36-38] this procedure should be carried out as a matter of course.

The major difficulty found in the measurement of the enthalpy data reported in this thesis was the relatively rapid deterioration

in the quality of the sample holder assembly after constant use over a period of about six months. This deterioration appears through the mismatch in thermal behaviour of the sample and reference holders. Since the thermal emissivity varies as the fourth power of the temperature, this mismatch becomes most pronounced at high temperatures, when marked baseline drift occurs. To some extent, this can be reduced by the adjustment of the slope control setting. The appearance of baseline drift is inevitable, sooner or later, with sample holders of the complex construction[39] used in the DSC-1. However, Rogers and Morris[40] have suggested methods of reducing the effect. The most recent DSC instrumentation, the DSC-2, has a much more robust sample holder assembly and essentially straight baselines are obtained over the entire temperature range. No less than three new DSC sample holder assemblies were required in the duration of this work.

The other thermochemical quantity measured in this thesis was the heat of sublimation of some of the heterocyclic metal complexes, MX_2L_n. This is described in the next chapter.

3 HEATS OF SUBLIMATION

It is preferable to refer the overall enthalpies of decomposition to the gas phase by incorporating the enthalpies of sublimation of the divalent metal halides, which are readily available,[41,42] and those of the heterocyclic metal complexes. The gas phase dissociation enthalpies i.e. the enthalpy of the reaction shown below, may then be used to calculate the mean bond dissociation

$$MX_2L_n\ (g) \longrightarrow MX_2\ (g) + nL\ (g)$$

energy of the metal ligand bond, $\bar{D}(M - L)$, if we make the assumption that the gaseous complexes are monomeric species. Since the olefinic and acetylenic complexes, $MXYZ_2.L$, decomposed near room temperature, their heats of sublimation could not be measured by the method described below.

The measurement of enthalpies of sublimation, ΔH_{sub}, by direct calorimetry or indirectly by vapour pressure determinations is time-consuming. Beech and Lintonbon[43] have described a rapid method of heat of sublimation measurement, suitable for thermally stable compounds, which uses the differential scanning calorimeter. However, this method is not suitable for the heterocyclic metal complexes, MX_2L_n, and the thermogravimetric method proposed by Ashcroft[44] was used. The theory of the technique and the experimental details are given in the following sections.

3.1 Theory of the thermogravimetric method to determine heats of sublimation

It has been shown[45] that the rate of sublimation in vacuo, m', per unit area of substance, is related to the vapour pressure, p, by the Langmuir equation given below

$$m' = \alpha \cdot \left[\frac{M}{2\pi RT}\right]^{\frac{1}{2}} \cdot p$$

where M is the molar mass of the gaseous substance; T is the temperature in ^{o}K and α is a sublimation coefficient usually assumed to be unity.

The Clausius-Clapeyron equation can be applied to a sublimation process in which the surface area of the sample remains constant. In general, for a phase transformation we may write

$$\frac{d\ln p}{dT} = \frac{\lambda}{RT^2}$$

and $$\frac{d\ln p}{d(1/T)} = -\frac{\lambda}{R}$$

where λ is the heat change of the phase transformation and is assumed to be constant over the temperature range of interest. It follows that

$$\ln\left[\frac{p_2}{p_1}\right] = -\frac{\lambda}{R}\left[\frac{1}{T_2} - \frac{1}{T_1}\right]$$

and for a sublimation process

$$\frac{d \ln p}{d(1/T)} = - \frac{\Delta H_{sub}}{R}$$

If the Langmuir expression for m' is rearranged, we may write

$$p = \frac{m'.(2\pi RT)^{\frac{1}{2}}}{M^{\frac{1}{2}}}$$

$$= m' (T^{\frac{1}{2}}) . \left[\frac{2\pi R}{M}\right]^{\frac{1}{2}}$$

$$\log p = \log m'.(T^{\frac{1}{2}}) + \frac{1}{2} \log \left[\frac{2\pi R}{M}\right]$$

hence

$$\log m'.(T^{\frac{1}{2}}) = \log p - \frac{1}{2} \log \left[\frac{2\pi R}{M}\right]$$

But, by the Clausius-Clapeyron equation, a plot of log p against 1/T is a straight line of slope $-(\Delta H_{sub}/2.303R)$ and intercept C on the log p axis. Therefore, we may write

$$\log m'.(T^{\frac{1}{2}}) = \frac{-\Delta H_{sub}}{2.303R} \left[\frac{1}{T}\right] + C - \frac{1}{2} \log \left[\frac{2\pi R}{M}\right]$$

$$= \frac{-\Delta H_{sub}}{2.303R} \left[\frac{1}{T}\right] + C'$$

where C' is a constant for a given compound. If the gas constant, R, is expressed in cal degree^{-1}mol^{-1}, ΔH_{sub} can be calculated in kcal mol^{-1} from the slope of a plot of log m'.$(T^{\frac{1}{2}})$ against $(10^3/T)$, where m' is measured in milligrams min^{-1}.

3.2 Experimental procedure

Any thermogravimetric equipment with facilities for isothermal and vacuum operation can be used. In this work, a Dupont 950 thermogravimetric analyser coupled to the basic instrument console of a Dupont 900 differential thermal analyser was used.

3.2.1 Instrumentation

The Dupont 950 model is a semi-micro balance designed to measure the weight of a material as a function of a linearly increasing temperature. The instrument is capable of attaining temperatures up to about 1470°K with any linear heating rate between 0.5 and 30°min^{-1}. It can also be utilised to study the weight change of a material as a function of time at some specified temperature. In this isothermal mode of operation, the time axis scale can be varied from 0.1 to 20 in min^{-1}.

The Dupont 950 model consists of three units; the furnace, balance and cabinet assemblies. A schematic representation of the Dupont 950 is given in Figure 3.1. A plate of the Dupont 950 model is shown in Figure 3.2, whilst a further plate, Figure 3.3, shows both the 950 and 900 models. The Dupont 950 model operates on a null balancing principle. The beam is balanced through a taut band electric meter movement, the balance arm being directly attached to this movement. When the balance arm is deflected from its reference position, the photocell amplifier adjusts the current in the movement coil until the balance arm returns to the null position. This current, after amplification, determines the position of the pen on the Y-axis of the X-Y plotter of the 900

Figure 3.1 Schematic representation of the Dupont 950 Thermogravimetric Analyser

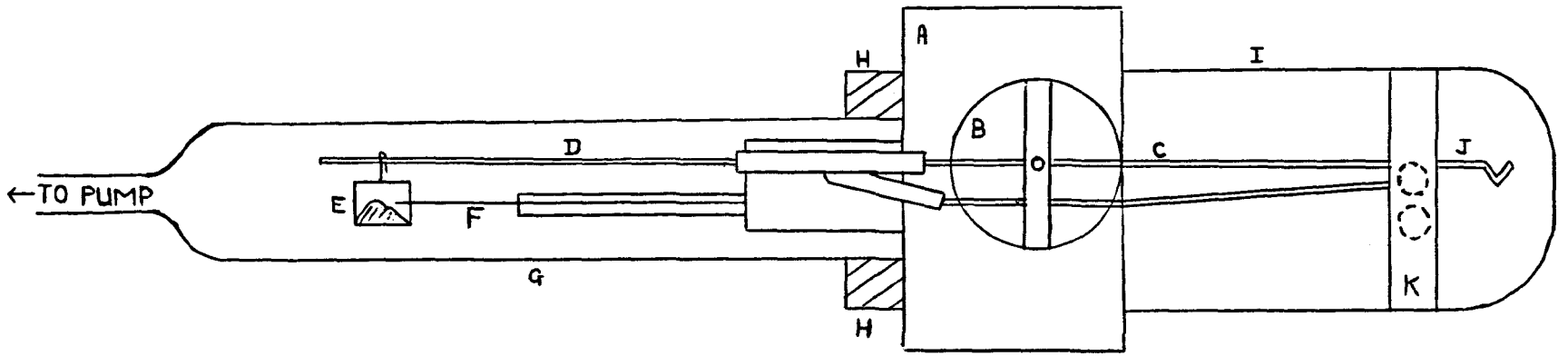

A = balance housing
B = taut band electric meter movement
C = rear of beam
D = quartz rod (removable "hot member")
E = sample pan
F = sample thermocouple
G = furnace tube
H = furnace tube retainer
I = pyrex glass envelope (or "cold side" of beam)
J = counterweight arm
K = photovoltaic cells and lamp housing behind

Figure 3.2.

The balance beam of the Dupont 950 model

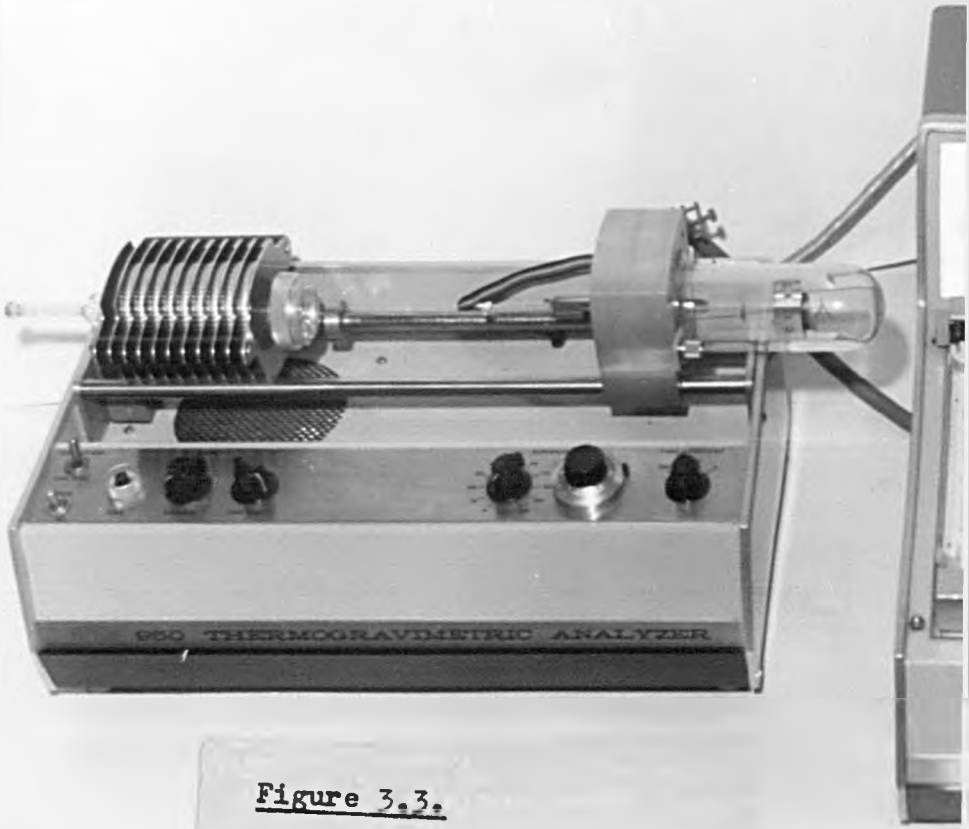

Figure 3.3.

The Dupont 950 and 900 models


900 DIFFERENTIAL THERMAL ANALYZER

console. The furnace of the Dupont 950 is programmed by the temperature programmer-controller of the 900 console. The temperature of the material being weighed is determined by a thermocouple, which is located close to the sample. This temperature is recorded on the X-axis of the X-Y plotter. Alternatively, the furnace can be held at a required temperature and the weight of the sample (on the Y-axis) recorded as a function of time (on the X-axis), at the given furnace temperature.

The furnace itself is a Kanthal wire wound resistance furnace with a low thermal mass. It can therefore be heated and cooled rapidly. The furnace temperature is monitored by a Platinel control thermocouple located in the furnace wall.

The balance assembly, mounted on horizontal support rods, has a glass "envelope" at each end. The larger Pyrex glass envelope encloses the control end of the balance or "cold section." The other envelope, referred to as the furnace tube, encloses the furnace end of the balance. Two furnace tubes are supplied; Pyrex for operation up to 773°K and quartz for operation up to 1473°K.

3.2.2 Calibration and determination of heats of sublimation

The balance beam was initially calibrated, in terms of its "span" and "suppression", for the particular quartz rod or "hot member" of the beam being used. The quartz rod was tared by the addition of weights to the counterweight arm of the cold section of the balance beam. The balance was then zeroed on the chart-paper zero and the span control of the 950 model adjusted, so that an accurate fifty milligram weight, hung from the quartz rod, registered exactly this weight on the Y-axis of the X-Y plotter.

The suppression controls, by which part or all of this standard weight can be cancelled out, were also adjusted. By use of the suppression control, small weight changes in a large sample can be observed at more sensitive scale settings.

After calibration of the balance beam, an aluminium sample pan was suspended from the end of the quartz rod and the balance beam was tared by the addition of more counterweights. The pen recorder was zeroed once more on the chart-paper zero. At least fifty milligrams of the finely divided metal complex were placed in the sample pan. The sample thermocouple was positioned just inside the sample pan and close to the surface of the sample. The exact weight of sample used need not be recorded, since the calculation for the heat of sublimation requires only values for the rates of sublimation. The furnace tube (the Pyrex one was used here) was placed over the furnace end of the balance. The furnace tube and the glass envelope around the cold section of the beam were sealed to the balance housing by O-rings. The whole assembly was moved, so that the furnace tube was correctly positioned within the furnace. The controls of the Dupont 900 console were adjusted to give a temperature programming rate of 5^{o} $min.^{-1}$ and an X-axis pen speed (in time-base operation) of 1.0 $in.min.^{-1}$. The furnace temperature control was adjusted to indicate a reading corresponding to room temperature. The "mode of operation" control of the 900 console was set to "isothermal". The vacuum source was connected at the end of the furnace tube and switched on, along with a fan below the furnace. The fan helped to protect the balance mechanism from damage due to an excessive heat flow. The vacuum pump used was

capable of reducing the pressure inside the furnace tube to a pressure of about 0.25 millimetres of mercury.

The furnace temperature control was then set at a higher temperature, found initially by trial and error, at which a low rate of sublimation of the sample occurred. The furnace took some time to equilibrate at this new temperature. By suppression of most of the sample weight, the maximum Y-axis sensitivity of 0.2 milligram in^{-1} could be used. When the X-axis was set in the temperature-base operation, the equilibration of the furnace temperature was seen as a loss in sample weight at a constant temperature, T_1. The X-axis was then operated in the time-base mode and the change in weight of the sample over a period of ten minutes was recorded, the final temperature, T_2, being noted. This procedure is indicated in Figure 3.4 (a) and (b). The temperatures, T_1 and T_2, should ideally be the same. For the purposes of the calculation, the rate of sublimation was obtained in milligram min^{-1} from the weight loss over the ten minute interval at a mean temperature, T_a, of $\frac{1}{2}(T_1 + T_2)$. The procedure was repeated at a slightly higher mean temperature, T_b, so that the sublimation rates were recorded for at least five essentially constant temperatures over a temperature interval of about 20 to 30°.

3.2.3 Errors associated with the heats of sublimation

By choosing the temperatures to give low rates of sublimation and small overall weight loss, ideally less than 2%, the assumptions inherent in the application of the Langmuir equation to a Clausius-Clapeyron plot are valid. Ashcroft[44] claims a reproducibility of $\simeq$ 5% after least squares analysis of the Clausius-Clapeyron plot.

Figure 3.4 The readout on the X-Y plotter of the Dupont 900 console during the determination of H_{sub}

(a) Time base operation for the X-axis

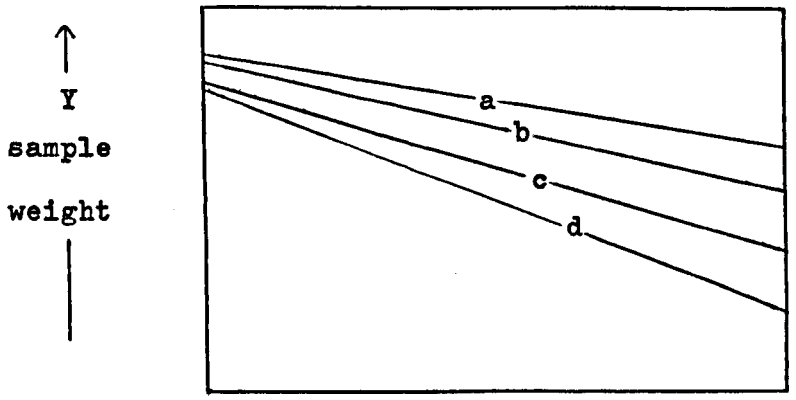

Isothermal operation

Y-axis sensitivity of 0.2 mg in^{-1}

X-axis sensitivity of 1.0 in min^{-1}

(b) Temperature base operation for the X-axis

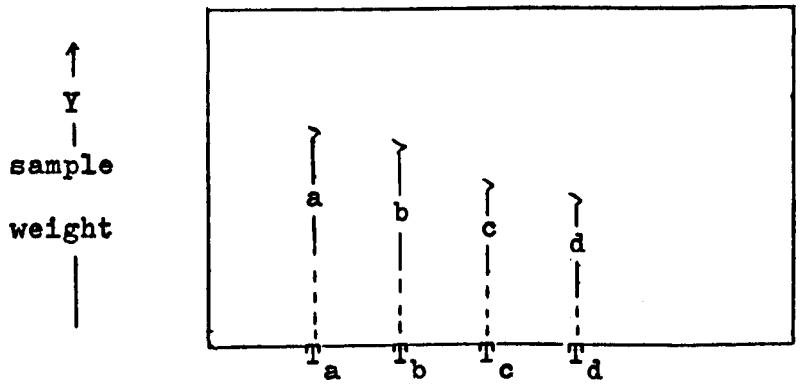

Isothermal operation

Y-axis sensitivity of 0.2 mg in^{-1}

X-axis sensitivity of 1 in = 10^{o}

(Curves a, b, c and d in Figure 3.4(a) indicate the gradually increasing rates of sublimation observed at the mean temperatures of T_a, T_b, T_c and T_d.)

He obtained fair agreement between heats of sublimation obtained by this method and those by other techniques. In many cases the thermogravimetric method yielded results at lower temperatures than the other techniques.

For the transition-metal complexes studied, the heat of sublimation values are the mean of at least four determinations and the associated error is the standard deviation of the mean. No least squares analyses of the plots were carried out. However, it is felt that the repetition of the measurements compensates for this omission. The main difficulties encountered were the length of time needed to equilibrate the furnace at each temperature setting, the appearance of "noise" on the recorder pen due to contamination of the slidewires of the X-Y plotter and, most of all, the possibility of partial decomposition accompanying sublimation. Theoretically, if decomposition does occur during sublimation, this should be indicated by a curvature of the plots which becomes apparent when decomposition first begins. However, this was not a good criterion for the recognition of this effect, since in most cases no curvature was observed even when it was obvious, by colour change of the sample, that decomposition had begun. Hence, to check this, the microanalysis of the sample residue in the pan, after a heat of sublimation determination, was carried out, as a matter of course, for each compound investigated. These analysis results are given along with the heat of sublimation results in Chapter 5. An arbitrary limit was set, whereby complexes which were found to have a carbon weight percentage, after the thermogravimetric work, of more than 1% below the calculated value were judged to have shown signs of decomposition concurrent with sublimation. The error on

each analysis value for the carbon weight percentage was estimated to be at least ± 0.4%.

The calculated values for the metal-ligand mean bond dissociation energies, $\bar{D}(M - L)$, for some of the heterocyclic metal complexes, MX_2L_n, through the use of these heats of sublimation, together with the DSC decomposition enthalpies, are given in Chapter 5.

4 THE PREPARATION AND ANALYSIS OF THE METAL COMPLEXES

In general, the scanning calorimeter gives the best results for enthalpies of decomposition for reactions of the type shown below

$$AL\ (c) \longrightarrow A\ (c) + L\ (g)$$

where the ligand L is swept out of contact with the product solid phase by the nitrogen purge gas. The platinum (11) complexes, $PtXMeZ_2.L$, and the iridium (1) complexes, $IrX(CO)(PPh_3)_2.L$ are ideally suited to a DSC investigation of their decomposition since the ligands, L, used were C_2F_4 and C_4F_6, which are gases at room temperature, and $CH_2CH(CN)$, which is a liquid at room temperature. The choice of which heterocyclic metal complexes, MX_2L_n, were to be prepared was, to a certain extent, governed by the requirement that the heterocyclic ligand L should preferably be a gas or a liquid of reasonably low boiling point.

The preparative details and analytical results have been subdivided into two sections which refer to the two very different groups of complexes studied; the heterocyclic metal complexes, MX_2L_n, and the olefinic and acetylenic complexes of platinum (II) and iridium (I), $MXYZ_2.L$. A list of the sources of the chemical reagents used has been omitted since in most cases the reagents were readily available. All the microanalysis data (except those denoted otherwise) were obtained at the University of Keele. The probable errors on these experimental values of carbon, hydrogen and nitrogen percentages in the complexes are ± 0.4%, ± 0.1% and ± 0.2% respectively. The overall weight loss percentage on decomposition during the DSC work was also used as a check on the purity of the complexes.

4.1. Preparation of the heterocyclic metal complexes, MX_2L_2

In all the preparations of these complexes the procedure was very similar and extremely simple. In general, the ligand itself, or the ligand in ethanolic solution, was added to an ethanolic solution of the hydrated metal dihalide; the appropriate stoichiometric amounts of reagents being used. In some cases, the ethanolic solutions were warmed before mixing. Metal dihalides which did not dissolve easily in ethanol were dissolved in aqueous-ethanolic solution. The precipitate of the complex, which gradually appeared after the two solutions were mixed, was filtered off and the crystals were washed with further ethanol or ether. The complexes were initially air-dried at room temperature and then dried over anhydrous calcium chloride. In most cases, the microanalysis data for the crystals indicated that no recrystallisations were necessary. Where the preparation differs significantly from the general method described above, a note is included in the text. In some cases, no previous report of the metal complex preparation could be found. Not all of the complexes prepared gave satisfactory results on the scanning calorimeter, usually because of the formation of intermediate liquid phases, which caused erratic pen recorder traces. Those complexes which gave DSC data are listed in Tables 5.1 and 5.2 of Chapter 5.

Most of the heterocyclic complexes prepared were of the stoichiometry MX_2L_2, except for the complexes of 3-methylpyrazole, where the majority were of the stoichiometry MX_2L_4, and a few other isolated cases, which are noted in the text. Table 4.1 gives the abbreviations used in this thesis for the heterocyclic ligands. The

Table 4.1 Abbreviations used for the heterocyclic ligands, L, in the metal complexes MX_2L_n

Ligand, L		Abbreviation
thiazole	=	(T)
2,4-dimethylthiazole	=	(24DiMeT)
benzothiazole	=	(BT)
2-methylbenzothiazole	=	(2MeBT)
2,6-dimethylbenzothiazole	=	(26DiMeBT)
benzoxazole	=	(BO)
2-methylbenzoxazole	=	(2MeBO)
2,5-dimethylbenzoxazole	=	(25DiMeBO)
2-methyl-5-methoxybenzoselenazole	=	(2Me5MeOBSe)
3(5)-methylpyrazole	=	(3(5)MePyz)
2-chloropyridine	=	(2Clpy)
2-bromopyridine	=	(2Brpy)
3-chloropyridine	=	(3Clpy)
3-bromopyridine	=	(3Brpy)
2-methoxypyridine	=	(2MeOpy)
2-ethylpyridine	=	(2Etpy)
pyridine	=	(py)
α-picoline	=	(α pic)
β-picoline	=	(β pic)
quinoline	=	(quin)
aniline	=	(an)

microanalysis data for the various heterocyclic metal complexes, MX_2L_n, are given in Table 4.2 along with references to the reported preparations.

4.1.1 Thiazole and substituted thiazole complexes

The analysis results are recorded in Table 4.2, section (a). For the 2,4-dimethylthiazole complexes, methanolic solutions of ligand and metal halide were used; the ratio of thiazole to metal ion being greater than 6 : 1.

4.1.2 Benzothiazole and substituted benzothiazole complexes

Most of the benzothiazole complexes prepared have been documented.[46] The three previously unreported complexes, $MnCl_2(BT)_2$, $CdCl_2(BT)_2$ and $CdBr_2(BT)_2$ were all white in colour. The 2-methylbenzothiazole complexes were prepared by the method of Duff, Hughes and Rutt,[47] which recommended that the ethanolic solutions should be refluxed for one hour after mixing. However, it was found that both of the copper (II) complexes, $CuCl_2(2MeBT)_2$ and $CuBr_2(2MeBT)_2$, precipitated immediately on mixing the ethanolic solutions. The preparation of metal complexes of 2,6-dimethylbenzothiazole does not seem to have been reported. The copper (II) complexes gave instant precipitation when the general synthetic method was used. However, on refluxing hydrated cobalt(II) chloride in ethanol with excess ligand for one hour, and cooling, no crystals separated out until after several weeks. The analysis results for the three complexes of 2,6-dimethylbenzothiazole prepared indicated that the stoichiometries were rather different. The dark grey copper(II) chloride complex gave agreement, if rather

poor, with the stoichiometry $CuCl_2(26DiMeBT)_3$. Good agreement was found for the other two complexes with the stoichiometries $CuBr_2(26DiMeBT)_4$ and $CoCl_2(26DiMeBT)_2$. These last two complexes were green and blue in colour respectively.

4.1.3 Benzoxazole and substituted benzoxazole complexes

The preparative method for benzoxazole metal complexes was that of Duff and Hughes[48], who advocated the use of ethyl acetate solutions of the ligand. The two previously unreported complexes, $CdCl_2(BO)_2$ and $ZnCl_2(BO)_2$, were both white in colour. Pale blue $CuCl_2(BO)_2$ precipitated immediately, but after filtering and drying in air appeared to go dark grey in colour. A similar occurrence was noted for $CuBr_2(BO)_2$, which changed colour from green to brown. Duff and Hughes[48] obtained blue $CuCl_2(BO)_2$ and reported only the formation of white $CuBr_2(BO)$. However, Duff[49] later recorded the preparation of green $CuBr_2(BO)_2$. Two of the 2-methylbenzoxazole complexes prepared, $MnCl_2(2MeBO)_2$ and $CdCl_2(2MeBO)_2$, gave apparently poor analysis results. However, the overall weight loss percentage after decomposition on the DSC was in good agreement with the calculated weight loss percentage.

Metal complexes, MX_2L_n, where L is 2,5-dimethylbenzoxazole, do not seem to have been reported. The general preparative method was used. Good analysis results were obtained for the complexes, $CoCl_2(25DiMeBO)_2$ (blue), $CoBr_2(25DiMeBO)_2$ (blue), $NiCl_2(25DiMeBO)_2$ (very pale yellow) and $CuCl_2(25DiMeBO)$ (orange/brown). The preparations with Manganese(II) chloride and copper(II) bromide gave precipitates whose stoichiometry was difficult to judge from their analysis data.

4.1.4 Selenium analogues

Some metal halide complexes with the ligand 2-methyl-5-methoxybenzoselenazole were prepared. No record of the previous preparation of such complexes is available. On using the general preparative method, immediate precipitation occurred for the case of $CuCl_2(2Me5MeOBSe)_2$ and $CuBr_2(2Me5MeOBSe)_2$. These two complexes were green/brown and red/brown in colour respectively. Precipitates were obtained for the case of $CoCl_2(2Me5MeOBSe)_2$ and $CoBr_2(2Me5MeOBSe)_2$ (both blue) after evaporation, overnight, of the solvent to small volume. Analysis results for these four complexes are given in Table 4.2, section (d). However, for various reasons, the DSC traces of these four complexes could not be interpreted. $CoBr_2(2Me5MeOBSe)_2$ gave inconsistent weight losses and $CoCl_2(2Me5MeOBSe)_2$, although giving a good overall weight loss, gave a final black residue, which was obviously not pale blue anhydrous cobalt(II) chloride.

4.1.5 Substituted pyrazole complexes

Imidazole, the nitrogen analogue of the thiazole and oxazole heterocyclic ring systems, is a high-melting solid (m.p. 363°K) and is not suitable for the preparation of complexes, MX_2L_n, for DSC study. Likewise, the use of benzimidazole (m.p. 443°K) is also precluded. However, pyrazole, the positional isomer of imidazole has a rather lower melting point, 342.5°K, and has a suitable derivative, 3-methylpyrazole, which is a liquid at room temperature. The preparation of complexes of this ligand, and of pyrazole itself, has been widely reported.[50-57]

The preparation of the complexes of 3-methylpyrazole used the general method, with the addition also of a few millilitres of ethyl orthoformate to the ethanolic metal salt solution to dehydrate the metal halide.[58] Because the acidic proton in pyrazoles may transfer from the one nitrogen to the other nitrogen in the ring, the 3-methyl derivative is more correctly denoted as 3(5)-methylpyrazole.

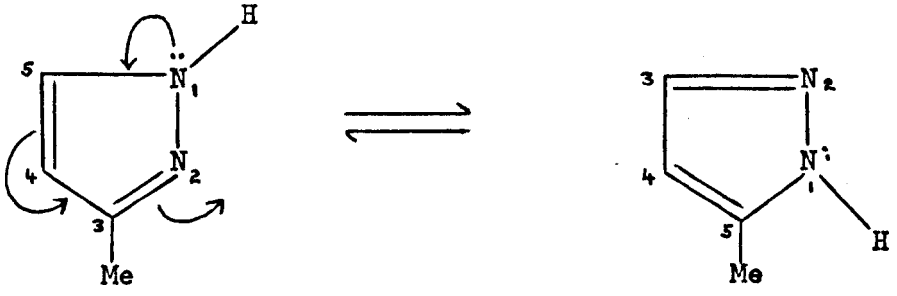

Reedjik[54] has shown that the ligand 3(5)-methylpyrazole coordinates via the imino lone pair of electrons, with the methyl group most probably located in the 5 position trans to the coordinated metal ion.

Only one of the 3(5)-methylpyrazole complexes prepared, $MnCl_2(3(5)MePyz)_2$, which was white in colour, does not seem to have been previously reported. The complex, $CoSO_4(3(5)MePyz)_4$, gave a poor analysis for nitrogen percentage, but the weight loss percentage on decomposition on the DSC was in good agreement with the calculated value.

4.1.6 Halogen-substituted pyridine complexes

Several complexes, MX_2L_n, were prepared, where L is 2-chloropyridine or 2-bromopyridine. The preparations of the complexes,

$MnCl_2(2Clpy)_2$, $CdCl_2(2Clpy)$ and $CdCl_2(2Brpy)$, all white in colour, do not appear to have been recorded in the literature. The preparations of NiX_2L_2, where X is Cl or Br and L is 2-chloro or 2-bromopyridine, were unsuccessful, as was also found by Billing and Underhill.[59] These workers suggested that this was due to the very low basicity of the ligand and the enforced tetracoordinated structure, making the formation of such complexes in solution unfavourable, relative to octahedral structures containing coordinated solvent.

The analysis results for $CdCl_2(2Brpy)$ gave poor agreement for the hydrogen percentage, but the overall weight loss percentage on decomposition on the DSC gave good agreement with the calculated value.

Complexes of stoichiometry MX_2L_2 were also prepared with the ligands, 3-chloropyridine and 3-bromopyridine. The complexes $ZnCl_2(3Clpy)_2$, $CdCl_2(3Clpy)_2$ and $CdCl_2(3Brpy)_2$, all white in colour, do not seem to have been reported in the literature.

It was hoped that complexes of 2-fluoropyridine might be prepared, but the general preparative method was not successful. The preparation of complexes MX_2L_n, where L is 2-fluoropyridine, does not appear to have been documented.

4.1.7 Other substituted pyridine complexes

For the ligand 2-methoxypyridine, the general method of preparation gave complexes MX_2L_2, where M was Cu or Co and X was Br or Cl. Compounds thought to be $CoCl_2(2EtOpy)_2$ and $CoBr_2(2EtOpy)_2$

gave poor analyses even on repetition of the preparations. No record of the preparation of complexes MX_2L_2, where L is 2-methoxypyridine or 2-ethoxypyridine has been found.

Although the DSC behaviour of the complexes MX_2L_2, where L is α, β or γ-picoline, has been fully investigated by Beech et al.,[25,60] the 2-ethylpyridine and 3-ethylpyridine complexes have not been studied. Three complexes of 2-ethylpyridine were made by the general preparative method. Unfortunately, all three gave unsatisfactory DSC traces. The preparations of the 3-ethylpyridine complexes were not attempted, but some reports on the preparations of some of these have been made.[61,62]

Several complexes were made which were needed for heat capacity data or heat of sublimation data, the DSC work for these having been already carried out by Beech et al..[25] These complexes were α-$CoCl_2(py)_2$, $CoCl_2(\alpha pic)_2$, $CoBr_2(\alpha pic)_2$, $CoCl_2(\beta pic)_2$, $CoCl_2(quin)_2$ and $CoCl_2(an)_2$. Analytical details of these complexes are included in section (g) of Table 4.2.

Table 4.2 Microanalysis data for the heterocyclic metal complexes

Complex	Observed			Calculated			Reference(s)
	C%	H%	N%	C%	H%	N%	
(a) Thiazole and substituted thiazole complexes							
L = thiazole							
$CoCl_2L_2$	23.3	2.79	9.1	24.0	2.02	9.34	(63) (64)
L = 2,4-dimethylthiazole							
$CoCl_2L_2$	33.4	4.24	7.6	33.7	3.96	7.87	(65)
$CuCl_2L_2$	33.2	4.26	7.6	33.3	3.91	7.77	(65)
$ZnCl_2L_2$	32.2	3.97	7.5	33.1	3.90	7.73	(65)
(b) Benzothiazole and substituted benzothiazole complexes							
L = benzothiazole							
$MnCl_2L_2$	42.2	2.83	6.9	42.5	2.54	7.07	(--)
$CoCl_2L_2$	42.7	2.54	7.0	42.2	2.00	7.00	(46)
$CoBr_2L_2$	34.1	2.04	5.8	34.5	2.00	5.75	(46)
CoI_2L_2	28.4	1.82	4.7	28.8	1.70	4.81	(46)
$NiCl_2L_2$	42.0	2.60	7.0	42.2	2.00	7.01	(46)
$CuCl_2L_2$	41.8	2.68	6.8	41.7	1.95	6.92	(46)
$Cu(NO_3)_2L_2$	36.7	2.16	12.1	36.7	2.20	12.2	(66)
$ZnCl_2L_2$	41.0	2.66	6.9	41.3	2.45	6.89	(46)
$ZnBr_2L_2$	33.5	2.81	5.6	33.9	2.00	5.65	(46)
$CdCl_2L_2$	36.8	2.17	6.2	37.1	2.22	6.18	(--)
$CdBr_2L_2$	31.3	2.39	5.2	31.0	1.86	5.16	(--)

Table 4.2(cont.) Microanalysis data for the heterocyclic metal complexes

Complex	Observed			Calculated			Reference(s)
	C%	H%	N%	C%	H%	N%	
L = 2-methylbenzothiazole							
$CoCl_2L_2$	44.2	3.39	6.4	44.9	3.30	6.55	(47)
$CoBr_2L_2$	36.9	2.92	5.3	37.2	2.70	5.42	(47)
$CuCl_2L_2$	44.0	3.49	6.4	44.4	3.24	6.48	(47)
$CuBr_2L_2$	36.5	3.32	5.2	36.8	2.69	5.37	(47)
$ZnCl_2L_2$	44.0	4.00	6.3	44.2	3.22	6.45	(47)
L = 2,6-dimethylbenzothiazole							
$CoCl_2L_2$	47.5	3.90	6.2	47.4	3.98	6.14	(--)
$CuCl_2L_3$	50.2	4.92	6.2	52.0	4.36	6.73	(--)
$CuBr_2L_2$	48.8	4.31	6.2	49.3	4.14	6.39	(--)
(c) Benzoxazole and substituted benzoxazole complexes							
L = benzoxazole							
$CoCl_2L_2$	44.6	3.31	7.5	46.2	2.95	7.61	(48)
$CoBr_2L_2$	37.0	2.38	6.1	36.8	2.35	6.15	(48)
CoI_2L_2	29.3	2.02	4.9	30.5	1.83	5.09	(48)
$ZnCl_2L_2$	43.9	3.05	7.1	44.9	2.69	7.48	(--)
$CdCl_2L_2$	40.3	2.78	6.5	39.9	2.39	6.65	(--)

Table 4.2(cont.) Microanalysis data for the heterocyclic metal complexes

Complex	Observed			Calculated			Reference(s)
	C%	H%	N%	C%	H%	N%	
L = 2-methylbenzoxazole							
$MnCl_2L_2$	40.3	3.95	5.8	49.0	3.60	7.14	(--)
$CoCl_2L_2$	47.7	3.83	7.1	48.4	3.56	7.07	(67)
$CoBr_2L_2$	39.6	3.00	5.7	39.6	2.91	5.78	(67)
$ZnCl_2L_2$	46.8	3.54	6.7	47.2	3.34	6.96	(67)
$CdCl_2L_2$	40.5	3.11	5.9	42.7	3.14	6.23	(--)
L = 2,5-dimethylbenzoxazole							
$CoCl_2L_2$	51.2	4.49	6.7	51.0	4.28	6.61	(--)
$CoBr_2L_2$	42.4	3.92	5.4	42.1	3.54	5.46	(--)
$NiCl_2L_2$	53.1	4.50	6.8	51.0	4.28	6.61	(--)
$CuCl_2L$	39.2	3.45	4.9	38.4	3.22	4.98	(--)
(d) Selenium analogues							
L = 2-methyl-5-methoxybenzoselenazole							
$CoCl_2L_2$	38.3	3.52	4.9	37.1	3.12	4.81	(--)
$CoBr_2L_2$	31.9	3.05	4.1	32.2	2.70	4.18	(--)
$CuCl_2L_2$	36.9	3.80	4.8	36.9	3.09	4.77	(--)
$CuBr_2L_2$	32.9	3.08	4.2	32.0	2.69	4.15	(--)

Table 4.2(cont.) Microanalysis data for the heterocyclic metal complexes

Complex	Observed			Calculated			Reference
	C%	H%	N%	C%	H%	N%	
(e) Substituted pyrazole complexes							
L = 3(5)-methylpyrazole							
$MnCl_2L_4$	41.9	5.81	24.7	42.3	5.33	24.7	(54)
$MnBr_2L_4$	35.5	4.98	20.7	35.4	4.46	20.6	(54)
$CoCl_2L_4$	42.5	5.51	24.3	41.9	5.25	24.4	(51)
$CoBr_2L_4$	34.6	4.55	19.8	35.1	4.40	20.4	(51)
$CoSO_4L_4$	39.6	5.31	22.6	39.8	5.00	29.2	(51)
$NiCl_2L_4$	42.4	5.58	24.6	42.0	5.28	24.5	(50)
$NiBr_2L_4$	36.0	4.85	20.9	35.1	4.42	20.5	(50)
$CuCl_2L_4$	42.2	5.78	23.7	41.5	5.23	24.2	(54)
$MnCl_2L_2$	32.2	4.10	18.8	33.1	4.17	19.3	(--)
$CuCl_2L_2$	32.1	4.99	18.7	32.2	4.05	18.8	(54)
$CdCl_2L_2$	26.9	4.00	15.7	27.7	3.48	16.1	(54)
(f) Halogen-substituted pyridine complexes							
L = 2-chloropyridine							
$MnCl_2L_2$	33.3	1.99	7.8	34.0	2.29	7.94	(--)
$CoCl_2L_2$	33.6	2.44	7.8	33.7	2.26	7.85	(68)
$CoBr_2L_2$	26.5	1.84	6.1	26.9	1.81	6.29	(68)
$CuCl_2L_2$	32.9	2.43	7.6	33.2	2.23	7.75	(68)
$CdCl_2L$	20.2	1.48	4.7	20.2	1.36	4.72	(--)

Table 4.2(cont.) Microanalysis data for the heterocyclic metal complexes

Complex	Observed			Calculated			Reference
	C%	H%	N%	C%	H%	N%	
L = 2-bromopyridine							
$CoCl_2L_2$	26.7	2.20	6.1	26.9	1.81	6.29	(68)
$CoBr_2L_2$	22.3	1.88	5.2	22.5	1.51	5.24	(68)
$CuCl_2L_2$	26.3	1.99	6.2	26.7	1.79	6.22	(68)
$CuBr_2L_2$	22.4	2.04	5.3	22.3	1.50	5.20	(68)
$ZnCl_2L_2$	26.0	2.35	5.8	26.6	1.78	6.20	(69)
$CdCl_2L$	18.6	1.76	4.3	17.6	1.18	4.10	(--)
L = 3-chloropyridine							
$MnCl_2L_2$	33.8	2.21	7.6	34.0	2.29	7.94	(61)
$CoCl_2L_2$	33.6	2.61	7.8	33.7	2.26	7.85	(59)
$CoBr_2L_2$	27.1	2.29	6.1	26.9	1.81	6.29	(59)
$NiCl_2L_2$	33.5	2.58	7.8	33.7	2.26	7.86	(59)
$CuCl_2L_2$	33.2	2.05	7.7	33.2	2.23	7.75	(62)
$CuBr_2L_2$	26.4	2.10	6.1	26.7	1.79	6.22	(62)
$ZnCl_2L_2$	32.7	2.58	7.4	33.1	2.22	7.71	(--)
$CdCl_2L_2$	29.0	1.92	6.7	29.3	1.97	6.83	(--)
L = 3-bromopyridine							
$MnCl_2L_2$	27.3	2.65	6.3	27.2	1.83	6.34	(61)
$CoCl_2L_2$	26.7	1.85	6.2	26.9	1.81	6.29	(59)

Table 4.2(cont.) Microanalysis data for the heterocyclic metal complexes

Complex	Observed			Calculated			Reference
	C%	H%	N%	C%	H%	N%	
L = 3-bromopyridine (cont.)							
$CoBr_2L_2$	22.7	2.25	5.2	22.5	1.51	5.24	(59)
$NiCl_2L_2$	27.0	2.45	6.2	27.0	1.81	6.29	(59)
$CuCl_2L_2$	26.9	2.17	6.2	26.7	1.79	6.22	(62)
$CuBr_2L_2$	22.4	1.71	5.0	22.3	1.50	5.20	(62)
$ZnCl_2L_2$	25.5	2.42	5.7	26.6	1.78	6.30	(--)
$CdCl_2L_2$	24.1	2.04	5.5	24.1	1.62	5.61	(--)
(g) Other substituted pyridine complexes							
L = 2-methoxypyridine							
$CoCl_2L_2$	40.1	4.38	7.8	41.4	4.05	8.05	(--)
$CoBr_2L_2$	33.0	3.64	6.3	33.0	3.23	6.41	(--)
$CuCl_2L_2$	40.7	4.23	7.9	40.9	4.00	7.94	(--)
$CuBr_2L_2$	32.6	3.70	6.4	32.6	3.19	6.35	(--)
L = 2-ethylpyridine							
$CoBr_2L_2$	38.9	4.30	6.6	38.8	4.19	6.47	(--)
$CuCl_2L_2$	48.1	5.61	8.3	48.2	5.20	8.05	(--)
$CuBr_2L_2$	38.4	4.78	6.4	38.4	4.14	6.40	(--)

Table 4.2(cont.) Microanalysis data for the heterocyclic metal complexes

Complex	Observed			Calculated			Reference
	C%	H%	N%	C%	H%	N%	
L = pyridine							
$CoCl_2L_2$* (oct.)	41.6	3.65	9.5	41.7	3.50	9.73	(70)
L = α-picoline							
$CoCl_2L_2$*	45.7	4.57	8.8	45.6	4.47	8.87	(26)
$CoBr_2L_2$*	35.2	3.37	6.8	35.6	3.49	6.92	(26)
L = β-picoline							
$CoCl_2L_2$*	45.8	4.52	8.8	45.6	4.47	8.87	(26)
L = quinoline							
$CoCl_2L_2$*	56.2	3.81	7.3	55.7	3.64	7.22	(71)
L = aniline							
$CoCl_2L_2$*	45.9	4.53	8.8	45.6	4.47	8.78	(72)

* The DSC enthalpies of decomposition for these complexes have already been determined by Beech et al..(reference 25)

4.2 Preparation of the olefinic and acetylenic complexes, $MXYZ_2.L$

The complexes can be subdivided into two main categories as follows.

(a) M = Ir(I)
X = F, Cl, Br or I
Y = CO
Z = PPh_3
L = C_2F_4, C_4F_6 or $CH_2CH(CN)$, (X = F, Cl or Br only.)

(b) M = Pt(II)
X = Cl or Br
Y = Me
Z = $AsMe_3$ or $AsMe_2Ph$, (L = C_4F_6 only.)
L = C_2F_4 or C_4F_6

4.2.1 Iridium(I) complexes $IrX(CO)(PPh_3)_2.L$

All the complexes of iridium(I) containing tetrafluoroethylene, C_2F_4, or hexafluorobut-2-yne, C_4F_6, were made, by a simple vacuum-line technique, at the University of Leicester by Dr. M.J. Hacker.[73] Tetrafluoroethylene (or hexafluorobut-2-yne) was condensed into a Carius tube containing a suspension of the parent complex, trans-$IrX(CO)(PPh_3)_2$, in dry, oxygen-free benzene at 77°K. The tube was sealed in vacuo and allowed to warm to room temperature with the gradual formation of a precipitate of the adduct. In some cases, this took up to eight days and the Carius tube had to be kept at about 330°K and mechanically shaken in order to obtain any product.

The analysis results, obtained at the University of Leicester, for these eight fluorocarbon complexes are given in Table 4.3. The author also spent some time at Leicester in attempting the preparation of $IrCl(CO)(PPh_2Me)_2.C_2F_4$[74] and $IrCl(CO)(AsPh_3)_2.C_2F_4$. (The latter compound does not seem to have been previously reported). However, pure samples of these could not be obtained. Several preparations were also tried of the adducts of C_2F_3Cl and hexafluoropropene with the parent complexes, $IrX(CO)(PPh_3)_2$, but no precipitates of the adducts were formed.

The complexes, $IrX(CO)(PPh_3)_2.CH_2CH(CN)$, where X is Cl or Br, were prepared (at Keele) according to the method of Baddeley[75] as reported for $IrCl(CO)(PPh_3)_2.CH_2CH(CN)$. Excess acrylonitrile, $CH_2CH(CN)$, was added to the parent complex, $IrCl(CO)(PPh_3)_2$ or $IrBr(CO)(PPh_3)_2$, under nitrogen. (Both of these parent complexes were purchased from Strem Chemicals Inc.). The mixture was stirred at room temperature and, after about two minutes, began to lighten in colour becoming white in ten minutes. The white powder was collected on a filter and washed with hexane. The preparation of $IrBr(CO)(PPh_3)_2.CH_2CH(CN)$ does not seem to have been reported before. Both $IrCl(CO)(PPh_3)_2.CH_2CH(CN)$ and $IrBr(CO)(PPh_3)_2.CH_2CH(CN)$ tend to revert slowly to their bright yellow parent complexes on standing in air. The conversion is complete after about one day. Because of this, no microanalysis data could be obtained. The infra-red spectra were recorded to establish the course of the preparation. Of necessity, the complexes were used on the DSC soon after filtration and the stoichiometry of the initial complex was calculated from the observed weight loss percentage on decomposition.

At the time this work was carried out, no record of the preparation of $IrF(CO)(PPh_3)_2.CH_2CH(CN)$ was available. The parent complex, trans-$IrF(CO)(PPh_3)_2$, was prepared from $IrCl(CO)(PPh_3)_2$ by the method of Vaska and Peone.[76] The fluoro acrylonitrile complex was then prepared by the method described for the chloro and bromo acrylonitrile complexes, except that the fluoro parent complex was suspended in oxygen-free benzene before the addition of the acrylonitrile. The yellow colour of the fluoro compound, $IrF(CO)(PPh_3)_2$, immediately disappeared to give a colourless solution. On slow evaporation of this solution, a buff-coloured solid was obtained after several days. Unlike the complexes of acrylonitrile with $IrCl(CO)(PPh_3)_2$ and $IrBr(CO)(PPh_3)_2$, the complex $IrF(CO)(PPh_3)_2.CH_2CH(CN)$ is stable indefinitely at room temperature. This observation has since been confirmed by Fitzgerald, Sakkab, Strange and Narutis.[77] A microanalysis was possible for $IrF(CO)(PPh_3)_2.CH_2CH(CN)$ and is given in Table 4.3. The low value for the nitrogen percentage is taken to indicate that rather less than one mole of acrylonitrile is coordinated to each mole of parent complex.

The preparation of the acrylonitrile complex of $IrCl(CO)(PPh_2Me)_2$ was attempted. The yellow colour of the parent immediately disappeared on addition of the acrylonitrile, but the product was an intractable brown oil. The attempted preparation of $IrCl(CO)(AsPPh_3)_2.CH_2CH(CN)$ resulted in a compound where both oxygen and acrylonitrile were coordinated. It has since been successfully prepared by Fitzgerald et al. [77]

The complexes of $IrCl(CO)(PPh_3)_2$ with tetracyanoethylene, $C_2(CN)_4$, and fumaronitrile, CH(CN)CH(CN), were also prepared by

Baddley's method.[75] These complexes are much more stable than the corresponding acrylonitrile complex and satisfactory analysis data were obtained. (See Table 4.3). The preparation of the tetrachloroethylene, C_2Cl_4, complex of $IrCl(CO)(PPh_3)_2$ was not successful. This complex does not appear to have been prepared elsewhere.

4.2.2 Platinum(II) complexes $PtXMeZ_2.L$

All of these platinum(II) complexes, $PtXMeZ_2.L$, where Z is $AsMe_3$, $AsMe_2Ph$, L is C_2F_4, C_4F_6, X is Cl or Br, were prepared at the University of Liverpool by Dr. R.J.Puddephatt. A vacuum-line procedure, similar to that for the C_2F_4 and C_4F_6 complexes of iridium(I) described in Section 4.3.1 was used. The preparations have been reported in the literature.[78-80] The analysis results (carried out at Liverpool University) are given in Table 4.4.

Table 4.3 Microanalysis data for the olefinic and acetylenic complexes of iridium(I), $IrX(CO)(PPh_3)_2.L$

(a) Tetrafluoroethylene and hexafluorobut-2-yne complexes*

Complex		Observed			Calculated		
L	X	C%	H%	F%	C%	H%	F%
C_2F_4	F	54.4	3.4	10.8	54.3	3.5	11.0
C_4F_6	F	52.9	3.3	14.1	53.2	3.3	14.3
C_2F_4	Cl	**					
C_4F_6	Cl	**					
C_2F_4	Br	51.1	3.4	- -	50.6	3.3	
C_4F_6	Br	48.3	3.0	- -	49.9	3.1	
C_2F_4	I	48.2	3.2	- -	48.2	3.1	
C_4F_6	I	47.2	2.8	- -	47.6	2.9	

(b) Cyano-olefin complexes

Complex		Observed			Calculated		
L	X	C%	H%	N%	C%	H%	N%
$CH_2CH(CN)$	F	59.2	4.27	1.2	58.8	4.07	1.72
$[CH(CN)]_2$	Cl	57.2	3.97	3.0	57.4	3.77	3.27
$C_2(CN)_4$	Cl	57.4	3.75	6.3	56.9	3.33	6.17

* These complexes were prepared and analysed at Leicester University.

** No analysis data are available for these complexes.

Table 4.4 Microanalysis data for the olefinic and acetylenic complexes of platinum(II), $PtXMeZ_2.L$*

Complex			Observed			Calculated		
Z	X	L	C%	H%	F%	C%	H%	F%
$AsMe_3$	Cl	C_2F_4	18.3	3.7	--	18.5	3.6	13.0
$AsMe_3$	Br	C_2F_4	16.8	3.8	11.9	17.2	3.4	12.1
$AsMe_3$	Cl	C_4F_6	19.9	3.8	--	20.4	3.3	17.6
$AsMe_3$	Br	C_4F_6	18.7	3.3	--	19.1	3.1	16.5
$AsMe_2Ph$	Cl	C_4F_6	32.7	3.4	--	32.7	3.3	14.8
$AsMe_2Ph$	Br	C_4F_6	30.7	3.1	13.2	30.9	3.1	13.9

* These complexes were prepared and analysed at the University of Liverpool.

5 ANALYTICAL AND THERMOCHEMICAL DATA FOR THE DECOMPOSITION OF THE HETEROCYCLIC METAL COMPLEXES, MX_2L_n

This chapter reports the enthalpies of decomposition, molar heat capacities and heats of sublimation obtained for the heterocyclic metal complexes, MX_2L_n.

5.1 Enthalpies of decomposition

Most of the decompositions of these complexes were found to occur in several stages. The enthalpy data for the individual stages of the decompositions, together with the enthalpies of overall decomposition, ΔH_{dec}, obtained by summation of the stepwise enthalpies, are reported in Tables 5.1 and 5.2 respectively. The stepwise enthalpies of decomposition, which refer to the peak temperature, T_p, correspond to the reaction given below.

$$MX_2L_x\ (c) \longrightarrow MX_2L_y\ (c) + (x - y)L\ (g)$$

The overall enthalpy of decomposition, ΔH_{dec}, is that of the following reaction, and refers to a temperature T_{mp}, which is the

$$MX_2L_n\ (c) \longrightarrow MX_2\ (c) + nL\ (g)$$

approximate mean of the peak temperatures of the individual decomposition stages.

The decomposition schemes for complexes of stoichiometry, MX_2L_2, were found to vary markedly with the nature of the heterocyclic ligand, L. For the complexes of this stoichiometry, where L is thiazole or 2,4-dimethylthiazole, simple loss of one ligand at a time appears to occur. This is also the situation found for the complexes containing the ligand 2-methylbenzothiazole.

However, for benzothiazole complexes, a more complicated decomposition scheme occurs, which depends on the nature of the metal dihalide. The benzoxazole and substituted benzoxazole complexes, MX_2L_2, decompose by the loss of one ligand at a time, except for the complex $CdCl_2(BO)_2$. The halogenopyridine complexes of this stoichiometry appear to decompose in this simple way also, although the occurrence of a single-stage decomposition seems quite frequent as in the complexes CoX_2L_2, where X is Cl or Br and L is 2-chloro- or 2-bromopyridine. All the cupric bromide complexes of the halogenopyridines give the cuprous bromide as the final product.

The complexes of stoichiometry MX_2L_4, which were found for the ligand 3(5)-methylpyrazole, also appear to have a complicated decomposition scheme.

Allan et al.[26] have suggested that the idealised scheme of thermal decomposition for CoX_2L_4, where L is pyridine, is as given below

$$\underset{\text{(oct.)}}{CoX_2L_4} \longrightarrow \underset{\text{(tet.)}}{CoX_2L_2} \longrightarrow \underset{\text{(oct.)}}{CoX_2L} \longrightarrow \underset{\text{(oct.)}}{CoX_2L_{\frac{1}{3}}} \longrightarrow \underset{\text{(oct.)}}{CoX_2}$$

The transition from the molecular octahedral complex CoX_2L_4, to a molecular tetrahedral complex CoX_2L_2, merely involves the loss of two molecules of ligand L, and a spatial rearrangement of the remaining ligands. This concept is in agreement with the ease with which this transformation occurs. The octahedral complexes, CoX_2L and $CoX_2L_{\frac{1}{3}}$, must be formulated with bridging halide ions. The violet complex, α-$CoCl_2(py)_2$ has a chain structure with chlorine atoms bridging between two cobalt atoms. Structures of

stoichiometry CoX_2L and $CoX_2L_{\frac{1}{3}}$ may be built up by removing pyridines from such a chain to give double or triple chains, in which each chlorine acts as a bridge between three metal atoms. If the chains are converted to infinite planes, this gives the structures of anhydrous cobaltous chloride and of cobaltous bromide. (These structures are the cadmium chloride and cadmium iodide layer lattices respectively.) Allan et al.[81] also suggest that, for NiX_2L_4, where L is pyridine, the decomposition is simpler as shown below

$$\underset{\text{(oct.)}}{NiX_2L_4} \longrightarrow \underset{\text{(oct.)}}{NiX_2L_2} \longrightarrow \underset{\text{(oct.)}}{NiX_2L} \longrightarrow \underset{\text{(oct.)}}{NiX_2L_{\frac{1}{3}}} \longrightarrow \underset{\text{(oct.)}}{NiX_2}$$

The only difference from the scheme for CoX_2L_4 is the preference for tetrahedral CoX_2L_2 but octahedral NiX_2L_2. However, it is more difficult to envisage a structural scheme involving the solid phases $MX_2L_{\frac{1}{2}}$, $MX_2L_{\frac{3}{4}}$ or $MX_2L_{\frac{1}{3}}$, as weight losses on decomposition imply, for some of the complexes reported in this thesis.

All the intermediate phases observed during the decomposition of the heterocyclic metal complexes, MX_2L_n, in the calorimeter were crystalline, except for the few cases noted in the data tables.

5.2 Heat capacities

Although the molar heat capacities, $\bar{C}_p$, have been measured for several of the heterocyclic metal complexes, MX_2L_n, the Kirchoff corrections were not calculable due to the absence of data for the gaseous heterocyclic ligands. However, the overall enthalpy of decomposition data of Table 5.2 indicate that for a given ligand L, the values of T_{mp} lie in a narrow temperature range, usually about

60°. The Kirchoff corrections to refer the ΔH_{dec} data to 298°K, for a given set of complexes MX_2L_n, are likely to be similar and differences between such corrections would be small compared with the errors associated with the enthalpy data.

The molar heat capacity data are reported in Table 5.3, in terms of the parameters "a" and "b", determined by a least squares analysis, assuming the relationship: $\bar{C}_p = (a + bT)$

5.3 Heats of sublimation

The values of the heats of sublimation, ΔH_{sub}, for some of the heterocyclic metal complexes of stoichiometry MX_2L_2, are reported in Table 5.4. The necessary microanalysis data for these complexes, which show that sublimation is not accompanied by decomposition, are reported in Table 5.5.

The values of the mean bond dissociation energy, $\bar{D}(M - L)$, of the metal-ligand bond in these MX_2L_2 complexes are also given in Table 5.4. These $\bar{D}(M - L)$ values were calculated from the simple thermochemical cycle shown below. No corrections were made to

$$\begin{array}{ccc} MX_2L_2\ (c) & \xrightarrow{\Delta H_{dec}} & MX_2\ (c) + 2L\ (g) \\ \downarrow \Delta H_{sub}\ (MX_2L_2) & & \downarrow \Delta H_{sub}\ (MX_2) \\ MX_2L_2\ (g) & \xrightarrow{2\bar{D}(M-L)} & MX_2\ (g) + 2L\ (g) \end{array}$$

$$2\bar{D}(M - L) = \Delta H_{dec} + \Delta H_{sub(MX_2)} - \Delta H_{sub(MX_2L_2)}$$

refer the enthalpies in this cycle to a common temperature or to refer the heat of sublimation of the heterocyclic metal complex to

the standard pressure value.

Table 5.6 reports some of the heterocyclic metal complexes for which the thermogravimetric method to determine the heat of sublimation proved unsatisfactory.

Table 5.1 Enthalpies of stepwise decomposition

$$MX_2L_x\ (c) \longrightarrow MX_2L_y\ (c) + (x - y)L\ (g)$$

Complex	Reaction		ΔH	T_i	T_p	T_f	Weight loss %	
	x	y	kcal mol^{-1}		°K		obs.	calc.
L = thiazole								
$CoCl_2L_2$	2	1	16.4 ± 0.1	380	450	455	28.3 ± 0.5	28.4
	1	0	18.8 ± 0.3	500	550, 580	590		
L = 2,4-dimethylthiazole								
$CoCl_2L_2$	2	1	14.4 ± 0.3	360	435	455	31.7 ± 0.7	31.8
	1	0	16.3 ± 0.1	455	505	520		
$CuCl_2L_2$	2	0	34.7 ± 0.7	390	460	500	63.9 ± 0.7	62.7
$ZnCl_2L_2$	2	1	14.9 ± 0.4	360	430	450	30.8 ± 0.1	31.2
	1	*	≃9	500	540	560		
L = benzothiazole								
$MnCl_2L_2$	2	⅓	23.1 ± 0.1	455	500	510	43.4 ± 0.5	43.6
	⅓	0	12.4 ± 0.4	540	585	595		
$CoCl_2L_2$	2	½	a	485	535		49.2 ± 1.2	50.7
	½	0			580	585		
$CoBr_2L_2$	2	½	a	480	535		41.2 ± 1.8	41.5
					570	590		

*The residue here appeared to be a liquid. Although the observed percentage weight loss for the overall decomposition, 62.5 ± 2.4 %, gave good agreement with the calculated value, 62.4 %, the enthalpy for the reaction was rather variable.

a Areas of peaks were insufficiently separated to obtain values for stepwise enthalpies, but approximate weight losses established the stoichiometry of the intermediate complexes.

Table 5.1 (cont.) Enthalpies of stepwise decomposition

$$MX_2L_x\ (c) \longrightarrow MX_2L_y\ (c) + (x - y)L\ (g)$$

Complex	Reaction		△H	T_i	T_p	T_f	Weight loss %	
	x	y	kcal mol^{-1}		°K		obs.	calc.
L = benzothiazole (cont.)								
$NiCl_2L_2$	2	$\frac{1}{3}$	21.8 ± 0.6	470	515	530	54.2 ± 0.8	56.3
	$\frac{1}{3}$	0	11.3 ± 0.2	540	580	595		
$CuCl_2L_2$	2	$\frac{2}{3}$	a	420	465		45.4 ± 0.3	44.5
	$\frac{2}{3}$	0			550	565		
$CdCl_2L_2$	2	1	17.1 ± 0.1	405	460	480	32.6 ± 0.3	29.8
	1	0	16.8 ± 0.4	495	570	585		
$CdBr_2L_2$	2	$\frac{3}{4}$	15.7 ± 0.2	385	420, 445	455	29.3 ± 0.6	31.1
L = 2-methylbenzothiazole								
$CoCl_2L_2$	2	1	19.2 ± 0.3	405	440	470	35.0 ± 0.3	34.8
	1	0	20.9 ± 0.3	500	565	580		
$CoBr_2L_2$	2	1	17.7 ± 0.1	420	465	480	29.6 ± 0.6	28.8
	1	0	20.8 ± 0.3	520	585	590		
L = 2,6-dimethylbenzothiazole								
$CoCl_2L_2$	2	1	22.6 ± 0.3	420	435, 480	485	35.9 ± 0.2	35.8
	1	0	17.3 ± 0.2	525	590	600		

a Areas of peaks were insufficiently separated to obtain values for stepwise enthalpies, but approximate weight losses established the stoichiometry of the intermediate complexes.

Table 5.1 (cont.) Enthalpies of stepwise decomposition

$$MX_2L_x\ (c) \longrightarrow MX_2L_y\ (c) + (x - y)L\ (g)$$

Complex	Reaction		ΔH	T_i	T_p	T_f	Weight loss %	
	x	y	kcal mol^{-1}		°K		obs.	calc.
L = benzoxazole								
$CoCl_2L_2$	2	1	16.0 ± 0.3	400	460	470	32.5 ± 0.2	32.4
	1	0	18.1 ± 0.3	470	530, 580	590		
$CoBr_2L_2$	2	1	16.4 ± 0.1	420	490	500	27.6 ± 1.7	26.1
	1	0	17.9 ± 0.1	500	555	565		
$CdCl_2L_2$	2	½	24.7 ± 0.5	370	440, 455	490	42.7 ± 0.2	42.4
	½	0	9.9 ± 0.3	500	540	560		
L = 2-methylbenzoxazole								
$MnCl_2L_2$	2	1	18.2 ± 0.3	365	395, 440	480	33.9 ± 0.9	34.0
	1	0	16.2 ± 0.2	485	540, 565	575		
$CoCl_2L_2$	2	1	15.0 ± 0.1	405	450	460	33.5 ± 0.1	33.6
	1	0	20.1 ± 0.2	495	565	575		
$CoBr_2L_2$	2	1	18.8 ± 0.4	450	505	515	27.2 ± 0.2	27.5
	1	0	19.5 ± 0.4	515	570	580		
$ZnCl_2L_2$	2	1	≃16	420	470	480	32.3 ± 0.3	33.1
	-	-	*	535	555	560		
$CdCl_2L_2$	2	1	11.4 ± 0.4	380	420	430	28.7 ± 1.0	29.6
	1	0	20.0 ± 0.3	460	525	545		

* The enthalpy for this decomposition stage was not reproducible.

Table 5.1 (cont.) Enthalpies of stepwise decomposition

$$MX_2L_x\ (c) \longrightarrow MX_2L_y\ (c) + (x - y)L\ (g)$$

Complex	Reaction x	Reaction y	ΔH kcal mol^{-1}	T_i °K	T_p °K	T_f °K	Weight loss % obs.	Weight loss % calc.
L = 2,5-dimethylbenzoxazole								
$CoCl_2L_2$	2	1	17.0 ± 0.3	395	445	465	35.8 ± 0.2	34.7
	1	0	20.4 ± 0.2	510	585	595		
$CoBr_2L_2$	2	1	15.4 ± 0.3	440	480	510	29.4 ± 0.2	28.7
	1	0	17.8 ± 0.4	530	585	590		
$NiCl_2L_2$	2	1	≃*17 ± 2	380	465	490	43.1 ± 0.4	34.7
	1	0	17.0 ± 0.2	515	565	590		
$CuCl_2L$	1	0	25.2 ± 0.6	440	475	515	50.1 ± 0.9	52.3
L = 2-methoxypyridine								
$CoCl_2L_2$	2	1	13.2 ± 0.4	390	430	440	28.7 ± 2.2	31.4
	a							
$CoBr_2L_2$	2	1	12.7 ± 0.3	405	440	480	27.0 ± 1.1	25.0
	a							
$CuCl_2L_2$	2	1	14.5 ± 0.1	370	425	435	34.1 ± 0.2	30.9
	1	0	15.4 ± 0.3	435	485	505		

* The long and straggly peak area made the baseline estimation difficult. Hence, there is a large error on the enthalpy and observed weight loss % for this stage.

a The second peak was very erratic due to the formation of a liquid phase.

Table 5.1 (cont.) Enthalpies of stepwise decomposition

$$MX_2L_x\ (c) \longrightarrow MX_2L_y\ (c) + (x - y)L\ (g)$$

Complex	Reaction		ΔH	T_i	T_p	T_f	Weight loss %	
	x	y	kcal mol^{-1}		°K		obs.	calc.
L = 2-chloropyridine								
$MnCl_2L_2$	2	1	15.6 ± 0.4	455	490	510	33.0 *	32.2
	1	0	17.5 ± 0.4	510	565	575		
$CoCl_2L_2$	2	0	27.5 ± 0.2	420	480	490	63.2 ± 0.5	63.6
$CoBr_2L_2$	2	0	29.8 ± 0.3	430	500	520	51.1 ± 0.3	50.9
$CuCl_2L_2$	2	1	14.0 ± 0.2	370	420	430	31.6 ± 0.2	31.4
	1	0	13.7 ± 0.4	430	490	500		
$CdCl_2L$	1	0	14.7 ± 0.2	460	535	545	38.2 ± 0.1	38.3
L = 2-bromopyridine								
$CoCl_2L_2$	2	0	30.2 ± 0.3	430	495	510	69.0 ± 0.2	70.9
$CoBr_2L_2$	2	0	30.9 ± 0.4	440	510	520	57.6 ± 0.2	59.1
$CuCl_2L_2$	2	0	24.7[a] ± 0.4	380 435 465	430 455 495	435 465 505	70.8 ± 0.2	70.1
$CuBr_2L_2$	b		30.4 ± 0.2	395	445, 470, 500	505	74.0 ± 0.1	73.4
$CdCl_2L$	1	0	12.6 ± 0.4	425	470, 510	525	47.9 ± 2.0	46.3

* Only one weight loss % was measured for this stage, due to the low yield on preparation of the complex.

a An initial peak, with T_p 355°K, ΔH of 0.62 ± 0.07 kcal mol^{-1} and weight loss % of 2.9 ± 0.6%, was thought to be due to the presence of ethanol. Stepwise ΔH and weight loss % data for the three peaks between 380°K and 505°K were not calculated.

b The reaction is $CuBr_2L_2\ (c) \rightarrow CuBr\ (c) + \frac{1}{2}Br_2\ (g) + 2L\ (g)$

Table 5.1 (cont.) Enthalpies of stepwise decomposition

$$MX_2L_x\ (c) \longrightarrow MX_2L_y\ (c) + (x - y)L\ (g)$$

Complex	Reaction		ΔH	T_i	T_p	T_f	Weight loss %	
	x	y	kcal mol^{-1}		°K		obs.	calc.
L = 3-chloropyridine								
$MnCl_2L_2$	2	1	16.0 ± 0.2	440	485	500	32.9 ± 0.3	32.2
	1	0	16.3 ± 0.3	515	570	585		
$CoCl_2L_2$	2	1	14.6 ± 0.3	425	490	500	32.8 ± 0.1	31.8
	1	0	17.6 ± 0.3	520	585	595		
$CoBr_2L_2$	2	1	17.0 ± 0.2	430	505	515	26.8 ± 0.1	25.5
	1	0	17.1 ± 0.4	515	580	590		
$NiCl_2L_2$	2	1	15.5 ± 0.2	465	520	530	33.3 ± 0.2	31.8
	1	0	18.5 ± 0.4	545	600	610		
$CuCl_2L_2$	2	1	16.2 ± 0.2	435	500	510	37.8 ± 1.8	32.4
	1	0	16.7 ± 0.5	510	575	580		
$CuBr_2L_2$	b		42.9 ± 0.5	450	520	535	67.9 ± 0.6	68.2
$CdCl_2L_2$	2	1	14.6 ± 0.2	425	475	485	29.1 ± 1.5	27.7
	1	0	16.6 ± 0.1	490	550	560		
L = 3-bromopyridine								
$MnCl_2L_2$	2	1	15.8 ± 0.3	435	485	500	35.9 ± 0.6	35.8
	1	0	16.5 ± 0.3	525	585	595		
$CoCl_2L_2$	2	1	14.3 ± 0.2	470	520	530	40.1 ± 0.4	35.4
	1	0	17.8 ± 0.1	540	600	610		

b The reaction is $CuBr_2L_2\ (c) \rightarrow CuBr\ (c) + \frac{1}{2}Br_2\ (g) + 2L\ (g)$

Table 5.1 (cont.) Enthalpies of stepwise decomposition

$$MX_2L_x\ (c) \longrightarrow MX_2L_y\ (c) + (x - y)L\ (g)$$

Complex	Reaction		ΔH	T_i	T_p	T_f	Weight loss %	
	x	y	kcal mol^{-1}		^oK		obs.	calc.
L = 3-bromopyridine (cont.)								
$CoBr_2L_2$	2	1	15.7 ± 0.2	460	520	530	33.1 ± 0.1	29.5
	1	0	18.4 ± 0.2	530	590	595		
$NiCl_2L_2$	2	1	15.4 ± 0.2	495	540	560	36.9 ± 0.4	35.5
	1	0	19.8 ± 0.3	560	610	620		
$CuCl_2L_2$	2	1	16.2 ± 0.2	450	520	530	39.0 ± 1.1	35.1
	1	0	18.8 ± 0.2	530	595	605		
$CuBr_2L_2$	*		40.9 ± 1.2	465	540	560	72.5 ± 0.1	73.4
$CdCl_2L_2$	2	1	14.8 ± 0.2	430	480	490	31.9 ± 0.4	31.7
	1	0	15.8 ± 0.2	505	560	570		
L = 3(5)-methylpyrazole								
$MnCl_2L_4$	4	2	59.0 ± 0.5	390	450, 490	500	38.8 ± 0.5	36.1
	2	0	15.6 ± 0.2	520	575	595		
$MnBr_2L_4$	4	1	51.3 ± 2.5	405	455, 480	510	46.4 ± 1.1	45.4
	1	0	13.3 ± 0.9	525	575	580		

* The reaction is $CuBr_2L_2\ (c) \longrightarrow CuBr\ (c) + \frac{1}{2}Br_2\ (g) + 2L\ (g)$

Table 5.1 (cont.) Enthalpies of stepwise decomposition

$$MX_2L_x\ (c) \longrightarrow MX_2L_y\ (c) + (x - y)L\ (g)$$

Complex	Reaction		△H	T_i	T_p	T_f	Weight loss %	
	x	y	kcal mol^{-1}		°K		obs.	calc.
L = 3(5)-methylpyrazole (cont.)								
$CoCl_2L_4$	4	1.5	38.1 ± 0.3	400	440	495	42.1 ± 1.1	44.8
	*							
$CoSO_4L_4$	4	1	58.1 ± 0.3	450	520	530	53.0 ± 0.2	51.0
	1	0	11.8 ± 0.2	565	575	590		
$NiCl_2L_4$	4	0.5	62.9 ± 0.5	440	510, 530	540	63.3 ± 0.2	62.7
	0.5	0	5.5 ± 0.4	610	660	670		
$MnCl_2L_2$	a		22.5 ± 0.6	440	490	500	39.6 ± 1.0	a
	a		13.4 ± 0.3	520	580	600		
$CdCl_2L_2$	2	⅓	21.9 ± 0.3	410	475	485	32.1 ± 0.6	31.5
	⅓	0	13.7 ± 0.2	510	570	580		

* The second peak occurred at a temperature around 600°K and was rather erratic, although the weight loss % at 640°K after the peak was 71% which is in good agreement with the calculated value of 71.7%.

a The observed weight loss % falls between that calculated for the loss of 1.5 ligand molecules, 42.7%, and that for the loss of 1.33 ligand molecules, 37.7%.

Table 5.2 Enthalpies of overall decomposition, ΔH_{dec}

$$MX_2L_n\ (c) \longrightarrow MX_2\ (c) + nL\ (g)$$

Complex	ΔH_{dec} kcal mol^{-1}	T_{mp} °K	Weight loss % obs.	calc.
L = thiazole				
$CoCl_2L_2$	35.2 ± 0.4	510	56.3 ± 0.2	56.7
L = 2,4-dimethylthiazole				
$CoCl_2L_2$	30.7 ± 0.4	470	63.2 ± 0.2	63.6
$CuCl_2L_2$	34.7 ± 0.7	460	63.9 ± 0.7	62.7
L = benzothiazole				
$MnCl_2L_2$	35.5 ± 0.5	540	56.0 ± 0.8	52.4
$CoCl_2L_2$	40.2 ± 0.8	550	67.5 ± 0.1	67.6
$CoBr_2L_2$	38.3 ± 0.4	550	53.7 ± 0.4	55.3
$NiCl_2L_2$	33.1 ± 0.8	540	64.8 ± 0.1	67.6
$CuCl_2L_2$	38.4 ± 0.7	505	64.5 ± 1.3	66.8
$CdCl_2L_2$	33.9 ± 0.5	510	59.4 ± 0.4	59.6
$CdBr_2L_2$	35.4 ± 0.4	480	49.7 ± 0.1	49.8
L = 2-methylbenzothiazole				
$CoCl_2L_2$	40.1 ± 0.6	500	69.0 ± 0.7	69.6
$CoBr_2L_2$	38.5 ± 0.4	525	57.0 ± 0.3	57.7

Table 5.2 (cont.) Enthalpies of overall decomposition, $\triangle H_{dec}$

$$MX_2L_n\ (c) \longrightarrow MX_2\ (c) + nL\ (g)$$

Complex	$\triangle H_{dec}$ kcal mol^{-1}	T_{mp} °K	Weight loss % obs.	calc.
L = 2,6-dimethylbenzothiazole				
$CoCl_2L_2$	39.9 ± 0.5	520	71.6 ± 0.1	71.6
L = benzoxazole				
$CoCl_2L_2$	34.1 ± 0.6	505	63.5 ± 0.2	64.8
$CoBr_2L_2$	34.3 ± 0.2	520	51.9 ± 0.4	52.1
$CdCl_2L_2$	34.6 ± 0.8	495	57.8 ± 0.5	56.5
L = 2-methylbenzoxazole				
$MnCl_2L_2$	34.4 ± 0.5	500	65.9 ± 1.4	67.9
$CoCl_2L_2$	35.1 ± 0.3	520	67.1 ± 0.1	67.2
$CoBr_2L_2$	38.3 ± 0.8	540	54.8 ± 0.1	54.9
$CdCl_2L_2$	31.4 ± 0.7	475	57.7 ± 0.2	59.2
L = 2,5-dimethylbenzoxazole				
$CoCl_2L_2$	37.4 ± 0.5	515	69.7 ± 0.2	69.4
$CoBr_2L_2$	33.2 ± 0.7	530	57.2 ± 0.1	57.4
$NiCl_2L_2$	≃34 ± 2	515	73.4 ± 0.5	69.4
L = 2-methoxypyridine				
$CuCl_2L_2$	29.9 ± 0.4	455	62.0 ± 0.3	61.9

Table 5.2 (cont.) Enthalpies of overall decomposition, ΔH_{dec}

$$MX_2L_n\ (c) \longrightarrow MX_2\ (c) + nL\ (g)$$

Complex	ΔH_{dec} kcal mol^{-1}	T_{mp} °K	Weight loss % obs.	calc.
L = 2-chloropyridine				
$MnCl_2L_2$	33.1 ± 0.8	530	61.9 ± 2.1	64.3
$CoCl_2L_2$	27.5 ± 0.2	480	63.2 ± 0.5	63.6
$CoBr_2L_2$	29.8 ± 0.3	500	51.1 ± 0.3	50.9
$CuCl_2L_2$	27.7 ± 0.6	455	62.1 ± 0.7	62.8
L = 2-bromopyridine				
$CoCl_2L_2$	30.2 ± 0.3	495	69.0 ± 0.2	70.9
$CoBr_2L_2$	30.9 ± 0.4	510	57.6 ± 0.2	59.1
$CuCl_2L_2$	24.7 ± 0.4	460	70.8 ± 0.2	70.1
$CuBr_2L_2$	*21.5 ± 0.2	-	-	-
L = 3-chloropyridine				
$MnCl_2L_2$	32.3 ± 0.5	530	63.8 ± 0.4	64.3
$CoCl_2L_2$	32.2 ± 0.6	540	65.0 ± 0.6	63.6
$CoBr_2L_2$	34.1 ± 0.6	545	51.4 ± 0.3	50.9
$NiCl_2L_2$	34.0 ± 0.6	560	63.4 ± 0.5	63.6
$CuCl_2L_2$	32.9 ± 0.7	540	64.4 ± 0.2	62.8
$CuBr_2L_2$	*34.0 ± 0.5	-	-	-
$CdCl_2L_2$	31.2 ± 0.3	515	55.4 ± 0.1	55.3

* ΔH_{dec} estimated by the use of the ΔH_f^o values for $CuBr_2$ and CuBr of -33.9 and -25.0 kcal mol^{-1} respectively.[22]

Table 5.2 (cont.) Enthalpies of overall decomposition, ΔH_{dec}

$$MX_2L_n\ (c) \longrightarrow MX_2\ (c) + nL\ (g)$$

Complex	ΔH_{dec} kcal mol^{-1}	T_{mp} °K	Weight loss % obs.	calc.
L = 3-bromopyridine				
$MnCl_2L_2$	32.3 ± 0.6	535	72.1 ± 0.2	71.5
$CoCl_2L_2$	32.1 ± 0.3	560	71.5 ± 0.2	70.9
$CoBr_2L_2$	34.1 ± 0.4	555	59.1 ± 0.9	59.1
$NiCl_2L_2$	35.2 ± 0.5	575	71.0 ± 0.1	70.9
$CuCl_2L_2$	35.0 ± 0.1	560	70.9 ± 0.4	70.1
$CuBr_2L_2$	*32.0 ± 1.2	-	-	-
$CdCl_2L_2$	30.6 ± 0.4	520	63.4 ± 0.1	63.3
L = 3(5)-methylpyrazole				
$MnCl_2L_4$	74.6 ± 0.7	520	73.4 ± 0.2	72.3
$MnBr_2L_4$	64.6 ± 3.4	520	60.4 ± 0.1	60.5
$CoSO_4L_4$	69.9 ± 0.5	545	67.2 ± 0.3	67.9
$NiCl_2L_4$	68.4 ± 0.9	590	71.8 ± 0.6	71.7
$MnCl_2L_2$	35.9 ± 0.9	535	58.2 ± 0.8	56.6
$CdCl_2L_2$	35.6 ± 0.5	520	46.6 ± 0.1	47.3

* ΔH_{dec} estimated by the use of the ΔH_f^o values for $CuBr_2$ and CuBr of -33.9 and -25.0 kcal mol^{-1} respectively.[22]

Table 5.3 Molar heat capacity data*for the complexes MX_2L_n

Complex	a cal mol^{-1}	b cal $deg^{-1}mol^{-1}$	Experimental temp. range ^oK
L = thiazole			
$CoCl_2L_2$	-19.3	0.244	320 - 360
L = benzothiazole			
$MnCl_2L_2$	16.0	0.225	320 - 400
$CoCl_2L_2$	22.4	0.190	320 - 430
$CoBr_2L_2$	26.5	0.195	320 - 450
CoI_2L_2	27.2	0.178	320 - 450
$NiCl_2L_2$	42.3	0.151	320 - 430
L = 2-methylbenzothiazole			
$CoCl_2L_2$	28.1	0.218	320 - 380
$CoBr_2L_2$	32.0	0.195	320 - 400
L = 2-methylbenzoxazole			
$CoCl_2L_2$	30.2	0.190	320 - 390
$CoBr_2L_2$	24.3	0.230	320 - 410
L = 2,5-dimethylbenzoxazole			
$CoCl_2L_2$	20.1	0.258	320 - 380
$CoBr_2L_2$	18.4	0.261	320 - 420

* $\bar{C}_p = a + bT$

Table 5.3 (cont.) Molar heat capacity data* for the complexes, MX_2L_n

Complex	a	b	Experimental
	cal mol^{-1}	cal deg^{-1} mol^{-1}	temp. range ^oK
L = 3(5)-methylpyrazole			
$MnCl_2L_4$	16.0	0.345	320 - 380
$MnBr_2L_4$	28.4	0.316	320 - 400
$CoCl_2L_4$	25.1	0.332	320 - 400
$CoBr_2L_4$	6.9	0.390	320 - 390
$CoSO_4L_4$	19.5	0.349	320 - 430
$NiCl_2L_4$	42.9	0.255	320 - 400
$NiBr_2L_4$	24.0	0.337	320 - 410
L = halogenopyridine			
$CoCl_2(2Brpy)_2$	15.2	0.177	330 - 390
$CoBr_2(2Brpy)_2$	26.7	0.134	330 - 410
$CoCl_2(3Brpy)_2$	28.8	0.134	320 - 420
$CoBr_2(2Clpy)_2$	28.9	0.138	320 - 400
$CuCl_2(2Clpy)_2$	12.4	0.184	320 - 360
$CoBr_2(3Clpy)_2$	18.3	0.149	320 - 400
L = other heterocyclic ligands			
$CoCl_2(py)_2$**	-4.1	0.216	320 - 360
$CoCl_2(an)_2$**	8.1	0.202	320 - 400
$CoCl_2(quin)_2$	6.0	0.252	320 - 410

* $\bar{C}_p = a + bT$

** The $\bar{C}_p$ values for these complexes are in reasonable agreement with the earlier values (reference 34), when a point by point comparison is made.

Table 5.4 The heats of sublimation and $\bar{D}(M - L)$ values for the heterocyclic metal complexes, MX_2L_2

Complex	Molec. Wt	$\Delta H_{sub}(MX_2L_2)$	Temp. range	$\Delta H^{o}_{sub}(MX_2)$[a]	$\bar{D}(M - L)$*
		kcal mol^{-1}	°K	← kcal mol^{-1} →	
L = benzothiazole					
$CoBr_2L_2$	489	29.8 ± 1.0	381 - 399	53 ± 1	30.8 ± 1.2
L = 2-methylbenzothiazole					
$CoCl_2L_2$	428	29.3 ± 0.3	332 - 356	56.0 ± 0.4	33.4 ± 0.7
$CoBr_2L_2$	517	27.5 ± 1.0	335 - 354	53 ± 1	32.0 ± 1.2
L = 2-methylbenzoxazole					
$CoCl_2L_2$	396	22.1 ± 0.6	327 - 348	56.0 ± 0.4	34.5 ± 0.7
$CoBr_2L_2$	485	26.6 ± 1.0	344 - 368	53 ± 1	32.3 ± 1.4
L = 2,5dimethylbenzoxazole					
$CoCl_2L_2$	424	22.8 ± 1.1	326 - 349	56.0 ± 0.4	35.3 ± 1.0
$CoBr_2L_2$	513	25.0 ± 1.2	345 - 364	53 ± 1	30.6 ± 1.5
L = α-picoline					
$CoCl_2L_2$	316	**20.7 ± 0.9	335 - 358	56.0 ± 0.4	30.8 ± 0.9
$CoBr_2L_2$	405	**16.6 ± 0.7	353 - 374	53 ± 1	28.8 ± 1.2

a These data are standard enthalpies of sublimation at 298°K and have been taken from reference 41, except that for $CoCl_2$, which has been taken from reference 42.

* The ΔH_{dec} values used in the calculation of $\bar{D}(M - L)$ have been reported in Table 5.2, except for the values for the α-picoline complexes which have been taken from reference 25.

** Some decomposition occurred with sublimation, hence the heat of sublimation is a maximum, and $\bar{D}(M - L)$ a minimum value.

Table 5.4. (cont.) The heats of sublimation and $\bar{D}(M - L)$ values for the heterocyclic metal complexes, MX_2L_2

Complex	Molec. Wt	$\triangle H_{sub}(MX_2L_2)$ kcal mol^{-1}	Temp. range ^oK	$\triangle H^o_{sub}(MX_2)$[a] kcal mol^{-1}	$\bar{D}(M - L)$* kcal mol^{-1}
L = 2-chloropyridine					
$CoCl_2L_2$	357	**24.2 ± 1.6	337 - 368	56.0 ± 0.4	29.7 ± 1.1
L = 2-bromopyridine					
$CoCl_2L_2$	446	28.8 ± 1.1	351 - 376	56.0 ± 0.4	28.7 ± 0.9
$CoBr_2L_2$	535	24.1 ± 0.5	348 - 382	53 ± 1	29.9 ± 1.0
L = 3-chloropyridine[c]					
$CoCl_2L_2$	357	**22.9 ± 0.8[b]	363 - 381	56.0 ± 0.4	32.7 ± 0.9
$CoBr_2L_2$	446	11.7 ± 1.5	345 - 371	53 ± 1	37.7 ± 1.6
$NiCl_2L_2$	357	17.2 ± 1.7	355 - 385	58.7 ± 1	37.8 ± 1.2
$CuCl_2L_2$	361	≃7 ± 1	347 - 386	47 ± 1	36.5 ± 1.4
L = 3-bromopyridine[c]					
$CoCl_2L_2$	446	18.4 ± 1.0	344 - 383	56.0 ± 0.4	34.0 ± 0.9
$NiCl_2L_2$	446	18.2 ± 1.2	374 - 403	58.7 ± 1	37.9 ± 1.4
$CuCl_2L_2$	451	13.6 ± 1.3	360 - 390	47 ± 1	34.2 ± 1.9

a See footnote on previous page.

* See footnote on previous page.

** See footnote on previous page.

b Only two determinations of the heat of sublimation were carried out.

c All the Co(II) complexes, CoX_2L_2, in Table 5.4 are tetrahedral, except those with these ligands, which are polymeric octahedral.

Table 5.5 Microanalysis data for the residues from the heat of sublimation determinations

Complex	Temperature* °K	C% obs.	C% calc.	H% obs.	H% calc.	N% obs.	N% calc.
L = benzothiazole							
$CoBr_2L_2$	397	34.4	34.5	2.43	2.00	5.7	5.75
L = 2-methylbenzothiazole							
$CoCl_2L_2$	355	44.9	44.9	3.57	3.30	6.4	6.55
$CoBr_2L_2$	355	37.3	37.2	3.31	2.70	5.2	5.42
L = 2-methylbenzoxazole							
$CoCl_2L_2$	343	48.0	48.4	3.60	3.56	6.7	7.07
$CoBr_2L_2$	367	39.5	39.6	3.47	2.91	5.6	5.78
L = 2,5-dimethylbenzoxazole							
$CoCl_2L_2$	349	51.0	51.0	4.16	4.28	6.6	6.61
$CoBr_2L_2$	367	41.3	42.1	3.78	3.54	5.2	5.46
L = 2-methylpyridine							
$CoCl_2L_2$**	359	44.0	45.6	4.77	4.47	8.8	8.87
$CoBr_2L_2$**	376	34.1	35.6	3.86	3.49	6.5	6.92

* This is the temperature of the sample at the end of the particular ΔH_{sub} determination.

** Some decomposition is occurring along with sublimation, since the observed C% is more than 1% lower than the calculated value.

Table 5.5 (cont.) Microanalysis data for the residues from the heat of sublimation determinations

Complex	Temperature*	C%		H%		N%	
	°K	obs.	calc.	obs.	calc.	obs.	calc.
L = 2-chloropyridine							
$CoCl_2L_2$**	366	30.5	33.7	2.30	2.26	7.2	7.85
L = 2-bromopyridine							
$CoCl_2L_2$	379	26.4	26.9	2.33	1.81	6.0	6.29
$CoBr_2L_2$	383	21.7	22.5	2.09	1.51	5.0	5.24
L = 3-chloropyridine							
$CoCl_2L_2$**	382	31.7	33.7	2.51	2.26	7.3	7.85
$CoBr_2L_2$	368	26.8	26.9	2.00	1.81	6.1	6.29
$NiCl_2L_2$	386	32.8	33.7	2.75	2.26	7.5	7.86
$CuCl_2L_2$	381	32.5	33.2	2.57	2.23	7.5	7.75
$CuBr_2L_2$	339	26.3	26.7	1.68	1.79	6.0	6.22
L = 3-bromopyridine							
$CoCl_2L_2$	383	26.8	26.9	1.92	1.81	6.3	6.29
$NiCl_2L_2$	399	26.6	27.0	2.59	1.81	6.0	6.29
$CuCl_2L_2$	389	26.6	26.7	2.33	1.79	6.0	6.22
$CuBr_2L_2$	347	22.1	22.3	1.63	1.50	5.1	5.20

* This is the temperature of the sample at the end of the particular ΔH_{sub} determination.

** Some decomposition is occurring along with sublimation, since the observed C% is more than 1% lower than the calculated value.

Table 5.6 Heterocyclic metal complexes which were found to give unsatisfactory heat of sublimation results

Complex	Reason for unsuitability
$CoCl_2(BT)_2$ $CoCl_2(3Mepy)_2$ $CoBr_2(2Clpy)_2$	Decomposition and sublimation occurred at the same time, resulting in a poor analysis for the residue
$CoBr_2(BO)_2$ $CoCl_2(3(5)MePyr)_4$ $CoSO_4(3(5)MePyr)_4$	Significant colour change of the sample occurred
$NiCl_2(BT)_2$ $CoCl_2(3Clpy)_2$ $MnCl_2(BT)_2$ $CuCl_2(BT)_2$	The samples were of such low density that insufficient material could be loaded into the sample pan.
$CoCl_2(24DiMeT)_2$ $CuCl_2(2Clpy)_2$ $CuCl_2(2Brpy)_2$	Very low temperatures of initial decomposition, $T_i \simeq 360^{\circ}K$, were observed during the DSC work
$CoCl_2(quin)_2$ $CuBr_2(3Brpy)_2$ $CuCl_2(3Clpy)_2$ $MnCl_2(3Brpy)_2$ $MnCl_2(3Clpy)_2$	These gave no indication of decomposition over the temperature ranges of sublimation of 368 - 385, 334 - 349, 328 - 340, 360 - 375 and 361 - 376°K respectively, but the heat of sublimation data obtained were rather erratic.
$CoCl_2(py)_2$ (oct.)	This gave rapid conversion to the blue, tetrahedral form, followed by excessive weight loss.

6 INTERPRETATION OF THE THERMOCHEMICAL DATA FOR THE HETEROCYCLIC METAL COMPLEXES, MX_2L_n

In this chapter the experimental $\bar{D}(M - L)$ values for the MX_2L_2 complexes are discussed. An estimate of the $\bar{D}(M - py)$ values for the corresponding $MX_2(py)_2$ complexes is made and these estimated values are compared with the experimental ones. The nature of the bonding in the M - L bond, where L is an azole or halogenopyridine, and in the M - py bond is discussed.

6.1 The stereochemistry of the heterocyclic metal complexes, MX_2L_2 and MX_2L_4

In most of the heterocyclic metal complexes, MX_2L_2 or MX_2L_4, for which data are reported in this thesis, the heterocyclic ligand is bonded to the metal ion via the imino-nitrogen (=N—) of the heterocyclic ring. As in analogous pyridine complexes, the σ-bond to the metal ion is formed by the donation of the non-bonding electron pair on the imino-nitrogen to the metal ion. The one exception to this is found in the complexes CoX_2L_2, where L is 2-methylbenzoxazole. Duff and Hughes[67] have proposed that here the ligand is bonded via its oxygen heteroatom. This is due to the electron-releasing effect of the 2-methyl group. The oxygen heteroatom is more electronegative than the nitrogen heteroatom and so it is rendered relatively more basic by the inductive effect of the 2-methyl group. In the corresponding 2-methylbenzothiazole complexes, the sulphur heteroatom is much less electronegative than the nitrogen heteroatom, so it is not influenced so much by the

presence of the 2-methyl group. Hence, in complexes of 2-methylbenzothiazole and of benzoxazole itself, bonding occurs via the nitrogen heteroatom. Although no literature report is available on the analogous complexes of 2,5-dimethylbenzoxazole, it is assumed that these also contain oxygen-bonded ligand.

It has been found that most of the MX_2L_2 or MX_2L_4 complexes have structures similar to their pyridine analogues. This is made apparent by comparison of their spectra, X-ray powder patterns and magnetic properties. Three main types of stereochemistry are observed for the MX_2L_4 and MX_2L_2 complexes. The complexes MX_2L_2 may be either tetrahedral and monomeric, or octahedral and polymeric with halogen-bridging. In some cases, the octahedra in the latter type may be distorted, as is usually observed in the copper(II) complexes. The MX_2L_4 complexes have monomeric trans-octahedral stereochemistry, with halogens above and below the ML_4 plane. The stereochemistries of MX_2L_2 and MX_2L_4 are indicated in Figure 6.1.

For those complexes, MX_2L_2, for which no structural data are available, the structural type has been taken to be the same as that of the corresponding $MX_2(py)_2$ complex. The metals Mn, Ni, Cu and Cd give polymeric octahedral MX_2L_2 complexes, whilst CoX_2L_2 may be either polymeric octahedral or tetrahedral. The tetrahedral structure of CoX_2L_2, where L is a 2-halogenopyridine, is due to steric effects.[59] A simple criterion for tetrahedral or octahedral CoX_2L_2 complexes, where X is Cl or Br, is that the former structure type is blue in colour and the latter type is violet. (The literature reports on the inferred stereochemistry of the MX_2L_n complexes are, in the main, the same references as for the preparations of these complexes. The latter references have been

Figure 6.1 Stereochemistries of MX_2L_2 and MX_2L_4 complexes

(a) MX_2L_2 complexes

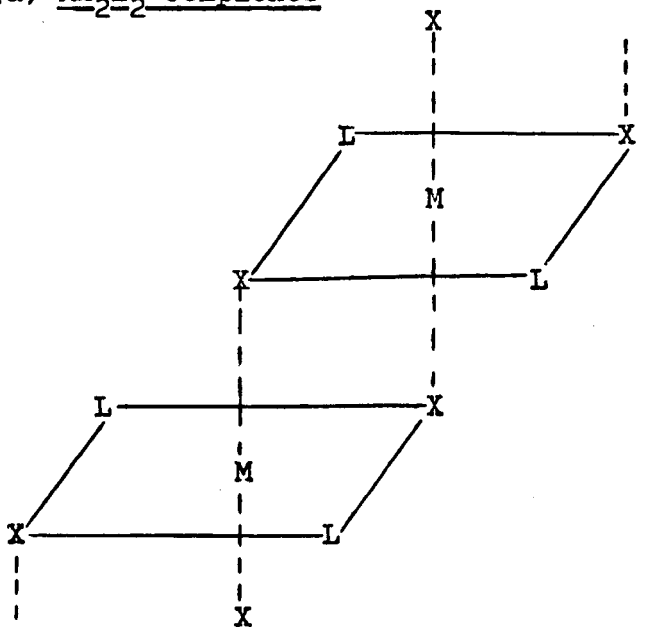

polymeric octahedral

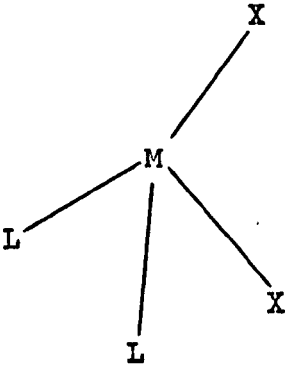

monomeric tetrahedral

(b) MX_2L_4 complexes

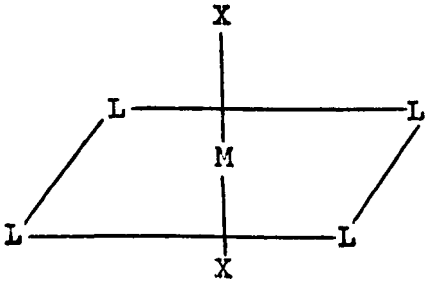

monomeric trans-octahedral

given in Chapter 4, Table 4.2.

6.2 The use of enthalpies of decomposition for the complexes MX_2L_n as a measure of the M - L bond strength

Earlier DSC work[25,60,82,83] on the heterocyclic metal complexes MX_2L_n, where L was pyridine, α , β or γ -picoline, quinoline, (methyl)pyrazine and aniline; n was 2 or 4; X was Cl, Br or I and M was a first-row transition-metal, used the assumption that the observed enthalpies of decomposition could be taken as a good guide to the gas phase heats of dissociation i.e. the difference between the heats of sublimation of MX_2 and MX_2L_2 (or MX_2 and MX_2L_4) was small and constant, irrespective of the nature of M, X and L. However, the experimental results for the heats of sublimation of the complexes studied here, Table 5.4, and data for the heats of sublimation of the metal dihalides,[41,42] indicate that these assumptions are not valid. Hence, the enthalpy of decomposition cannot be used as a measure of the gas phase dissociation reaction and, therefore, of the metal-ligand bond strength. This, unfortunately, means that although enthalpy of decomposition data have been evaluated for almost fifty MX_2L_2 and MX_2L_4 complexes, any further discussion must be limited to the eighteen complexes, mainly of the stoichiometry CoX_2L_2, for which experimental heats of sublimation, and, hence, $\bar{D}$(M - L) values were obtained.

6.3 The metal-ligand bond strength, as determined by the value of $\bar{D}(M - L)$

Before a detailed interpretation of the $\bar{D}(M - L)$ values is given, a further critical comment must be made concerning the heats of sublimation obtained for the complexes MX_2L_2. Whereas it is possible to interpret the sublimation of a tetrahedral, crystalline complex, MX_2L_2, as yielding a similar, possibly distorted, stereochemical species in the gas phase, it is obvious that the sublimation of a polymeric octahedral complex, MX_2L_2, must involve a large reorganisation of stereochemistry, after the initial breakage of halogen-bridges. The assumption is made that all the MX_2L_2 complexes, for which heat of sublimation data have been reported in this thesis, give monomeric gaseous species of the same stereochemical type, irrespective of the nature of M, X or L. Also, there are no available data for the nature of the gaseous species arising from the sublimation of the metal dihalides thenselves. It is assumed that the gaseous species, derived from the metal dihalides, is monomeric. If these assumptions are valid, then the values of $\bar{D}(M - L)$ for the complexes MX_2L_2 may be directly compared, since in each case $\bar{D}(M - L)$ refers to the following reaction.

$$MX_2L_2\ (g) \xrightarrow{2\bar{D}(M - L)} MX_2\ (g) + 2L\ (g)$$

Table 6.1 gives the $\bar{D}(M - L)$ values for the complexes MX_2L_2. (More detailed data have been given in Table 5.4). From the data in Table 6.1, the following observations may be made.

Table 6.1 The $\bar{D}$(M - L) values for the heterocyclic metal complexes, MX_2L_2

Complex	$\bar{D}$(M - L)[a] kcal mol^{-1}
(a) $CoCl_2L_2$ complexes	
L = 2MeBT	33.4 ± 0.7
L = 2MeBO	*34.5 ± 0.7
L = 25DiMeBO	*35.3 ± 1.0
L = 3Clpy	**32.7 ± 0.9
L = 3Brpy	34.9 ± 0.9
L = 2Mepy	**30.8 ± 0.9
L = 2Clpy	**29.7 ± 1.1
L = 2Brpy	28.7 ± 0.9
(b) $CoBr_2L_2$ complexes	
L = BT	30.8 ± 1.2
L = 2MeBT	32.0 ± 1.2
L = 2MeBO	*32.3 ± 1.4
L = 25DiMeBO	*30.6 ± 1.5
L = 2Mepy	**28.8 ± 1.2
L = 2Brpy	29.9 ± 1.0

a These $\bar{D}$(M - L) values are taken from Table 5.4.

* These $\bar{D}$(M - L) values refer to oxygen-bonded ligands; all the other $\bar{D}$(M - L) values refer to nitrogen-bonded ligands.

** These $\bar{D}$(M - L) values are minimum values.

Table 6.1 (cont.) The $\bar{D}(M - L)$ values for the heterocyclic metal complexes, MX_2L_2

Complex	$\bar{D}(M - L)$[a] kcal mol^{-1}
(c) $NiCl_2L_2$ complexes	
L = 3Clpy	37.8 ± 1.2
L = 3Brpy	37.9 ± 1.4
(d) $CuCl_2L_2$ complexes	
L = 3Clpy	36.5 ± 1.4
L = 3Brpy	34.2 ± 1.9

a These $\bar{D}(M - L)$ values are taken from Table 5.4 and refer to nitrogen-bonded ligands.

(1) The $\bar{D}$(Co - L) values of the $CoCl_2L_2$ complexes are within the approximate range of 35 ± 1 to 29 ± 1 kcal mol^{-1}. The higher $\bar{D}$(Co - L) values are observed for the complexes of the azole and 3-halogenopyridine ligands, whilst $CoCl_2(2Brpy)_2$ gives the lowest $\bar{D}$(Co - L) value.

(2) The $\bar{D}$(Co - L) values of the $CoBr_2L_2$ complexes are very similar, the approximate range of $\bar{D}$(Co - L) values being only 32 ± 1 to 29 ± 1 kcal mol^{-1}.

(3) The $\bar{D}$(Co - L) values for analogous CoX_2L_2 complexes, where X is Cl or Br, are the same, within experimental error, except for the case of the complexes of 2,5-dimethylbenzoxazole, where $\bar{D}$(Co - L) for the chloro complex is significantly greater than for the bromo complex.

(4) For both the $CoCl_2L_2$ and $CoBr_2L_2$ complexes, the values of $\bar{D}$(Co - L), where L is an oxygen-bonded azole, are very similar to the $\bar{D}$(Co - L) values, where L is a nitrogen-bonded azole.

(5) For MCl_2L_2, where L is a 3-halogenopyridine, the $\bar{D}$(M - L) values are in the orders Ni $\simeq$ Cu > Co for L = 3-chloropyridine, and Ni > Cu $\simeq$ Co for L = 3-bromopyridine.

It would be of interest to compare these experimentally obtained $\bar{D}$(M - L) values with those of the corresponding pyridine complexes. Unfortunately, α-$CoCl_2(py)_2$ did not give satisfactory results when the determination of its heat of sublimation was attempted by the thermogravimetric method described in Chapter 3.

However, it is possible to obtain an estimate for the heats of sublimation of β-$CoCl_2(py)_2$ and $CoBr_2(py)_2$, and of α-$CoCl_2(py)_2$ and $NiCl_2(py)_2$ in the following way. The assumption is made that the heat of sublimation of tetrahedral complexes, CoX_2L_2, where X is Cl or Br, is directly proportional to the molecular weight of the complex. Figure 6.2 shows a graph of the heat of sublimation of tetrahedral CoX_2L_2 complexes against the molecular weight. It has been assumed that the origin must be a point on this plot, although the extrapolation to this point is hypothetical. Data for the graph have been taken from Table 5.4.

The estimated values for the heats of sublimation of β-$CoCl_2(py)_2$ and $CoBr_2(py)_2$ are 16 and 21 kcal mol^{-1}, respectively. The use of such a graph to estimate heats of sublimation for MX_2L_2 must incur large errors on the values obtained. It is suggested that the error on these estimated heat of sublimation values be of the order of $\pm$ 3 kcal mol^{-1}. The heat of sublimation of $CoCl_2(an)_2$ can also be estimated as 17 $\pm$ 3 kcal mol^{-1}. This value for $CoCl_2(an)_2$ is in agreement with that proposed by Ablov and Konunova[84] of 14 kcal mol^{-1}, obtained by the application of Trouton's Rule to the boiling points of organometallic compounds of the same molecular weight.

A similar plot (Figure 6.3) for the octahedral complexes MCl_2L_2, where M is Co or Ni, yields a value of 13 $\pm$ 3 kcal mol^{-1} for the heat of sublimation of both α-$CoCl_2(py)_2$ and $NiCl_2(py)_2$, which have the same molecular weight.

Figure 6.2. Graph of ΔH_{sub} against the molecular weight for the tetrahedral complexes, CoX_2L_2, X = Cl or Br

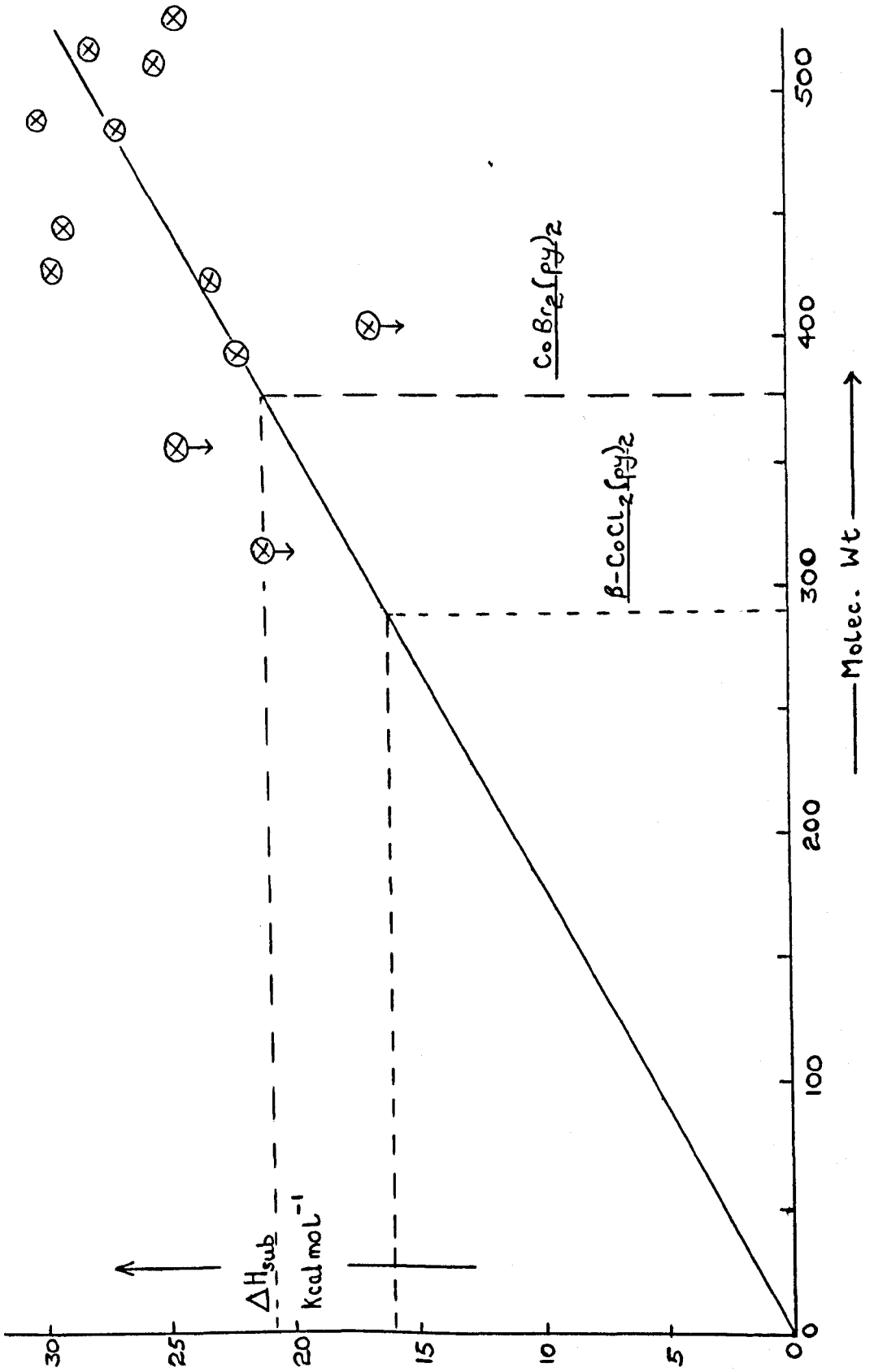

Figure 6.3. Graph of ΔH_{sub} against the molecular weight for the octahedral complexes, $NiCl_2L_2$ and $CoCl_2L_2$

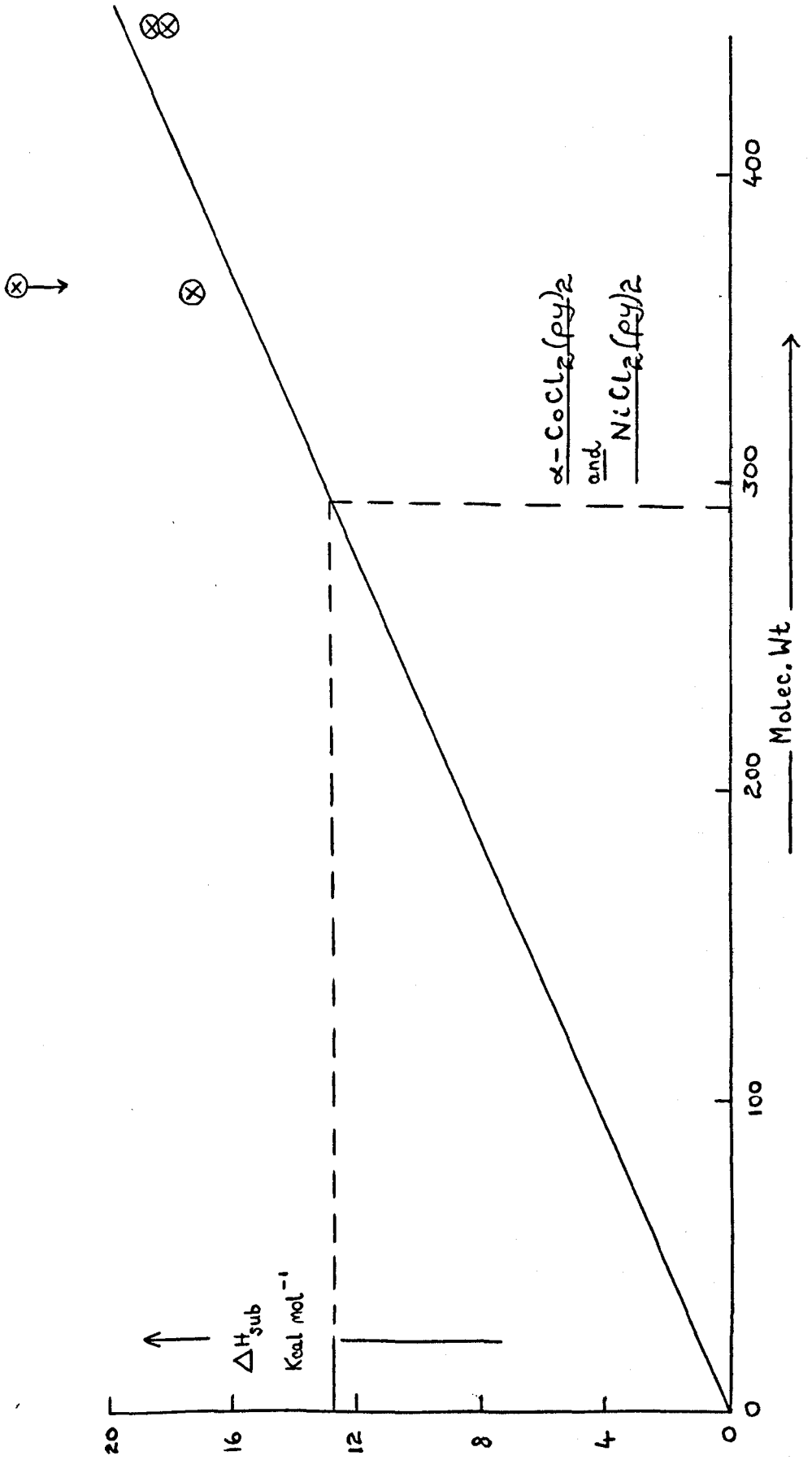

The calculation of the $\bar{D}$(M - py) values, using these estimated heats of sublimation, the heats of sublimation of the metal dihalides[41,42] and earlier DSC data for the enthalpies of decomposition[25,83] of α-$CoCl_2(py)_2$, β-$CoCl_2(py)_2$, $NiCl_2(py)_2$ and $CoBr_2(py)_2$, leads to the following $\bar{D}$(M - py) values.

Complex	$\bar{D}$(M - py) / kcal mol^{-1}
α-$CoCl_2(py)_2$	38 ± 2
β-$CoCl_2(py)_2$	34 ± 2
$CoBr_2(py)_2$	30 ± 3
$NiCl_2(py)_2$	40 ± 2

The main points that arise from these estimated $\bar{D}$(M - py) values are given below.

(1) The $\bar{D}$(Co - py) values derived from α-$CoCl_2(py)_2$ and β-$CoCl_2(py)_2$ are the same, within experimental error, as they should be, since $\bar{D}$(Co - py) refers to the same gas phase reaction in each case. A mean value for $\bar{D}$(Co - py) in $CoCl_2(py)_2$ may be taken as 36 ± 2 kcal mol^{-1}.

(2) The $\bar{D}$(Co - py) value for $CoCl_2(py)_2$ of 36 ± 2 kcal mol^{-1} is higher than that for $CoBr_2(py)_2$ of 30 ± 3 kcal mol^{-1}.

(3) The $\bar{D}$(M - py) values for the complexes $MCl_2(py)_2$ are in the order M = Ni > Co.

The $\bar{D}$(M - L) values in Table 6.1 can now be compared with the estimated $\bar{D}$(M - py) values. Table 6.2 gives such a comparison.

Table 6.2 Comparison of the experimental $\bar{D}$(M - L) values for MX_2L_2 complexes with the estimated values for $\bar{D}$(M - py) of the corresponding $MX_2(py)_2$ complexes

Complex	$\bar{D}$(M - L) - $\bar{D}$(M - py) kcal mol^{-1}
(a) $CoCl_2L_2$ complexes	
L = 2MeBT	-3 ± 3
L = 2MeBO*	-2 ± 3
L = 25DiMeBO*	-1 ± 3
L = 3Clpy	-3 ± 3**
L = 3Brpy	-1 ± 3
L = 2Mepy	-5 ± 3**
L = 2Clpy	-6 ± 3**
L = 2Brpy	-7 ± 3
(b) $CoBr_2L_2$ complexes	
L = BT	+1 ± 4
L = 2MeBT	+2 ± 4
L = 2MeBO*	+2 ± 4
L = 25DiMeBO*	+1 ± 4
L = 2Mepy	-1 ± 4**
L = 2Brpy	0 ± 4
(c) $NiCl_2L_2$ complexes	
L = 3Clpy	-2 ± 3
L = 3Brpy	-2 ± 3

* These ligands are bonded via oxygen.

** $\bar{D}$(M - L) for these cases was a low estimate.

The following observations can be made.

(1) For the complexes $CoCl_2L_2$, the $\bar{D}$(Co - azole) values are the same, within experimental error, as $\bar{D}$(Co - py). However, $\bar{D}$(Co - 2Brpy) for $CoCl_2(2Brpy)_2$ is significantly less than $\bar{D}$(Co - py). The $\bar{D}$(Co - 3Brpy) value is the same as $\bar{D}$(Co - py). Similarly, $\bar{D}$(Co - 3Clpy) is likely to be at least the same as the $\bar{D}$(Co - py) value.

(2) For the complexes $CoBr_2L_2$, the $\bar{D}$(Co - azole) values are the same as $\bar{D}$(Co - py) of $CoBr_2(py)_2$. This is also the case for the $\bar{D}$(Co - 2Brpy) value.

(3) For the $NiCl_2L_2$ complexes, where L is a 3-halogenopyridine, $\bar{D}$(Ni - 3Clpy) and $\bar{D}$(Ni - 3Brpy) are the same as $\bar{D}$(Ni - py).

It would appear then that in the majority of cases the $\bar{D}$(M - azole) or $\bar{D}$(M - halogenopyridine) values are the same as the corresponding $\bar{D}$(M - py) values. This is the major observation which must be explained.

The $\bar{D}$(M - L) values are a measure of the total bond strength of the metal-ligand bond. Therefore, $\bar{D}$(M - L) measures the summation of both σ and π-bonding effects. The reasons for the similarity of the $\bar{D}$(M - azole), $\bar{D}$(M - halogenopyridine) and $\bar{D}$(M - pyridine) values can be discussed in terms of the relative contributions of σ and π-bonding effects in the complexes MX_2L_2.

6.4 The strength of the σ-bonding component in the metal-ligand bond

The basicities of the ligands, as judged by their pK_a values, are a measure of their affinity for a proton, in aqueous solution. However, we might expect the pK_a to be an indication of the strength of the σ-bonds between the ligand donor atom and the metal ion in the gas phase. The pK_a data that are available are given in Table 6.3. These data indicate that the azole ligands, with the exception of imidazole, are very much less basic than pyridine. The pK_a values for oxazole and the benzoxazoles are not available in the literature. They are concluded to be very low, since oxazole does not give any picrate complexes, whilst benzoxazole and its 2-methyl derivative decompose in aqueous solution. A pK_a value of $\simeq 2.3$ may be estimated for 2-methylbenzothiazole by analogy to the pK_a values of pyrazole and 3(5)-methylpyrazole. The pK_a of 2-bromopyridine does not appear to have been documented.

It is apparent from the pK_a values of Table 6.3 that changes in σ-bond strength alone cannot account for the similarity observed between the $\bar{D}(M - L)$ values. The pK_a values would suggest, if σ-bonding effects only are operative, that $\bar{D}(M - azole)$ and $\bar{D}(M - halogenopyridine)$ should be significantly less than the $\bar{D}(M - py)$ value for analogous MX_2L_2 complexes.

It would, therefore, appear that some other factor gives rise to the observed independence of $\bar{D}(M - L)$ with the nature of L. It is not likely that the low σ-donor ability of the azoles and halogenopyridine pyridines is compensated by a closer approach of

Table 6.3 The basicities of the heterocyclic ligands, L

Ligand	pK_a	Reference
imidazole	7.0	85
2-methylpyridine	6.0	86
pyridine	5.2	86
3(5)-methylpyrazole	3.6	85
3-bromopyridine	2.9	59
3-chloropyridine	2.8	86
thiazole	2.5	85
pyrazole	2.5	85
2-methylbenzothiazole	2.3	(estimated)
benzothiazole	1.2	85
2-chloropyridine	0.7	86

the ligand donor atom to the metal ion in these complexes, MX_2L_2. The factors influencing the degree of π-bonding in these complexes must, therefore, also be considered.

6.5 The strength of the π-bonding component in the metal-ligand bond

The kind of π-bonding that is envisaged in these complexes is of the $d - \pi^*_\pi$ type.[87] This involves the transfer of electron density from a filled metal d-orbital, or a suitable dp-hybrid, to an empty anti-bonding π-orbital of the ligand. The occurrence of such π-bonding in carbonyl complexes is supported by considerable evidence. However, the extent of π-bonding in metal complexes of heterocyclic ligands has been the subject of much debate.

Several groups of workers have invoked π-bonding to explain experimental results for metal-heterocyclic amine complexes. Nelson and Shepherd[88] have interpreted the electronic spectra of some NiX_2L_4 complexes, where L is isoquinoline, pyridine or methylpyridine in terms of the π-acceptor order of the amine L given below.

isoquinoline > 4-methylpyridine $\simeq$ pyridine > 3-methylpyridine

Lever et al.[89] have carried out a similar analysis of the electronic spectra of some NiX_2L_2 complexes, where L is an amine. The derived effective crystal field splitting energy (10Dq') of the amine was frequently greater in the bromo than in the chloro

complexes, and the ratio 10Dq' (bromide) : 10Dq' (chloride) was correlated with the expected relative degree of metal→amine π-bonding. They proposed the following order of π-acceptor ability for the amine L :

methylpyrazine > isoquinoline ≃ pyridine ≃ 4-methylpyridine > 3-methylpyridine

Thermodynamic evidence for a moderate degree of π-bonding in the six-coordinate cobalt-pyridine complexes, $CoX_2(py)_4$, has been reported by King et al..[90,91] They also found that the extent of metal→pyridine π-bonding was in the order X = I > Br > Cl. Wong and Brewer[92] have interpreted the coordination bond in metal complexes of the 4-substituted pyridines in terms of both σ and π-bonding and have measured the relative degree of π-bonding as the substituent is varied. Cabral et al.[93] have studied the relative stabilities of some tetrahedral, CoX_2L_2, and octahedral, CoX_2L_4, complexes. They interpreted their results in terms of the variations in the π-acceptor properties of the amines L, which were found to be in the following order:

isoquinoline > pyridine ≥ 4-alkylpyridine > 3-alkylpyridine

It would, therefore, appear that the same order of π-acceptor ability for isoquinoline, pyridine and the alkylpyridines has been reached by the application of a number of different techniques.

Gill et al.[94] have studied the IR spectra of pyridine coordinated to a variety of metals and non-metals and free pyridine. Only very small changes in some of the vibrational frequencies are observed for the pyridine molecule on coordination. They concluded that the electron density over the pyridine ring remains constant, whatever the acceptor atom, and attributed this to a degree of π-bonding in these complexes. This would be in agreement with the great stability of α, α'-dipyridyl and ortho-phenanthroline complexes, which is also believed to be due to similar back-coordination.[95,96]

Thus, it can be concluded that the "σ-bonding only" concept for the metal-heterocyclic ligand bond is not sufficient to explain the experimental data obtained by several groups of workers. Pettit[87] has reasoned that, "since the evidence for back-coordination from metal to benzene systems is considerable and broad-based, metal to pyridine back-bonding must be highly reasonable." It is very probable that the true extent of π-bonding has been over-rated, however, and that in metal-pyridine complexes, at least, the extent will be small. That this is the case can be shown by the following two observations.

(1) The IR data[97] for some substituted molybdenum carbonyl complexes are given in Table 6.4. The carbonyl molecule is increasingly better at competing with the trans ligand for π-electron density from the metal as the series is traversed from the good π-acceptor, phosphorus trichloride, to diethylene-triamine, dien, which can only form σ-bonds with the metal atom.

Table 6.4 Stretching frequencies of the carbonyl group in some molybdenum complexes*

Complex	ν_{CO} cm^{-1}
$(PCl_3)_3Mo(CO)_3$	1989, 2041
$(PhPCl_2)_3Mo(CO)_3$	1943, 2016
$(Ph_2PCl)_3Mo(CO)_3$	1885, 1977
$(Ph_3P)_3Mo(CO)_3$	1835, 1949
$(py)_3Mo(CO)_3$	1746, 1888
(dien)$Mo(CO)_3$ **	1723, 1883

* These IR data are taken from reference 97.

** (dien) is diethylenetriamine

(2) One might also expect, if π-bonding from metal to pyridine were of a significant extent, that the choice of stereochemical configuration in complexes such as $M(acac)_2(py)_2$, where (acac) is the acetylacetonate anion, would be in favour of a structure where metal to pyridine π-bonding was maximised. The structure would, therefore, be one in which the pyridine molecules were staggered. This structure is found for $Co(acac)_2(py)_2$,[98] but $Ni(acac)_2(py)_2$[99] contains eclipsed pyridine molecules. Hence, packing effects in the crystal are responsible for the choice of configuration and not π-bonding effects.

Therefore, it is concluded that metal→pyridine π-bonding is possible, but that it does not make any great contribution to the bonding. However, it is shown, in the following sections, that the extent of π-bonding between metal and the halogeno-pyridines and between metal and the azole ligands will be greater than that between metal and pyridine itself.

6.5.1 The strength of the metal to ligand π-bonding in metal-azole complexes, relative to that in metal-pyridine complexes

The azole ligands, with the exception of imidazole, are likely to be better π-acceptors than pyridine. This can be shown by initially considering the electron density distributions[100] in pyridine itself and in the five-membered heterocycle, pyrrole. (It is a simple step to consider the electron density distributions in the oxazole, thiazole and pyrazole molecules

from that in the pyrrole molecule.) The resonance canonicals contributing to the overall resonance hybrids for pyridine and pyrrole are shown in Figures 6.4 and 6.5. Similar canonicals to those for pyrrole may be envisaged for furan and thiophene. Thiophene is the most aromatic of these three heterocycles and furan the least aromatic, because of the relative contributions of the charged canonicals.

It is seen from Figures 6.4 and 6.5 that the typical reaction of the pyridine molecule will be nucleophilic reactions at the ring carbon atoms, while the five-membered heterocycles will undergo electrophilic reactions at the ring carbon atoms. The introduction of an imino-nitrogen, =N– , to replace one of the =CH– groups of pyrrole, thiophene and furan to give imidazole or pyrazole, thiazole and oxazole, respectively, leads to heterocyclic compounds which take part in a variety of reactions typical of both the pyrrole and pyridine types of heterocycles. Oxazole, as expected, is the least aromatic of the simple azoles and thiazole resembles pyridine rather than pyrrole.

We have taken the pK_a values of the ligands as a measure of the σ-bond strength to a metal ion. Another measure of this is the ability of these heterocyclic ligands to participate in electrophilic reactions, since the positively charged metal ion can be considered as an electrophile. Similarly, the ability of the ligand to undergo nucleophilic attack is a measure of its π-acceptor ability.

In these five-membered heterocycles containing two hetero-atoms, there is a balance between the mesomeric effect, which would increase the electron density on the nitrogen atom and,

Figure 6.4 The resonance canonicals of the pyridine molecule

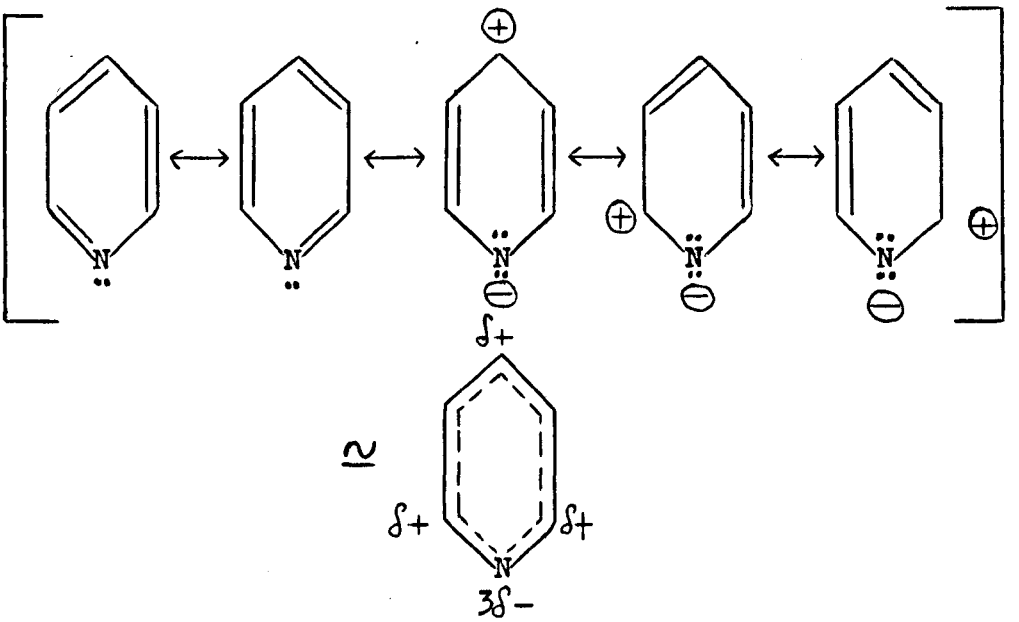

Figure 6.5 The resonance canonicals of the pyrrole molecule

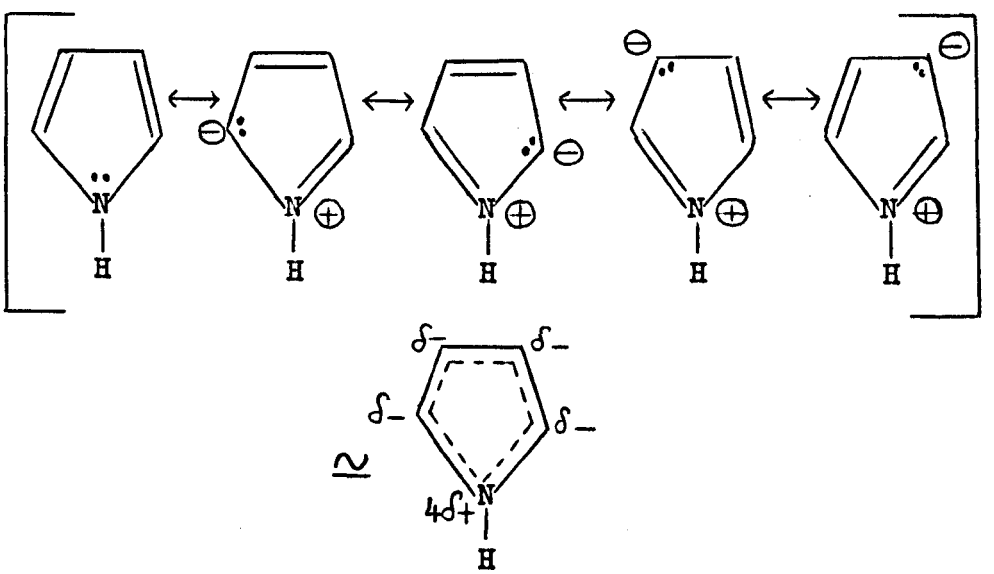

hence, increase the pK_a value, and the inductive electron-withdrawing effect, which would tend to decrease the pK_a value, c.f. the pK_a values of NH_3, N_2H_4, NH_2OH are 9.5, 8.0 and 6.0, respectively.[86]

The mesomeric effect in these five-membered heterocycles

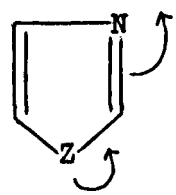

Z = NH imidazole

Z = S thiazole

Z = O oxazole

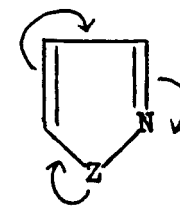

Z = NH pyrazole

If both heteroatoms are nitrogen, the mesomeric effect appears to predominate when they are in the 1 : 3 positions.[86] However, the inductive effect predominates when they are in the 1 : 2 positions. The pK_a value of imidazole is 7.0 and that of pyrazole is 2.5. When Z is oxygen or sulphur the inductive, base-weakening effect increases and the pK_a values are 2.5 and $\simeq 0$. The increased importance of the inductive electron-withdrawal by the other heteroatom causes nucleophilic attack on the uncharged ligands to occur under milder conditions than in the pyridines.[86] On this evidence one might expect, therefore, that the order of π-acceptor ability would be as follows:

oxazole > thiazole > pyridine

and

pyrazole > pyridine > imidazole

A similar argument has been applied to the question of the π-acceptor capacity of the ligand pyrazine. (Pyrazine is the ligand 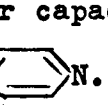 .) It has been inferred in several cases[86,89,101] that pyrazine would be a better π-acceptor than pyridine in the complexes MX_2L_2. This is consistent with the low pK_a of pyrazine (0.4),[86] due to the electron-withdrawal effect of the second nitrogen heteroatom, relative to the pK_a of pyridine (5.2) and the increased ease of nucleophilic attack in pyrazines[86,102] because of this inductive effect. Indeed reagents which only react with quaternised pyridine derivatives will sometimes react with diazines like pyrazine.[86]

Since quinoline undergoes nucleophilic attack rather more easily than pyridine[86], and isoquinoline appears to be a rather better π-acceptor than pyridine,[88] we can infer that benzothiazole and benzoxazole will be better at encouraging metal to ligand π-bonding than their corresponding non-annelated derivatives.

Evidence in support of the conclusion that imidazole is a rather poorer π-acceptor than pyridine is found in some work by Epstein et al.[103] on the Mössbauer spectra of some porphyrin complexes of pyridine, piperidine and imidazole. Further evidence for the proposed orders of π-acceptor behaviour is found in the stoichiometries of the metal dihalide complexes, MX_2L_n, usually formed with these ligands. The greater the basic strength of the ligand, then the greater the net build-up of charge on the metal ion. Because halide ions have strong donor properties, the formation of MX_2L_4 is not so favourable as the formation of $\left[ML_6\right]^{++}2X^-$.[63] Increasing the π-acceptor properties and

decreasing the pK_a value increases the stabilisation of complexes where halide is coordinated. Thus, the maximum ligated copper complexes with imidazole, benzimidazole, 2-methylimidazole and ammonia are $CuCl_2L_4$, whereas pyridine, thiazole, alkylthiazoles and benzothiazole form predominantly $CuCl_2L_2$.[65] (The thiazoles, being weaker σ-donors and better π-acceptors than the imidazoles, will favour structures in which four halides (MX_2L_2) rather than four heterocyclic bases (MX_2L_4) are coordinated.) Hughes and Rutt[64] and Eilbeck et al.[63] agree with the position of thiazole as a good π-acceptor.

It is, therefore, suggested that with the exception of imidazole the azole ligands are rather better π-acceptors than pyridine. This compensates for their poorer σ-bonding ability. Although the degree of π-bonding in the metal-azole bond will still probably be small, it can increase the ligand to metal σ-bonding synergically. This gives rise to the similarity in metal-ligand bond strength for analogous MX_2L_2 complexes, where L is an azole or pyridine. Although definite orders of π-acceptor ability for the azole ligands have been suggested, the thermochemical data for $\bar{D}$(M - azole) are not sufficiently precise to allow any conclusion to be made about the relative degree of π-bonding in the metal-azole bonds.

The similarity between the $\bar{D}$(M - L) values, where L is a 3-halogenopyridine, and the $\bar{D}$(M - py) values, indicated in Table 6.2, can now also be explained in a similar way.

6.5.2 The strength of the metal to ligand π-bonding in the metal-halogenopyridine complexes, relative to that in metal-pyridine complexes

The ease of electrophilic attack by a positively charged metal ion at the nitrogen atom of pyridine will depend on the electron density on that atom. Strongly electron-withdrawing substituents will make such reactions more difficult and, since the effect is largely inductive, the effect will be greatest for such substituents in the 2-position. Thus, the pK_a values for the halogenopyridines will be in the order given below. Strongly

pK_a increasing $\longrightarrow$

2Clpy < 2Brpy < 3Clpy < 3Brpy < py

0.7 5.2

electron-donating substituents make electrophilic attack at the nitrogen atom easier. This is due to the mesomeric effect and is therefore of larger influence when the substituent is in the 2 or 4 position. Methyl and phenyl groups have little effect on the pK_a values; on the whole the pK_a values are increased slightly.

The ease of nucleophilic attack, which can be taken as a measure of the π-acceptor ability, will be aided by the presence of electron-withdrawing substituents. Therefore, it can be concluded that the approximate order of π-acceptor ability will be as follows.

halogenopyridines > pyridine > alkyl and phenylpyridines

Methylpyridines have positive inductive effects and mesomeric effects, which accounts for their decreased π-acceptor nature.[59]

Cabral et al.[93] have interpreted some stability constants in chloroform in terms of this. Halogenopyridines have negative inductive effects and positive mesomeric effects. (See Figure 6.6.) Since the inductive effect appears to predominate, in that the pK_a values are lower than that of pyridine, this increases their π-acceptor ability relative to that of pyridine. On this basis we might infer that the order of π-acceptor ability of the chloropyridines would be as follows.

2Clpy > 3Clpy > 4Clpy > py

However, we must also consider not only the overall charge density on the pyridine ring, but also how this charge is distributed.[93] The occurrence of π-bonding will localise charge principally on the 2, 4 and 6 positions.[88] (See Figure 6.6.) Thus, any substituent such as 3-alkyl or 3-halogeno which directs π-electron density onto these positions via positive mesomeric effects will inhibit π-bonding. (This is supported by the observation that the 3-halogenopyridines are less reactive to nucleophilic substitution[86] than the 2 and 4 isomers.) Alkyl substituents in the 2 or 4 position direct charge mainly onto the 1, 3 and 5 positions. Hence, π-bonding is not inhibited to the same degree.[88,93] Thus, the predicted orders of π-acceptor ability are as given below.

chloropyridine > bromopyridine > pyridine

4Clpy $\simeq$ 2Clpy > 3Clpy > py

py > 4-alkylpy $\simeq$ 2-alkylpy > 3-alkylpy[88]

Figure 6.6 Electronic effects in the halogenopyridines

(a) Inductive effect

(b) Mesomeric effect

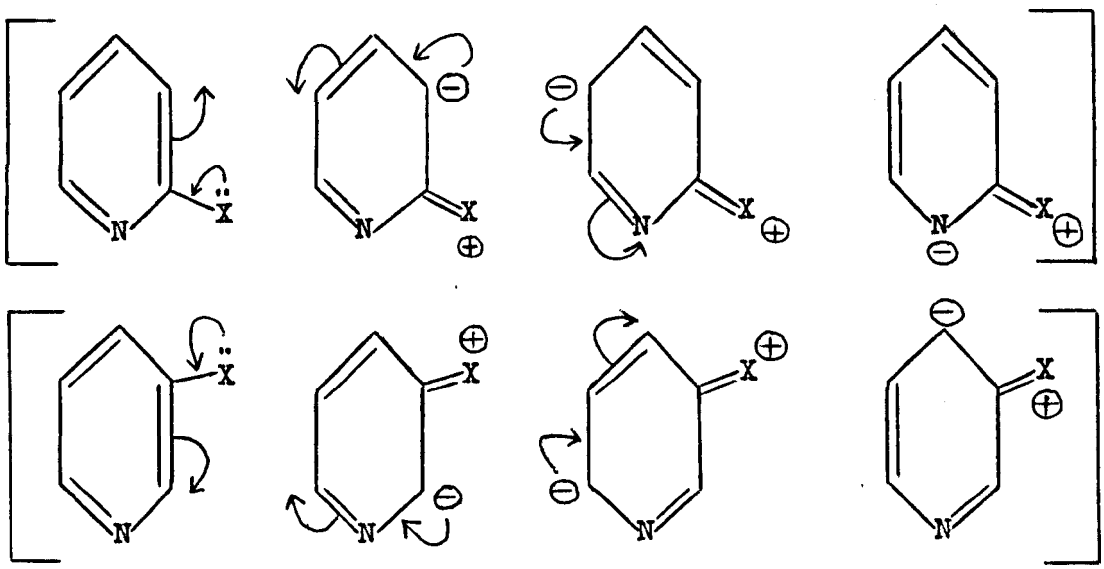

(c) Metal to (halogeno)pyridine π-bonding

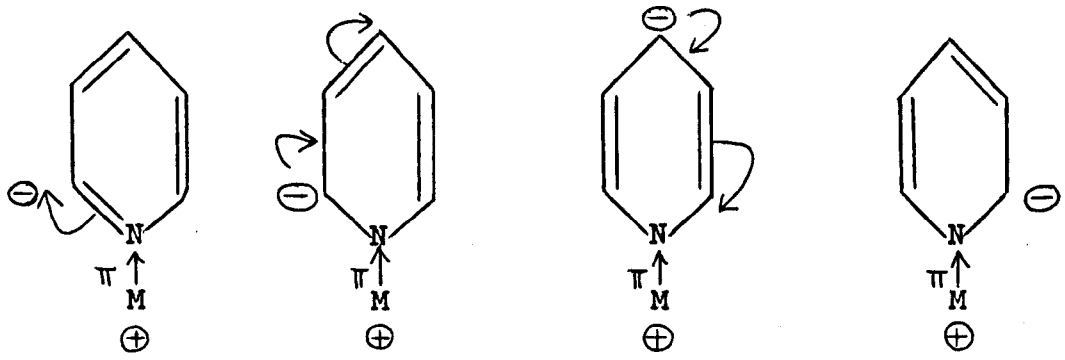

The similarity of the $\bar{D}$(M - 3Clpy) and $\bar{D}$(M - 3Brpy) values with the corresponding $\bar{D}$(M - py) value, where M is Co, Ni, is, therefore, explained by the lower σ-bonding ability of the 3-halogenopyridines, relative to pyridine, being compensated by their greater π-acceptor capacity. On the grounds of the proposed orders of π-acceptor ability, the $\bar{D}$(M - 2halogeno-pyridine) values should also be at least the same as $\bar{D}$(M - py). However, the situation for the 2-substituted pyridine complexes is complicated by the additional factor of steric effects. This is shown, for example, by the heats of reaction of pyridine, 2-methylpyridine and 2,6-dimethylpyridine with boron trifluoride, which are 32.9, 31.2 and 25.4 kcal mol^{-1}, respectively.[104] The steric effect is also manifested in the tetrahedral structures, in the crystalline state, for the cobalt dihalide complexes of the 2-halogenopyridines and the 2-alkylpyridines.[59] The existence of the steric effect would seem to explain the observation that $\bar{D}$(Co - 2Brpy) for $CoCl_2(2Brpy)_2$ is significantly less than $\bar{D}$(Co - py) of $CoCl_2(py)_2$.

For the ligands where bonding occurs via the nitrogen atom i.e. (benzo)thiazole, pyrazole, imidazole and (substituted)pyridine, we might expect the position in the spectrochemical series to be approximately the same. However, the series is sensitive to π-bonding effects,[105] since ligands that are good π-acceptors are usually placed high in the series. Although the evidence that is available is fragmentary, it is consistent with the proposed orders of π-acceptor ability.

Taylor and Underhill[106] have suggested, from data for the ligand field splitting parameter, 10Dq, for some NiX_2L_4 complexes, that pyridine comes higher in the spectrochemical series than imidazole. Reedjik[53] has deduced that pyrazole is higher in the series than imidazole. No data are available for the position of benzothiazole or its derivatives in the spectrochemical series. However, data reported by Billing and Underhill[59] imply that 3-bromopyridine is rather higher in the series than pyridine, whilst McWhinnie[68] merely concludes that 2-chloropyridine and 2-bromopyridine have similar ligand field strengths.

It might be anticipated that the values of the metal-nitrogen stretching frequencies, ν_{M-N}, for those complexes that contain nitrogen-bonded ligands might be a good guide to the metal-ligand bond strength. There is an abundance of data on the values of ν_{M-N}. Ferraro[107] has reviewed such data for a variety of complexes. However, ν_{M-N} values are not a good guide to the prediction of $\bar{D}(M - L)$ values, and no simple relationship with the pK_a values of the ligands is found. The effect of the ligand mass on ν_{M-N} is difficult to dissect out.

Thus, the similarity of the experimental $\bar{D}(M - L)$ values with the estimated $\bar{D}(M - py)$ values, for analogous MX_2L_2 and $MX_2(py)_2$ complexes, where L is an azole or halogenopyridine, can be explained in terms of the relative contributions of σ and π-bonding to the metal-ligand bond. The metal-pyridine bond has a high σ-bonding contribution, whilst the metal-halogenopyridine and metal-azole bonds have a rather lower σ-bonding contribution but a greater π-bonding contribution.

7 ANALYTICAL AND THERMOCHEMICAL DATA FOR THE DECOMPOSITION OF THE OLEFINIC AND ACETYLENIC COMPLEXES

The decomposition of the iridium(I) and platinum(II) olefinic and acetylenic complexes was found to occur in a single stage denoted by the equations given below.

$$IrX(CO)(PPh_3)_2.L\ (c) \longrightarrow trans\text{-}IrX(CO)(PPh_3)_2\ (c) + L\ (g)$$

X = F, Cl, Br or I; L = C_2F_4, C_4F_6 and $CH_2CH(CN)$ (X = F, Cl and Br only)

or

$$PtXMeZ_2.L\ (c) \longrightarrow trans\text{-}PtXMeZ_2\ (c) + L\ (g)$$

X = Cl or Br; L = C_2F_4 or C_4F_6 ; Z = $AsMe_3$ and $AsMe_2Ph$ (L = C_4F_6 only)

The enthalpies of decomposition, ΔH_{dec}, are given in Tables 7.1 and 7.2 for the iridium(I) and platinum(II) fluorocarbon complexes respectively. These Tables show that the platinum complexes decompose in the temperature range 355 - 405°K, denoted by the T_p values, whilst the iridium fluorocarbon complexes decompose at slightly higher temperatures, between 430 and 480°K. The acrylonitrile complexes of iridium, for which temperature and weight loss data are also included in Table 7.1, decompose relatively near room temperature over the interval 330 to 385°K.

The weight loss percentage on decomposition for the C_2F_4 and C_4F_6 complexes provided a further check on the purity of these complexes. For the iridium complexes, the stretching frequency of the carbonyl group, ν_{CO}, in the adduct and the residual product

after thermal decomposition, was determined on a Perkin-Elmer 337 grating infra-red spectrometer. All the infra-red spectra were recorded for samples in a nujol mull. A film of polystyrene was used as a calibrating standard for the absorption wavenumber (cm^{-1}). With the spectrometer used, the wavenumbers obtained have a probable associated error of $\pm 3cm^{-1}$. In general, good agreement was found between the literature and observed values for ν_{CO}. Table 7.3 gives the infra-red data for the iridium(I) complexes of C_2F_4 and C_4F_6.

The acrylonitrile complexes of $IrCl(CO)(PPh_3)_2$ and $IrBr(CO)(PPh_3)_2$ were unstable at room temperature and the DSC work was done immediately after the preparation and initial IR spectrum had been completed. Hence, the stoichiometries of the prepared complexes were deduced from the percentage weight losses observed after decomposition. The calculated and observed weight losses for the decomposition of the acrylonitrile complexes of $IrX(CO)(PPh_3)_2$, where X is Cl or Br, are given in Table 7.1. For the chloro-acrylonitrile complex, the observed weight loss was used to calculate an effective molecular weight of 819.6, corresponding to the stoichiometry $IrCl(CO)(PPh_3)_2.0.74CH_2CH(CN)$. The high observed weight loss for the bromo-acrylonitrile complex was taken to imply the presence of further acrylonitrile as solvent. The effective stoichiometry was calculated to be $IrBr(CO)(PPh_3)_2.1.46CH_2CH(CN)$.

The acrylonitrile complex of $IrF(CO)(PPh_3)_2$ was found to be stable at room temperature. However, microanalysis data, given overleaf, indicated that only 0.7 moles of acrylonitrile were

coordinated per mole of $IrF(CO)(PPh_3)_2$. The high observed weight loss on decomposition was presumably due to the presence of

Microanalysis data for the fluoro-acrylonitrile complex

	C%	H%	N%
Observed	59.2	4.27	1.2
Calculated*	58.8	4.07	1.72
Calculated**	59.8	4.17	1.18

* Calculated for $IrF(CO)(PPh_3)_2.CH_2CH(CN)$

** Calculated for $IrF(CO)(PPh_3)_2.0.7CH_2CH(CN).0.4C_6H_6$

benzene, in which the complex had been prepared. The observed weight loss and microanalysis data together implied the stoichiometry $IrF(CO)(PPh_3)_2.0.7CH_2CH(CN).0.4C_6H_6$.

However, since none of the prepared acrylonitrile complexes of $IrX(CO)(PPh_3)_2$ had the stoichiometry $IrX(CO)(PPh_3)_2.CH_2CH(CN)$, no enthalpy data were calculated. Infra-red data for the prepared acrylonitrile complexes are given in Table 7.4. The greater stability of the fluoro-acrylonitrile complex is apparent from these data.

The complexes $IrCl(CO)(PPh_3)_2.C_2(CN)_4$ and $IrCl(CO)(PPh_3)_2.CH(CN)CH(CN)$ were also studied by the DSC method. However, both of these complexes showed no sign of decomposition until temperatures around 540°K, when complete breakdown of the complexes occurred, resulting in dark green/black residues.

No specific heat or heat of sublimation data were obtained for any of the iridium(I) or platinum(II) olefinic or acetylenic complexes.

Table 7.1 Enthalpies of decomposition, ΔH_{dec}, for $IrX(CO)(PPh_3)_2.L$

$$IrX(CO)(PPh_3)_2.L\ (c) \longrightarrow IrX(CO)(PPh_3)_2\ (c) + L\ (g)$$

Complex		ΔH_{dec}	T_i	T_p	T_f	Weight loss %	
L	X	kcal mol^{-1}		°K		obs.	calc.
C_4F_6	F	23.7 ± 0.1	410	450	500	17.5 ± 0.1	17.5
	Cl	22.9 ± 0.4	355	430	450	18.1 ± 0.7	17.2
	Br	18.8 ± 0.1	405	450	470	16.0 ± 0.2*	16.4
	I	19.7 ± 0.4	405**	430	440	16.3 ± 0.2	15.7
			440	480	490		
C_2F_4	F	19.0 ± 0.4	420	480	495	11.8 ± 0.2	11.6
	Cl	16.5 ± 0.3	385	445, 475	490	10.9 ± 0.6	11.4
	Br	9.8 ± 0.2	410	435, 470	480	11.3 ± 0.1	10.8
	I	13.7 ± 0.2	420	455, 470	480	10.9 ± 0.1	10.3
$CH_2CH(CN)$	F	-	350	385	410	8.0 ± 0.6	6.5
	Cl	-	310	335	345	4.8 ± 0.1	6.4
	Br	-	305	330	340	8.6 ± 0.7	6.1

* This is based on a sample from which benzene had been removed by heating to 390°K. The original sample contained 5.36% by weight of benzene.

** The observed weight loss for the first peak only is 3.25%, which corresponds to the loss of 0.2 moles of C_4F_6. The enthalpy for this peak is 3.29 ± 0.1 kcal mol^{-1}.

Table 7.2 Enthalpies of decomposition, ΔH_{dec}, for $PtXMeZ_2.L$

$$PtXMeZ_2.L\ (c) \longrightarrow PtXMeZ_2\ (c) + L\ (g)$$

Complex			ΔH_{dec}	T_i	T_p	T_f	Weight loss %	
Z	X	L	kcal mol^{-1}		°K		obs.	calc.
$AsMe_3$	Cl	C_2F_4	12.3 ± 0.1	355	380	390	17.0 ± 0.1	17.1
$AsMe_3$	Br	C_2F_4	11.5 ± 0.1	365	385	405	15.8 ± 0.1	15.9
$AsMe_3$	Cl	C_4F_6	16.4 ± 0.2	350	385	400	25.2 ± 0.1	25.0
$AsMe_3$	Br	C_4F_6	14.6 ± 0.2	345	385, 405	*410	23.5 ± 0.1	23.4
$AsMe_2Ph$	Cl	C_4F_6	17.6 ± 0.2	310	345, 370	**380	21.3 ± 0.3	21.0
$AsMe_2Ph$	Br	C_4F_6	19.2 ± 0.1	320	355	370	20.0 ± 0.4	19.9

* Two peaks were observed; the second was very small.

** Two quite distinct, although not completely separated peaks were observed. The enthalpy value corresponding to the first peak is $\simeq 8.3$ kcal mol^{-1}.

Table 7.3 Infra-red data for the iridium complexes, $IrX(CO)(PPh_3)_2.L$, where L is C_2F_4 or C_4F_6

		$IrX(CO)(PPh_3)_2.L$				$IrX(CO)(PPh_3)_2$*	
		ν_{CO} cm^{-1}		ν_{CC} cm^{-1}		ν_{CO} cm^{-1}	
X	L	obs.	lit.	obs.	lit.	obs.	lit.
F	C_2F_4	2029	---	---	---	1939, 1942	1944 [77]
F	C_4F_6	2007	---	1797	---		
Cl	C_2F_4	1995	2040 [108] (KBr)	---	---	1954, 1949	1960 [77]
Cl	C_4F_6	2022	2025 [108]	1773	1775 [108]		
Br	C_2F_4	2033	---	---	---	1951, 1953	1966 [76] ($CHCl_3$)
Br**	C_4F_6	1995	---	1763	---		
I	C_2F_4	2040	---	---	---	1955, 1953	1967 [76] ($CHCl_3$)
I[a]	C_4F_6	1994, 1984	---	1778	---		

* This is the residual parent complex, after decomposition on the DSC. All IR data in Table 7.3 refer to samples in a nujol mull, unless otherwise stated.

** The prepared complex was heated to 390°K to remove solvent.

a The IR data for this complex, after the removal of 0.2 moles of C_4F_6 at 440°K, were ν_{CO} 1997,1983; ν_{CC} 1775 cm^{-1}. No IR band corresponding to the parent complex was observed.

Table 7.4 Infra-red data for the acrylonitrile complexes of $IrX(CO)(PPh_3)_2$, where X is F, Cl or Br

acrylonitrile complex of $IrX(CO)(PPh_3)_2$*	ν_{CO} cm^{-1}				
	initial complex		complex after 24 hrs	residue after DSC work	
X	obs.	lit.		obs.	lit.
F	2010, 1947 [a]	2008 [77]	no change	1946	1944 [77]
Cl	2020	2017 [75]	2016, 1948 [b]	1952	1960 [77]
Br	2019	----	2020, 1950 [b]	1954	1966 [76] ($CHCl_3$)

* None of the complexes had the exact stoichiometry, $IrX(CO)(PPh_3)_2.CH_2CH(CN)$. The stoichiometries of the complexes are given in the text. All IR data in Table 7.4 refer to samples in nujol mulls, except where stated otherwise.

a The figure of 1947 cm^{-1} indicates the presence of a trace of the parent complex.

b The chloro and bromo acrylonitrile complexes decompose on standing in air at room temperature. The parent peak is the major one.

8 DISCUSSION OF THE THERMOCHEMICAL DATA FOR THE OLEFINIC AND ACETYLENIC METAL COMPLEXES, $MXYZ_2.L$

Very few thermochemical data are available for the strength of π-bonds between carbon and the platinum metals, although compounds containing such bonds are likely to be formed during catalytic processes. Barnes and Pettit[109] have reviewed the available information about the stability and structure of olefin and acetylene complexes of the transition metals. Hartley[110,111] has collated thermodynamic data for such complexes, but the data refer, in the main, to complexes in solution.

In Chapter 7, the enthalpies of decomposition of some olefinic and acetylenic complexes of Ir(I) and Pt(II) were reported. In the present chapter, these decomposition enthalpies are discussed in the light of the available information on the structure and bonding in these complexes.

8.1 The platinum(II) complexes, $PtXMeZ_2.L$

The catalytic polymerisation of unsaturated organic compounds by transition-metal complexes is believed to proceed by a series of reactions involving complex formation followed by insertion,

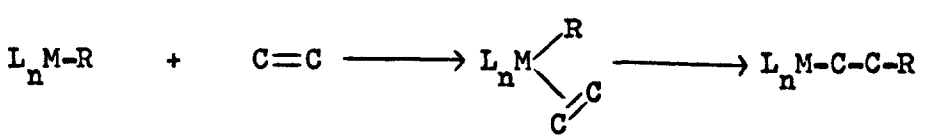

1 2

where R is a σ-bonded organic group. However, only rarely[112] have either the intermediate complex (1) or the product of a single

insertion (2) been isolated. Clark and Puddephatt[78-80] have reported the preparation of complexes of type (1) by the action of C_2F_4 and C_4F_6 on some methyl-platinum(II) complexes. In some cases, rearrangement of such complexes gave the insertion products of type (2). The platinum complexes studied here, $PtXMeZ_2.L$, are the intermediates formed during the insertion reaction of C_2F_4 and C_4F_6 with the platinum-carbon bond of methyl-platinum complexes of the type trans-$PtXMeZ_2$. Clark and Puddephatt[78,79] observed that the rate of insertion of these methyl-platinum complexes was dependent on the stability of the intermediate complex.

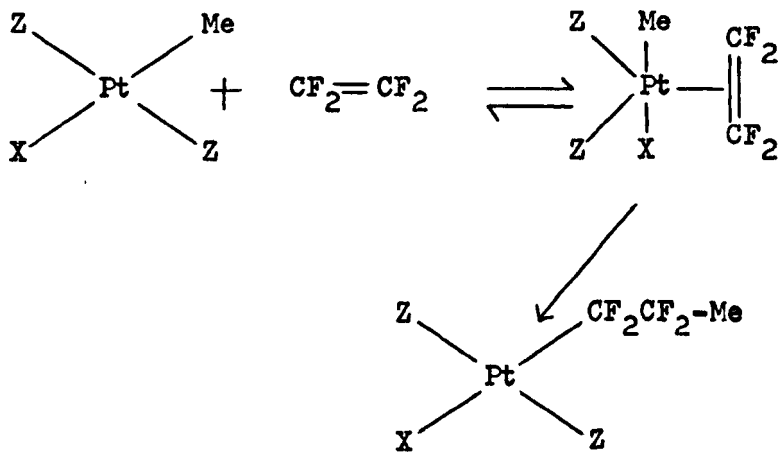

The formation of intermediates of the type indicated above is analogous to the oxidative adducts formed with Vaska's chloride complex, $IrCl(CO)(PPh_3)_2$.

In this work, the decomposition enthalpies of these intermediates are used to confirm the previous observations of Clark and Puddephatt[78,79] regarding the stability of such complexes. For one such complex, where X-ray structural data are available, the bond energy of the platinum-C_4F_6 interaction in this complex, $E(Pt - C_4F_6)$, can be calculated.

Before considering the DSC enthalpy data, the structure and bonding in these complexes are described.

8.1.1 Structure and bonding

Nuclear magnetic resonance data have indicated[78] that the structure of the C_4F_6 intermediates is as shown below. In this

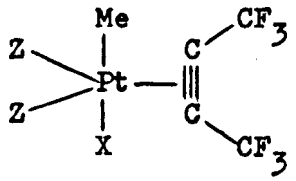

structure the acetylene ligand is rigidly bonded and approximately coplanar with the PtZ_2 unit. Infra-red and Raman spectral assignments confirm this structural interpretation. The C_2F_4 complexes have been assigned the same structure from the similarity of their spectra to those of the C_4F_6 complexes.[78]

Chatt and co-workers,[113] in their studies of transition-metal acetylene complexes, characterised two types of complexes. These two types are indicated in the diagrams below.

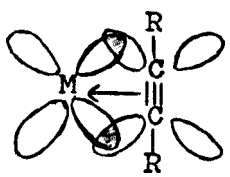

(A)

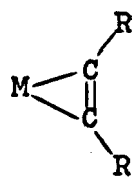

(B)

Structure (A) implies that bonding is caused by donation of acetylene π-electron density into an empty p or d-orbital of the metal and back donation of electron density from a filled metal d or dp hybrid to an acetylene π^*-orbital. Structure (B) implies

that the electron density in the acetylene has been reorganised to give an arrangement close to that for an olefin and that the resulting two unpaired electrons combine with two unpaired electrons on the metal to give two σ-bonds between the acetylene and the metal in a "metallocyclopropene" ring.

The argument was based on the values of $\Delta\nu_{C\equiv C}$ found in (A) and (B) respectively. The smaller value of $\Delta\nu_{C\equiv C}$ in (A) was taken to imply weaker bonding of the acetylene to the metal, less distortion of the acetylenic geometry from linear and a shorter acetylenic carbon-carbon bond. It was also assumed that the acetylene was bonded perpendicular to the coordination plane of the metal. The larger value of $\Delta\nu_{C\equiv C}$ in (B) was taken to imply a stronger bonding of the acetylene to the metal, greater distortion of the acetylene from linearity and a longer acetylenic carbon-carbon bond. If two Pt - C bonds are formed in (B), then the oxidation state of the Pt would be increased by two and the acetylene would take up two coordination positions in the plane.

Chatt later suggested[114] the possibility of a series of complexes with a gradual transition from bonding type (A) to (B), depending on the nature of the substituent groups, R, on the acetylene.

However, Greaves et al.[115] have proposed a more general scheme for acetylenic complexes which uses only Chatt's first model, (A). The bonding type (B) then arises from this as one point in a continuous range of bond types. Similar conclusions have been reached for olefin complexes.[116,6]

Greaves et al.[115] suggest that three criteria determine whether significant bond formation between metal and acetylene occurs. These

are as follows:

(a) Orbitals of the same symmetry must exist on the metal and on the ligand.

(b) The orbitals are able to overlap significantly.

(c) The energy of the overlapping orbitals must be similar.

Assuming that the criteria (a) and (b) are satisfied, then (c) will be the deciding factor. The energy of the metal valence electrons relative to the energy of the acetylene π and π^* orbitals will determine the type of bonding that occurs between the metal and acetylene. Figure 8.1 indicates the various situations that can occur and the bonding type that is expected for each case. Although Greaves et al.[115] originally considered only metal-acetylene complexes, the argument is also valid for metal-olefin complexes, since the electronic states are very similar.

The four cases, C to F, (See Figure 8.1) in which interaction between metal and acetylene occurs, represent points on a continuum of bond types, the extremes being represented below. Complexes of

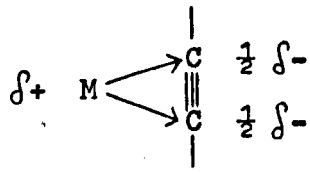

bonding type C

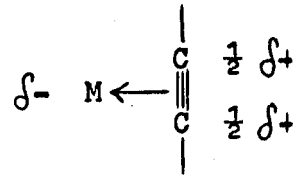

bonding type F

type C would be stabilised by metals in very low oxidation states carrying electron-donating ligands and by acetylenes with electron-withdrawing substituents. Hence, tetracyanoethylene complexes of Pt(0) would be nearer the type C extreme, whilst tetramethyl-ethylene complexes of platinum(II) would be nearer the other

Figure 8.1 Bonding types in transition metal acetylene complexes[115]

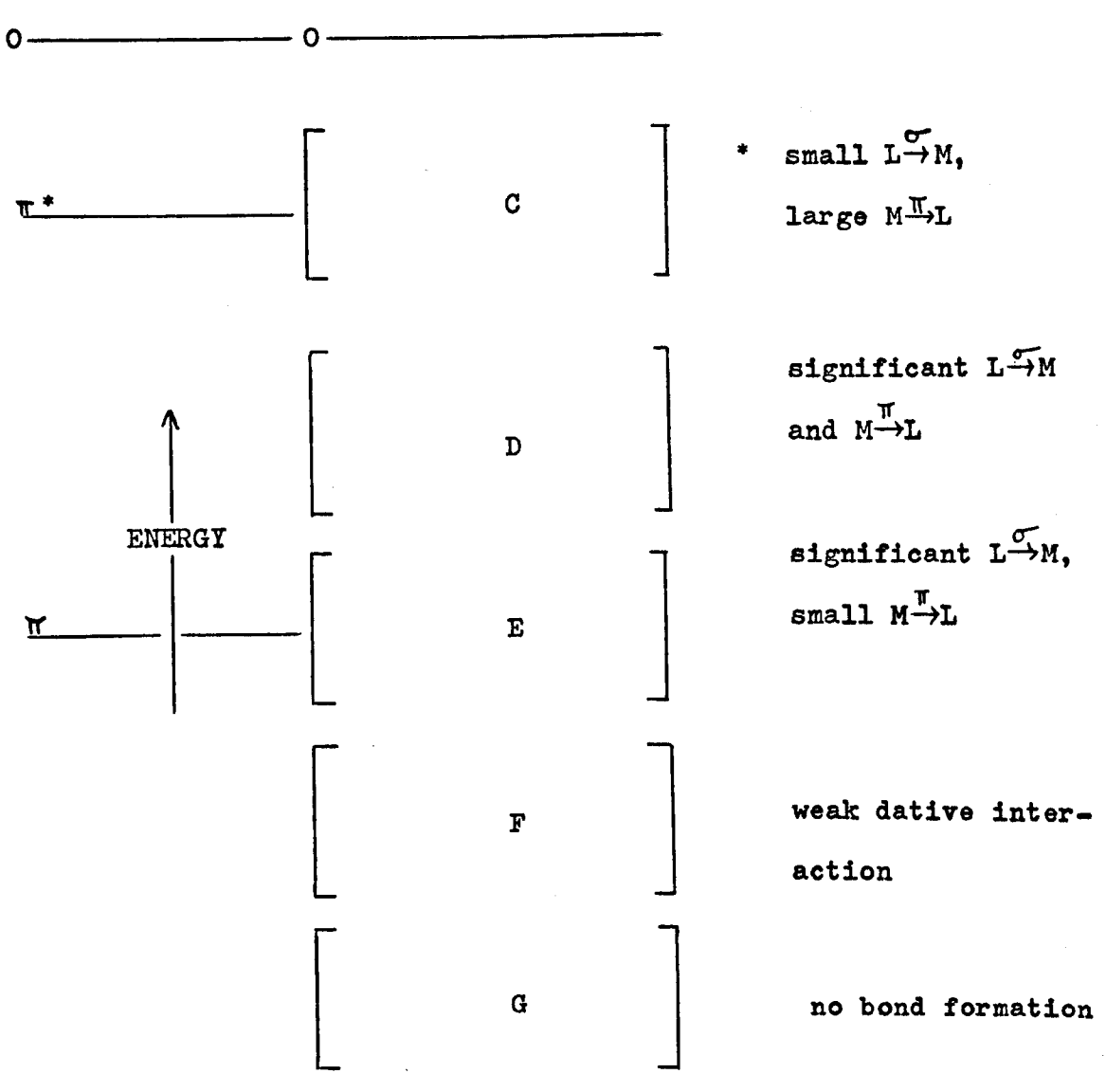

* The carbon-carbon bond order is greater than in case D and the distortion of the acetylene will be less than in D, since the coordinated acetylene resembles the anion rather than the excited state.

The bonding in type C is somewhat analogous to that implied by the "metallocyclopropene ring" description proposed by Chatt et al. [113] Complexes of bonding type F would be difficult to isolate, so that in practice the bonding type of metal-olefin and metal-acetylene complexes will be somewhere between the extremes C and E.

Simple symmetry arguments show that the maximum overlap of possible bonding orbitals occurs when the ligand is either in the coordination plane or at 90° to it.

It would, therefore, appear that metal-olefin and metal-acetylene bonds are best represented schematically as indicated below.

8.1.2 Extent of charge transfer

The position of the complexes, $PtXMeZ_2.L$, with respect to the bond types C to F, Figure 8.1, can be inferred from infra-red data. For the bond type C, a large change in the stretching frequency of the olefinic or acetylenic carbon-carbon bond on coordination is expected, whilst for the type E and especially type F this change in stretching frequency will be much smaller.

Table 8.1 gives infra-red data for several metal-C_4F_6 complexes. From these data it has been inferred that the $PtXMeZ_2.C_4F_6$ complexes are of type D. Corresponding IR data for the $PtXMeZ_2.C_2F_4$ complexes are more difficult to obtain.

Table 8.1 Infra-red data for some C_4F_6 complexes

Complex	$\nu_{C\equiv C}$ cm^{-1}	$\Delta\nu^{*}_{C\equiv C}$ cm^{-1}	Reference
$(\pi cp)Mn(CO)_2 \cdot C_4F_6$	1919	381	117
$RhCl(PPh_3)_2 \cdot C_4F_6$	1917	383	118
$PtClMe(AsMe_2Ph)_2 \cdot C_4F_6$	1870	430	80
$PtIMe(AsMe_2Ph)_2 \cdot C_4F_6$	1868	432	80
$PtClMe(SbMe_3)_2 \cdot C_4F_6$	1865	435	78
$PtClMe(AsMe_3)_2 \cdot C_4F_6$	1838	462	78
$PtClMe(PMe_3)_2 \cdot C_4F_6$	1827	473	78
$Pd(PPh_3)_2 \cdot C_4F_6$	1811, 1838*	476	115
$Pd[(nbut)_3P]_2 \cdot C_4F_6$	1795, 1837*	479	115
$Pd(PPhMe_2)_2 \cdot C_4F_6$	1800, 1837*	482	115
$V(\pi cp)_2 \cdot C_4F_6$	1800	500	119
$Ni(PPh_3)_2 \cdot C_4F_6$	1790	510	115
$Pt(AsPh_3)_2 \cdot C_4F_6$	1775	525	117
$Pt(PPh_3)_2 \cdot C_4F_6$	1775	525	117
$Pt(PMe_2Ph)_2 \cdot C_4F_6$	1767	533	115
$Pt(P(nbut_3))_2 \cdot C_4F_6$	1758	542	115
$IrF(CO)(PPh_3)_2 \cdot C_4F_6$	1797	503	this work
$IrCl(CO)(PPh_3)_2 \cdot C_4F_6$	1773	527	this work
$IrBr(CO)(PPh_3)_2 \cdot C_4F_6$	1763	537	this work
$IrI(CO)(PPh_3)_2 \cdot C_4F_6$	1778	522	this work

* $\Delta\nu_{C\equiv C}$ is calculated by using the value of $\nu_{C\equiv C}$ of the free ligand of 2300 cm^{-1}. [120]

* The reason why $\nu_{C\equiv C}$ is split is not known.

The extent of the electron transfer is also indicated by the lengthening of the carbon-carbon bond of the olefin or acetylene on coordination with respect to that of the free ligand. X-ray data have been reported for only one of these complexes for which we report enthalpy data, $PtClMe(AsMe_3)_2.C_4F_6$. The structure[121] is indicated in Figure 8.2.

The main feature of the $PtClMe(AsMe_3)_2.C_4F_6$ structure is the lengthening of the carbon-carbon bond of the coordinated C_4F_6 molecule from 1.22(9) Å [122] in the free ligand to 1.32(4) Å. The latter figure is quite close to that found for the carbon-carbon bond length of free ethylene, 1.339(2) Å.[123] The long Pt - Cl bond is due to the high trans effect of the methyl group. The difference between the bond lengths for the platinum-carbon (of C_4F_6) bonds is not significant. The platinum, arsenic and carbon (of C_4F_6) atoms all lie in the same plane. Considerable distortion of the C_4F_6 molecule from linearity is observed.

The data imply that only one of the two π-bonds of the C_4F_6 molecule is involved in bonding to the platinum atom. In the compound, $Co_2(CO)_6(PhC{\equiv}CPh)$, where both of the acetylenic π-bonds are used in bonding to the cobalt, the carbon-carbon distance is much longer at 1.46 Å.[124] Moreover, the mean Pt - C distance in $PtClMe(AsMe_3)_2.C_4F_6$ of 2.07(4) Å is very similar to that of 2.03(3) Å [125] found in $Pt(PPh_3)_2.C_2Cl_4$. Davies et al.[121] have inferred from the carbon-carbon bond length that the bonding in $PtClMe(AsMe_3)_2.C_4F_6$ corresponds to type D, as suggested by the earlier IR data.

Mason et al.[126,127] have showed that, on coordination, acetylene would take up its first excited state, which would be

Figure 8.2 Structural data for $PtClMe(AsMe_3)_2 \cdot C_4F_6$[121]

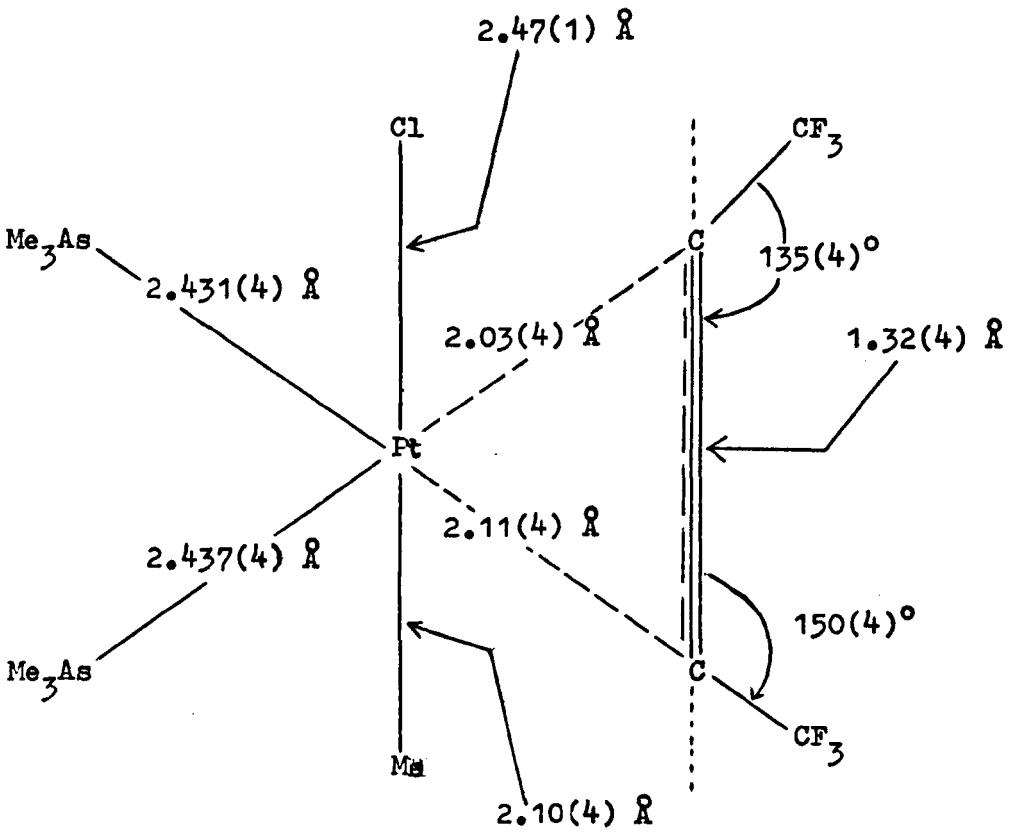

cis-bent. It has been estimated[128] that the bond angle in the excited state would be 142° and the carbon-carbon bond length would be 1.38 Å. The experimental data are in good agreement with these values, as also is the bond angle of 140° found[129] in $Pt(PPh_3)_2.(PhC{\equiv}CPh)$. The bonding type D of the scheme proposed by Greaves et al.[115] predicts that the distortion of the olefin or acetylene occurs to give the geometry of an excited state.

Having thus described the nature of the bonding in the $PtXMeZ_2.L$ complexes, we may now consider in detail the decomposition enthalpy data obtained for them.

8.1.3 Enthalpies of decomposition and stabilities of the platinum complexes

The enthalpies of decomposition of these complexes are summarised in Table 8.2. (More detailed information has already been presented in Table 7.2.) The temperatures, to which the enthalpy data refer, vary over a comparatively narrow range of 40°, the mean being 365°K. It is assumed that only small errors, compared with the quoted uncertainties, will be introduced by ignoring these temperature differences. When using the enthalpies of reactions as a measure of the strength of chemical bonds, it is preferable that such data should refer to gas phase reactions. However, because of the lack of heat of sublimation data for these complexes, it has not been possible to correct the measured enthalpies so that they refer to the gas phase. The assumption is made that the differences between the heats of sublimation of the solid reactant and product, $PtXMeZ_2.L$ and $PtXMeZ_2$, are reasonably

Table 8.2 Enthalpies of decomposition of $PtXMeZ_2.L$

$$PtXMeZ_2.L\ (c) \longrightarrow PtXMeZ_2\ (c) + L\ (g)$$

Complex			ΔH_{dec}	T_p
Z	X	L	kcal mol^{-1}	^oK
$AsMe_3$	Cl	C_2F_4	12.3 ± 0.1	380
$AsMe_3$	Br	C_2F_4	11.5 ± 0.1	385
$AsMe_3$	Cl	C_4F_6	16.4 ± 0.2	385
$AsMe_3$	Br	C_4F_6	14.6 ± 0.2	385,405
$AsMe_2Ph$	Cl	C_4F_6	17.6 ± 0.2	345,370
$AsMe_2Ph$	Br	C_4F_6	19.2 ± 0.1	355

constant and small for differing halogen X, and arsine ligand, Z. If this assumption is justified, then the measured enthalpies of decomposition will be very similar to those in the gas phase for any particular reaction. Thus, the gas phase dissociation energies, D(Pt - L), are likely to be very similar to the enthalpy values of Table 8.2. It will be noted, however, that in Chapter 6 a similar assumption concerning the heats of sublimation of solid heterocyclic metal complex and residual metal dihalide, MX_2L_n and MX_2, was shown to be incorrect. However, it is proposed that the assumption for the type of complex now under discussion is valid, since the unsaturated molecule, L, in $PtXMeZ_2.L$ makes little contribution ($\simeq$10%) to the molecular weight of the complex and presumably, therefore, the interactions in the crystalline lattice are not so much affected by its presence. However, it should be emphasized that whereas the thermochemical data for the condensed phase are precise, the correction to the gas phase depends on an assumption which may not be strictly correct.

8.1.3.1 The stability of $PtXMeZ_2.L$ as a function of the ligand L

A consideration of the dissociation enthalpies in Table 8.2 shows that, in the complexes where Z is $AsMe_3$, the enthalpy value is only about 3.5 kcal mol^{-1} greater for the acetylenic ligand, C_4F_6, than for the olefinic ligand, C_2F_4. This is in keeping with the deduction, from the X-ray data[121] for $PtClMe(AsMe_3)_2.C_4F_6$, that only one of the two π-bonds of the C_4F_6 molecule is involved in bonding it to the platinum atom. The higher stability of the C_4F_6 complexes over the C_2F_4 complexes is in agreement with the experimental observations of Clark and Puddephatt,[78,130] who

reported the following order of stability of $PtXMeZ_2.L$:

$$L = C_2(CN)_4 > C_4F_6 > C_2F_4 > CF_2CFCF_3 > CF_2CFCl$$

The stability of these $PtXMeZ_2.L$ complexes will depend critically on the balance between the σ-donor and π-acceptor nature of the ligand L. In the platinum(0) complexes, $Pt(PPh_3)_2.$olefin, a different stability order is found on the basis of carbon-carbon bond lengths.[121] The order found is given below.

$$L = C_2H_4 < C_2Cl_4 > C_2F_4 > C_2(CN)_4$$

This indicates that the balance in the metal-ligand bond strength due to σ-donor and π-acceptor components is maximised at C_2Cl_4.[125] It appears, therefore, that in these platinum(0) complexes the stability depends relatively more on the σ-donor nature of the olefin than in the olefin complexes of platinum(II). Mason et al.[131] have explained ESCA data for complexes, $Pt(PPh_3)_2.$olefin by saying that the Lewis basicity of the bis(triphenylphosphine)platinum(0) moiety is so strong that the extent of charge transfer, $M \xrightarrow{\pi} L$, is not affected by the nature of the substituent groups on the olefin. This is confirmed by data, also from the ESCA technique, of Cook et al.[132] which have shown that the net transfer of charge from metal to ligand in $Pt(PPh_3)_2.PhC{\equiv}CPh$ and in $Pt(PPh_3)_2.C_2H_4$ is very similar.

It would appear then that the stability of the $PtXMeZ_2.L$ complexes depends critically on the π-acceptor nature of L, unlike the case of the platinum(0) olefin and acetylene complexes.

8.1.3.2 The stability of $PtXMeZ_2.L$ as a function of the arsine, Z

The enthalpy data of Table 8.2 also suggest that the complexes $PtXMeZ_2.L$ are more stable when Z is $AsMe_2Ph$ than when Z is $AsMe_3$. Clark and Puddephatt[78] observed the following order of stability, with respect to the nature of Z, for the complexes $PtXMeZ_2.C_4F_6$.

$$Z = AsMe_3 \simeq AsMe_2Ph \gg SbMe_3 > PMe_3 > PEt_3 > PMe_2Ph$$

8.1.3.3 The stability of $PtXMeZ_2.L$ as a function of the halogen, X

The data of Table 8.2 also imply that the stability with respect to the nature of the halogen, X, cannot be generalised. Clark and Puddephatt[79] have reported that the stability of such complexes does not appear to depend on the nature of the halogen.

It is further suggested[78] that, since the formation of these complexes, $PtXMeZ_2.L$, may be considered as partial oxidative addition, then the factors promoting oxidative addition might be expected to stabilise the complexes. This would explain the inability to isolate similar palladium(II) complexes. Clark and Puddephatt[78] further suggest that, since the ligand, L, is trans to the arsine groups, Z, the stability of the complexes will also be dependent on the trans effect of Z. The ability to promote oxidative additions, for which the order is stibine > arsine > phosphine,[133-135] is balanced by the trans effect, for which the order (as observed in $cis\text{-}PtCl_2L_2$) is phosphine > stibine > arsine,[136, 137] thus resulting in the observed stability order of Clark and Puddephatt.

An important point can be made here with relation to the inference of stability orders from infra-red data. The values of $\Delta\nu_{C\equiv C}$ of Table 8.1 would suggest stability orders, for the complexes $PtXMeZ_2.L$, which are completely different to those obtained from the DSC data. The use of small differences in the values of $\Delta\nu_{C\equiv C}$ is not a good criterion, therefore, for stability evaluation. Hartley[111] has indicated that $\Delta\nu_{C=C}$ for coordinated olefins will be altered by coupling to other vibrations, strain and substituent effects.

Having made some general comments on the stability of the $PtXMeZ_2.L$ complexes in terms of the dissociation enthalpies, an alternative way of expressing the strength of the platinum-ligand interaction in such complexes may be considered. On dissociation, the C_2F_4 or C_4F_6 molecule will undergo extensive reorganisation and the energy of this reorganisation may be taken into account, as indicated in the following section.

8.1.4 Estimation of $E(Pt - C_4F_6)$ in $PtClMe(AsMe_3)_2.C_4F_6$

The X-ray data[121] for this complex, shown in Figure 8.2, indicate that the carbon-carbon bond of C_4F_6 has become lengthened on coordination to a value approaching that of the carbon-carbon bond in free ethylene. Therefore, it would seem likely that in the complex the strength of the carbon-carbon bond will be very similar to that of the double bond in ethylene, $E(C=C) \simeq 143$ kcal mol^{-1}.[138] On dissociation, the bond strength will increase, probably by about 51 kcal mol^{-1} to a value close to that of the triple bond in acetylene, $E(C\equiv C) \simeq 194$ kcal mol^{-1}.[138] Consequently, the bond

Figure 8.3 Schematic representation of the estimation of $E(Pt - C_4F_6)$ in the complex $PtClMe(AsMe_3)_2 \cdot C_4F_6$

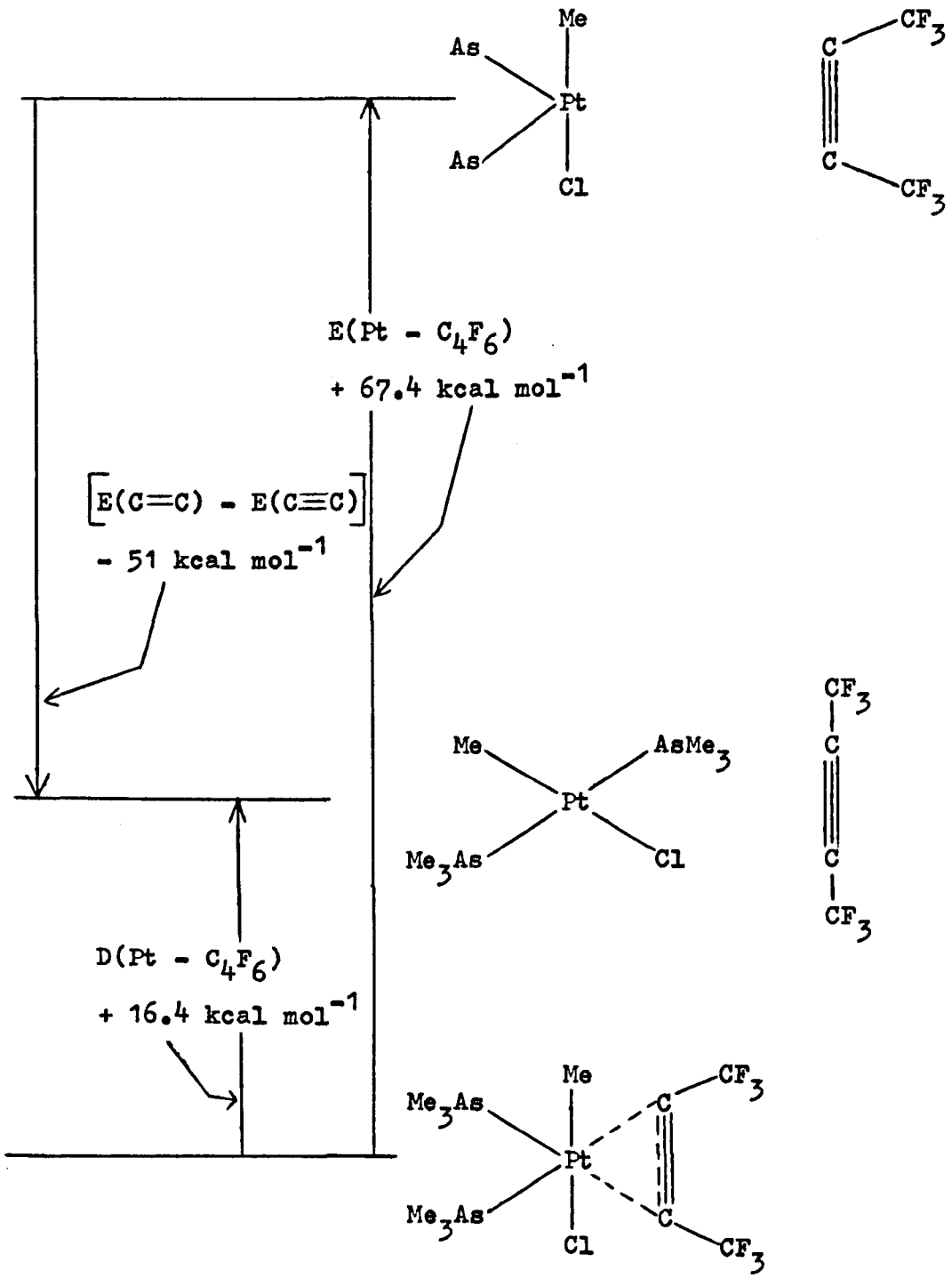

energy of the platinum-C_4F_6 linkage in this complex is about 67 kcal mol^{-1}. This method of estimation of the E(Pt - C_4F_6) value is indicated schematically in Figure 8.3.

The iridium(I) complexes, for which data are reported in this thesis, $IrX(CO)(PPh_3)_2.L$, may now be discussed and comparison drawn, where possible, with the platinum(II) complexes, $PtXMeZ_2.L$.

8.2 The iridium(I) complexes, $IrX(CO)(PPh_3)_2.L$

The iridium(I) complexes are the oxidative adducts formed by the attack of the simple, unsaturated molecules C_2F_4, C_4F_6 and $CH_2CH(CN)$ on the complexes trans-$IrX(CO)(PPh_3)_2$, where X is F, Cl, Br or I. A wealth of data has been accumulated for the oxidative addition reactions of the complex $IrCl(CO)(PPh_3)_2$ in particular. Unfortunately, the majority of thermodynamic data for such adducts refer to complexes in solution. Thus, thermodynamic data for the solid-state decomposition of oxidative adducts of $IrX(CO)(PPh_3)_2$ are especially valuable.

The interpretation of the stability of these adducts has been based on various criteria including the reversibility of the addition, thermal decomposition temperatures, infra-red stretching frequencies and X-ray data. However, there are indications that there is some inconsistency amongst the interpretations.

In this section, the stability orders of the C_2F_4 and C_4F_6 adducts, in particular, of $IrX(CO)(PPh_3)_2$ are discussed. Special

reference is made to the stability of $IrCl(CO)(PPh_3)_2.L$, as a function of L, and to the observed stability order of $IrX(CO)(PPh_3)_2.L$ with respect to the halogen, X, as the ligand L is varied.

8.2.1 Structure and bonding

The bonding scheme proposed by Greaves et al.[115] for metal-acetylene complexes, which is equally applicable to metal-olefin complexes, has already been described in Section 8.1.1. The contribution from the $M \xrightarrow{\pi} L$ component of the bonding can be estimated from the second ionisation potential of iridium, for iridium(I) complexes, and from the third ionisation potential of platinum, for platinum(II) complexes. From this, it is concluded that the ability of iridium(I) to participate in oxidative additions will be greater than that of platinum(II). The spectroscopic data for some metal-C_4F_6 complexes in Table 8.1, Section 8.1.2, confirm this expected trend.

Unfortunately, no X-ray data are available for any of the $IrX(CO)(PPh_3)_2.L$ complexes, for which enthalpy data are reported in this thesis. However, some indication as to the stereochemical disposition of the coordinated ligands around the iridium atom is available.

Ibers et al.[139] have proposed that in $IrI(CO)(PPh_3)_2.C_2F_4$ the phosphine groups are cis to each other and trans to the C_2F_4 ligand. This stereochemistry is confirmed by N.M.R. data of Clarke et al.[74] for the closely related complex $IrCl(CO)(PPh_2Me)_2.C_2F_4$. However, Clarke et al.[74] also found that in $IrCl(CO)(PPh_2Me)_2.C_4F_6$ the phosphine groups are trans to each other. (The structures of

$IrCl(CO)(PPh_2Me)_2.L$, where L is C_2F_4 and C_4F_6, are given in Figure 8.4.) It is assumed that $IrCl(CO)(PPh_3)_2.C_4F_6$ has the same stereochemistry as $IrCl(CO)(PPh_2Me)_2.C_4F_6$.

Hence, it is seen that, unlike the $PtXMeZ_2.L$ complexes, where both the C_2F_4 and C_4F_6 complexes had the same structural type, the C_2F_4 and C_4F_6 complexes of $IrX(CO)(PPh_3)_2$ do not.

No literature reports are available on the structure of the acrylonitrile adducts. The instability of $IrCl(CO)(PPh_3)_2.CH_2CH(CN)$ and $IrBr(CO)(PPh_3)_2.CH_2CH(CN)$ at room temperature precludes X-ray investigation. The only structural inference for an ethylene complex, from N.M.R. evidence,[140] is that the complex $Ir(SnCl_3)(CO)(PPh_2Me)_2.C_2H_4$ contains trans phosphine groups. The structures of a fumaronitrile (trans-1,2-dicyanoethylene) and of a tetracyanoethylene adduct of iridium(I) are known[141,6] to contain cis phosphine groups. McClure and Baddeley[142] propose a similar stereochemistry for $IrX(CO)(EPh_3)_2.(CN)C{\equiv}C(CN)$, where X is Cl, Br or I; and E is As or P. Thus, the stereochemistry in the acrylonitrile complexes cannot be inferred from comparisons with other ethylene and cyano-olefin adducts of $IrX(CO)(PPh_3)_2$.

A summary of the stereochemistries found in some $IrX(CO)(phosphine)_2.L$ complexes, where the ligand L is not dissociated on coordination, is given in Table 8.3. It is seen that the more common arrangement is that in which the phosphine groups are trans to each other. The cis configuration seems to occur only where L is C_2F_4, or some cyanoethylenes in which there is at least one cyanide substituent on each carbon atom, or dicyanoacetylene.

Figure 8.4 The stereochemistries of the complexes, $IrCl(CO)(PPh_2Me)_2.L$, where L is C_2F_4 and C_4F_6

(a) $IrCl(CO)(PPh_2Me)_2.C_2F_4$

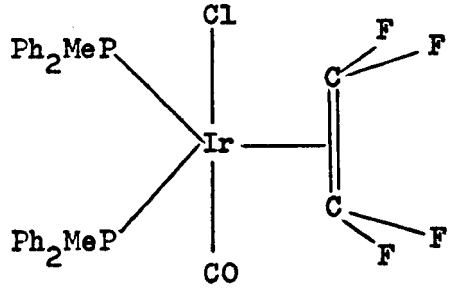

(b) $IrCl(CO)(PPh_2Me)_2.C_4F_6$

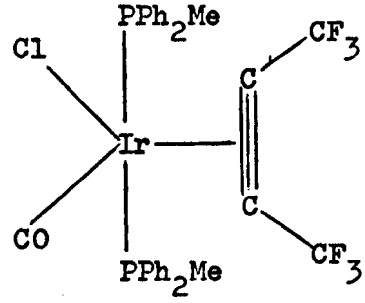

Table 8.3 The stereochemistries of the complexes, $IrX(CO)(phosphine)_2.L$

Complex			Stereochemistry		Reference
X	phosphine	L	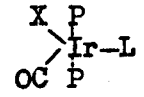		
Cl	PPh_3	SO_2	✓		143
Cl	PPh_3	CO	✓		144
Cl	PPh_2Me	C_4F_6	✓		74
Cl	PPh_2Me	C_2F_4		✓	74
I	PPh_3	C_2F_4		✓	139
Br	PPh_3	$C_2(CN)_4$		✓	6
Cl	PPh_2Me	$[C(CF_3)(CN)]_2$		✓	145
Cl	PPh_3	$C(CN)_2C(CF_3)_2$	✓		146
Cl	PPh_2Me	$CF_2CF(Br)$	✓		146
Cl	PPh_2Me	$CF_2CF(CF_3)$	✓		146
I	PPh_3	CS_2	✓		147
Cl	PPh_3	$SC{=}C(CF_3)_2$	✓		148
Cl	PPh_3	$OC{=}C(CF_3)_2$	✓		146
Cl	PPh_2Me	$OC{=}C(CF_3)_2$	✓		146
I	PPh_3	O_2	✓		5
Cl	PPh_3	O_2	✓		4,3
Cl	PPh_2Et	O_2	✓		149
Cl*	PPh_3	$(CN)C{\equiv}C(CN)$		✓	142

* also X = Br and I.

In discussing the DSC data for the C_4F_6 and C_2F_4 adducts of $IrX(CO)(PPh_3)_2$, the difference in stereochemistry must be borne in mind. It will be assumed that no change in stereochemical type is caused by varying the nature of X.

8.2.2 Enthalpies of decomposition and stabilities of the iridium(I) complexes

In order to consider the decomposition enthalpies of the iridium(I) complexes as a measure of the gas-phase bond dissociation energies, D(M - L), the same assumptions as outlined in Section 8.1.3 for the platinum(II) complexes have to be made. Hence, although the DSC data are precise, the assumption that they are a measure of D(Ir - L) may not be strictly justifiable.

The enthalpies of decomposition for $IrX(CO)(PPh_3)_2.L$ are summarised in Table 8.4. (More detailed data have been given in Table 7.1.) Variations in the stability of $IrX(CO)(PPh_3)_2.L$ can be discussed in terms of the ligand L, and halogen X.

8.2.2.1 The stability of $IrX(CO)(PPh_3)_2.L$ as a function of the ligand, L

The values for the enthalpies of decomposition for the C_4F_6 complexes are, in all cases, greater than for the corresponding C_2F_4 complexes, the mean difference in ΔH_{dec} being 6.5 kcal mol^{-1}. These results are similar to those found in the $PtXMeZ_2.L$ complexes, where D(Pt - C_4F_6) was greater than D(Pt - C_2F_4), but by only $\simeq$3.5 kcal mol^{-1}. The DSC data are in agreement with the qualitative

Table 8.4 Enthalpies of decomposition of $IrX(CO)(PPh_3)_2.L$

$$IrX(CO)(PPh_3)_2.L\ (c) \longrightarrow IrX(CO)(PPh_3)_2\ (c) + L\ (g)$$

Complex		ΔH_{dec}	T_p
L	X	kcal mol^{-1}	^oK
C_4F_6	F	23.7 ± 0.1	450
	Cl	22.9 ± 0.4	430
	Br	18.8 ± 0.1	450
	I	19.7 ± 0.4	430,480
C_2F_4	F	19.0 ± 0.4	480
	Cl	16.5 ± 0.3	445,475
	Br	9.8 ± 0.2	435,470
	I	13.7 ± 0.2	455,470
$CH_2CH(CN)$	F	- - -	385
	Cl	- - -	335
	Br	- - -	330

stability order of $IrCl(CO)(PPh_3)_2.L$, where L is C_4F_6 and C_2F_4, of Parshall and Jones.[108] The observation that $IrCl(CO)(PPh_3)_2.C_2(CN)_4$ and $IrCl(CO)(PPh_3)_2.CH(CN)CH(CN)$ did not decompose until about 540°K suggests that these complexes are very much more stable than any of the $IrX(CO)(PPh_3)_2.L$ complexes, where L is C_2F_4 or C_4F_6. The instability of the acrylonitrile complex of $IrCl(CO)(PPh_3)_2$, with respect to decomposition at room temperature, suggests that it is rather less stable than the corresponding C_2F_4 and C_4F_6 complexes. If the inability to prepare the C_2Cl_4 complex of $IrCl(CO)(PPh_3)_2$ is assumed not to be due to kinetic reasons, this would imply that C_2Cl_4 has a very low affinity for $IrCl(CO)(PPh_3)_2$. Hence, we may, on the observations reported in this thesis, express the stability of the oxidative adducts, $IrCl(CO)(PPh_3)_2.L$, in the following order.

$$L = C_2(CN)_4,\ CH(CN)CH(CN) > C_4F_6 > C_2F_4 > CH_2CH(CN) > C_2Cl_4$$

The stability of $IrCl(CO)(PPh_3)_2.L$ will depend on the balance between the σ-donor and π-acceptor nature of the ligand L. A similar stability order, $L = C_2(CN)_4 > C_4F_6 > C_2F_4$, has been found[130] for the $PtXMeZ_2.L$ complexes, where it has already been shown, in this thesis, that the stability depends critically on the π-acceptor nature of L. The same situation would seem to be the case for the stability of $IrCl(CO)(PPh_3)_2.L$. This is confirmed by the ESCA data of Mason et al.,[131] who propose that the complex $IrCl(CO)(PPh_3)_2$ has a relatively low basicity and that the $Ir \rightleftarrows L$ bonding is significantly determined by the π-acceptor ability of L. Only with the very strong π-acid, tetracyanoethylene, did the metal binding energies approximate to those of formal Ir(III)

systems. Vaska[2] has also concluded that the stability of adducts of $IrCl(CO)(PPh_3)_2$ "appears to parallel the extent of electron transfer from the metal to the addendum." The same conclusion is reached by Baddley[75] in his explanation for the increasing stability of the cyano-olefin complexes of $IrCl(CO)(PPh_3)_2$ as the number of cyano groups increases. Scott et al.[150] also suggest that the dominant type of interaction between iridium and the ligand L, in the adducts $IrCl(CO)(PPh_3)_2L$, is metal to ligand donor-acceptor bonding. They note that the acceptor ligand BF_3 forms an adduct with $IrCl(CO)(PPh_3)_2$.

The decomposition temperatures of the adducts is sometimes taken as a measure of their stability. However, Table 8.4 shows that the stability of $IrX(CO)(PPh_3)_2.L$ cannot always be gauged by the values of the DSC peak temperatures, T_p, when only small differences in T_p are involved. However, for the acrylonitrile complexes, the T_p values are considerably lower than those for the C_2F_4 and C_4F_6 complexes. This is in agreement with the experimentally observed instability of $IrCl(CO)(PPh_3)_2.CH_2CH(CN)$ and $IrBr(CO)(PPh_3)_2.CH_2CH(CN)$ at room temperature. The large difference in T_p value, $\simeq 50^\circ$, between the acrylonitrile complexes of $IrF(CO)(PPh_3)_2$ and $IrCl(CO)(PPh_3)_2$ is in accordance with the experimental observations, and the report of Fitzgerald et al.[77]

8.2.2.2 The stability of $IrX(CO)(PPh_3)_2.C_2F_4$ and $IrX(CO)(PPh_3)_2.C_4F_6$ as a function of the halogen, X

Table 8.4 shows that for both the C_4F_6 and C_2F_4 complexes of

$IrX(CO)(PPh_3)_2$, the heat of decomposition values decrease in the order F > Cl > Br < I. The minimum value of ΔH_{dec}, when X is Br, is especially pronounced for the case of the C_2F_4 complex.

The explanation for the observed order, F > Cl > Br < I, may lie in the balance between the σ and π-bonding components of the Ir - L bond. The observed order may be interpreted in terms of the "classical" electronegativity and polarisability of X. If the σ-bonding component of the Ir - L bond were the more important, then one might expect the stability of $IrX(CO)(PPh_3)_2.L$ to be in the order F > Cl > Br > I, since the very electronegative fluorine atom would reduce the electron density distribution on the iridium atom and encourage σ-bonding. However, if the π-bonding component were the more important, the stability of $IrX(CO)(PPh_3)_2.L$ would be expected to be in the reverse order i.e. I > Br > Cl > F, since the higher nephelauxetic effect, which can be measured by the polarisability, of the heavier halogens can expand the metal d-electron cloud and promote the ability of the metal to participate in Ir $\rightarrow$ L π-bonding. This is the explanation given for the differing rates of oxygenation and deoxygenation of $IrX(CO)(PPh_3)_2$, where X is F, Cl, Br or I.[151] Since an intermediate stability order, with respect to the halogen, of F > Cl > Br < I, has been found for the C_2F_4 and C_4F_6 adducts of $IrX(CO)(PPh_3)_2$, it is suggested that there is a fine balance between the relative contributions of the σ and π-bonds in the Ir - C_2F_4 and Ir - C_4F_6 bonds.

The relatively large variation in the heats of decomposition for the $IrX(CO)(PPh_3)_2.C_2F_4$ and $IrX(CO)(PPh_3)_2.C_4F_6$ complexes, $\simeq$30% and $\simeq$ 20% respectively, as a function of X, is surprising in view

of recent X-ray, photoelectron and Mössbauer spectroscopic data.[152] The latter have shown that the variation of X in $IrX(CO)(PPh_3)_2$ only slightly affects the total electron density on iridium, the s-electron density and the electric field gradient at the nucleus. Changes in the distribution of electron density caused by the variation of X are balanced by compensating changes in the electron density distribution within the carbonyl ligand. This is indicated by the ν_{CO} (in $CHCl_3$) values[76] for $IrX(CO)(PPh_3)_2$, where X is F, Cl, Br and I, of 1957, 1965, 1966 and 1967 cm^{-1}. This order of ν_{CO} values is not that expected in terms of "classical" electronegativities of the halogens. Vaska and Peone[76] have explained the ν_{CO} order by the concept of "total electronegativity". They propose that, both the withdrawal of charge by purely inductive effects and also the removal of electron density from the iridium atom, into unfilled d-orbitals of the halogen, must be considered. This results in a "total electronegativity" order of I > Br $\simeq$ Cl > F. If the observed stability order for the C_2F_4 and C_4F_6 complexes of F > Cl > Br < I is regarded in the light of this new concept, the greatest stability for the fluoro complex is explained by the lower "total electronegativity" of fluorine compared with the other halogens, which enables a greater degree of Ir $\rightarrow$ L π-bonding to occur in the adducts formed from $IrF(CO)(PPh_3)_2$. The difference between the "total electronegativity" of the halogens is very small. Thus, the relatively large variation of the heats of decomposition is unexpected.

8.2.3 Comparison of the observed stability orders for $IrX(CO)(PPh_3)_2.L$ with those found by other workers

8.2.3.1 Other oxidative adducts of $IrCl(CO)(PPh_3)_2$

Very few data are available in the literature for the solid-state decomposition of other oxidative adducts of $IrCl(CO)(PPh_3)_2$. The DSC enthalpy of decomposition for $IrCl(CO)(PPh_3)_2.SO_2$ has been reported to be 8.4 ± 0.2 kcal mol^{-1} at $457^{\circ}K$.[8] The SO_2 ligand is only weakly attached to the iridium atom in this adduct, since the observed Ir - S bond length is 2.49 Å [143] as compared with the value of 2.07 Å found[153] in other metal-SO_2 complexes. Hence, it would appear that both $IrCl(CO)(PPh_3)_2.C_4F_6$ and $IrCl(CO)(PPh_3)_2.C_2F_4$ are much more stable adducts than $IrCl(CO)(PPh_3)_2.SO_2$. This is in agreement with the conclusion that the stability of $IrCl(CO)(PPh_3)_2.L$ depends on the π-acceptor nature of L, since the electron affinity of SO_2 will be less than that of C_2F_4 and C_4F_6.

Vaska[2] has obtained thermodynamic data for the stability of several other adducts of $IrCl(CO)(PPh_3)_2$ in chlorobenzene at $303^{\circ}K$. The thermodynamic data were calculated from the rate and/or equilibrium constants measured at different temperatures in the range 273 to $333^{\circ}K$. The enthalpy values for the following reaction were determined to be 17.1, 10.8 and 10.1 kcal mol^{-1}

$$IrCl(CO)(PPh_3)_2.L \longrightarrow IrCl(CO)(PPh_3)_2 + L$$

respectively for the adducts, where L is O_2, CO and SO_2. Similarly, enthalpy values of 12, 9.3 and 1 kcal mol^{-1} were found for the C_2H_4, C_2H_2 and CO adducts of $IrI(CO)(PPh_3)_2$.[154] These stability data again

agree with the expected stability trend in terms of the π-acceptor nature of the addendum.

8.2.3.2 The stability of other adducts $IrX(CO)(PPh_3)_2.L$ as a function of the halogen, X

It would be of interest to compare literature reports for the stability of $IrX(CO)(PPh_3)_2.L$, as a function of X, with the observed stability order, F > Cl > Br < I, for the cases of L = C_2F_4 and C_4F_6. Peone[155] has observed from the relatively large differences in the temperature range of decomposition of $IrX(CO)(PPh_3)_2.SO_2$, where X is F, Cl, Br or I, that the stability order is F > Cl > Br > I. This order is very similar to that observed for the C_2F_4 and C_4F_6 complexes. Similarly, the mean decomposition temperatures[156,75] of $IrX(CO)(PPh_3)_2.C_2(CN)_4$, where X is F, Cl, Br or I, of >573, 540, 500 and 487°K indicate the stability order F > Cl > Br > I. We have also observed in this work that the stability order of $IrX(CO)(PPh_3)_2.CH_2CH(CN)$ appears to be F > Cl, a similar order being found for the crotononitrile ($CH(CH_3)CH(CN)$) complexes by Fitzgerald et al.[77]

It would appear, then, that the available solid-state observations suggest that for adducts $IrX(CO)(PPh_3)_2.L$, where L is $C_2(CN)_4$, C_4F_6, C_2F_4, $CH_2CH(CN)$ and $CH(CH_3)CH(CN)$ i.e. ligands of good π-acceptor ability, the stability is greatest for the fluoro complex.

However, data for other adducts, $IrX(CO)(PPh_3)_2.L$, in solution, do not indicate that the fluoro complex is always the most stable. Vaska et al.[151,154] have shown that the stability of the oxygen adducts is in the order I > Br > Cl > F and that a similar

order is the case for the ethylene and acetylene complexes. Strohmeier and Fleischmann[157] have found, however, that the stability of the adducts of maleic anhydride and the dimethyl esters of maleic and fumaric acids is in the order Cl > Br > I. The situation is further complicated by the observation by Peone,[155] that the stability of $IrX(CO)(PPh_3)_2.SO_2$, as measured by equilibrium constant data obtained spectrophotometrically, is in the order I > Br > Cl > F i.e. the reverse of that found from the decomposition temperatures of the crystalline adducts. Furthermore, at a temperature around 323°K, the stability order of the adducts in solution is reversed from that at 303°K and becomes F > Cl > Br > I. This is the only reported case of such a reversal in stability order, but no explanation is proposed for it by Peone. This observation, together with that of Vaska,[154] that the order of stability, as measured by equilibrium constants for the CO adducts, I > Br > Cl, does not agree with that derived from enthalpy values, Cl > Br > I, suggests that a discussion of the stability order of $IrX(CO)(PPh_3)_2.L$, with respect to X, as determined for adducts in solution, is not justifiable. Vaska[154] has suggested that the variance in stability orders, as measured by equilibrium constants or enthalpy values, reflects the relatively large differences in the entropy changes.

At the beginning of this section on iridium(I) complexes, it was pointed out that, in comparing the stability of the adducts $IrX(CO)(PPh_3)_2.L$, we are not necessarily comparing complexes of exactly the same stereochemistry.

For the complexes $PtXMeZ_2.L$, Clark and Puddephatt[78] observed that their stability was, to some extent, dependent on the trans

effect of the ligand trans to the ligand L. If this same criterion is applied to the complexes $IrX(CO)(PPh_3)_2.L$, the possible influence of varying stereochemistry may become apparent. However, both the C_4F_6 and SO_2 adducts, which have phosphine groups trans to one another, and the C_2F_4 and $C_2(CN)_4$ adducts, which have cis phosphines give a stability order where the fluoro complex is the most stable. This suggests that the influence of the stereochemistry, and, therefore, of the trans effect, is not significant in determining the stability order with respect to X.

It must, therefore, be concluded that the stability order of the adducts $IrX(CO)(PPh_3)_2.L$ appears to depend on the π-acceptor nature of the ligand L. This is in agreement with data from other sources. The DSC data for the C_4F_6 and C_2F_4 adducts are in agreement with other data for the $C_2(CN)_4$ and SO_2 adducts, that the stability is a maximum at the fluoro complex. However, we must admit, like Fitzgerald et al.,[77] that the factors governing the basicity of $IrX(CO)(PPh_3)_2$, as a function of X, and hence, the stability of $IrX(CO)(PPh_3)_2.L$, are not entirely clear.

If the DSC data for the $PtXMeZ_2.L$ and $IrX(CO)(PPh_3)_2.L$ complexes are compared, several general comments can be made.

	$IrCl(CO)(PPh_3)_2.L$	$PtClMe(AsMe_3)_2.L$
$D(M - C_2F_4)$*	16.5	12.3
$D(M - C_4F_6)$*	22.9	16.4

The two sets of complexes are by no means analogous, but there is

[*$D(M - C_2F_4)$ and $D(M - C_4F_6)$ are in kcal mol^{-1}.]

evidence[78] that replacement of arsine by phosphine in the platinum(II) complexes makes them less stable. The data are, therefore, in agreement with the greater tendency of iridium(I) complexes to undergo oxidative addition than platinum(II) complexes.

9 EVALUATION OF KINETIC PARAMETERS

Differential scanning calorimetry provides an opportunity for measuring not only the enthalpy change of a reaction, but also the rate of a reaction. This can lead, in principle, to information about the kinetic parameters and mechanisms of the process.

9.1 The use of the scanning calorimeter to obtain kinetic data

To obtain a measure of the reaction rate, the calorimeter may be used in either the isothermal, or in the temperature-scanning mode.

9.1.1 Isothermal mode

In the isothermal mode the extent of reaction is measured directly as a function of the temperature and time. Several separate samples are held in the calorimeter at a given temperature, but for varying intervals of time. They are then programmed through their decompositions. The decrease in the peak area, per unit sample weight, as a function of the previous isothermal exposure time, is a measure of the reaction rate at the set temperature. By repetition of the procedure at various temperatures, data can be obtained for the variation of reaction rate with temperature. Duswalt[158] has used this method to obtain kinetic data for some highly exothermic decompositions. Kambe, Mita and Horie[159] have used a slightly modified method to study polymerisation reactions. Rogers[160] has also used an isothermal

method to study systems that melt with decomposition.

9.1.2. Temperature-scanning mode

In this method, the sample is scanned through a temperature range and the thermogram is recorded. The usual starting-point for the analysis of experimental data is to use the equation given below,

$$-\frac{dc}{dt} = k\,c^{n} \qquad \ldots\ldots\ldots\ldots\ldots\ldots\ldots\ldots (1)$$

where k is the rate constant and c is the concentration of the reactant. However, for the systems studied here, the concentration, c, is constant throughout. Hence, the data must be analysed in terms of α, the degree of conversion, and $d\alpha/dt$. The value of α, as a function of temperature, can be obtained from the ratio of the area swept out by the pen recorder up to that temperature, and the total peak area. Difficulty arises in deriving the rate constant, k, for the solid-state reactions. The terms "energy of activation", "order of reaction" and "frequency factor" must be used with an appreciation of their more diffuse interpretation in solid-state reactions as compared to ideal gas kinetics.

The calculation of kinetic parameters is often based on the assumption that the reaction can be described by the following differential equation,

$$\frac{d\alpha}{dt} = k(T)\, f(\alpha) \qquad \ldots\ldots\ldots\ldots\ldots\ldots\ldots (2)$$

where k(T) is the temperature-dependent rate constant and $f(\alpha)$ is

a function which represents the hypothetical model for the reaction mechanism. The possible mechanisms in solid-state processes have been derived mathematically by Šesták and Berggren,[161] who conclude that the most convenient analytical approximation for the differential equation is

$$\frac{d\alpha}{dt} = k\,(1-\alpha)^{n}\,\alpha^{m}\left[-\ln\,(1-\alpha)\right]^{p} \quad \ldots\ldots\ldots(3)$$

where the values of n, m and p are temperature independent and are chosen so as to represent the model of the reaction path.

It has been commonly supposed that solid-state processes take place in three stages: an induction or nucleation period, during which reaction centres form within the solid: the interfacial reaction, where these centres expand, so that the interface between product and reactant increases; and finally decay, when the centres overlap and the interfaces between product and reactant begin to decrease. Hence, a plot of α against time will be sigmoid-shaped for such processes.[162]

Šesták and Berggren[161] have suggested that for certain processes controlled by an induction (nucleation) period, equation (3) reduces to the form

$$\frac{d\alpha}{dt} = k(T)\,\alpha^{m} \qquad (\text{i.e. } n = p = 0) \quad \ldots\ldots\ldots(4)$$

For those processes which are controlled by the rate of the interfacial reaction, the relevant equation is

$$\frac{d\alpha}{dt} = k(T)\,(1-\alpha)^{n} \quad (\text{i.e. } m = p = 0) \quad \ldots\ldots\ldots(5)$$

where n may have, on theoretical grounds, only the values 0, 0.5 and 0.66.[163] For the later stages of the reaction (the unimolecular decay) the equation becomes

$$\frac{d\alpha}{dt} = k(T)\,(1 - \alpha) \quad \text{(i.e. } n = 1,\ m = p = 0) \ldots\ldots (6)$$

Most workers have chosen to adopt equation (5) as a basis for their calculations, with the implication that the derived parameters refer to the interfacial reaction. Moreover, Šesták and Berggren[161] accept the view that true solid-state reactions are activated processes for which an activation energy may be calculated from the exponential character of k(T). Thus, the incorporation into equation (5) of the equality $k(T) = C\, e^{-E_A/RT}$, where E_A is the activation energy of the interfacial reaction and C is a constant, leads to the equation

$$-\log \frac{d\alpha}{dt} + n \log (1 - \alpha) = \frac{+E_A}{2.303RT} - \log C \ldots\ldots (7)$$

In studying reactions of the type $X\,(s) \rightarrow Y\,(s) + Z\,(g)$, the usual practice has been to select a value of n, so as to give a best linear plot of $[-\log d\alpha/dt + n \log (1 - \alpha)]$ against 1/T. This has been criticised by Brindley et al.[163] who point out that equation (5) has no general validity for heterogeneous solid-state reactions, except for the cases when n is 0, 0.5 and 0.66. However, equation (7) has been used as the basis for evaluating kinetic parameters by several groups of workers. Kauffman and Beech[164] have used values of n varying between 0.23 and 1.8, depending on the particular part of the decomposition reaction of the transition-

metal isothiocyanate complex being investigated in the α range 0.01 to 0.91. Beech et al. have also used this method to obtain kinetic data for the decomposition of other transition-metal complexes.[165-167] Uricheck[168] has used a value of n = 1 for work on the decomposition of sodium carbonate. Rogers and Smith[169] have adopted the value n = 1.3 for the thermal decomposition of RDX (hexahydro-1,3,5-trinitro-s-triazine) in the α range 0.07 to 0.80. In other work, Rogers and Morris[170] have preferred the value n = 0 in their study of the decomposition kinetics of some organic explosives.

In a DSC study of the dehydration of manganous hydrate formate, $Mn(HCOO)_2.2H_2O$, Thomas and Clarke[171] have shown that for differential scanning calorimetry, DSC, the rate of reaction, $d\alpha/dt$, where α is the degree of conversion, is given by the relationship $d\alpha/dt = dH/dt \cdot 1/A$, where dH/dt is the pen-deflection at a given temperature (or peak height at this temperature) and A is the total peak area. They suggest that, for the reaction stage where the value of α depends linearly on the time, t, the rate constant represents the specific advance of the interface. They have taken n = 0 in equation (7) and have used the following equation,

$$-\log\left[\frac{dH}{dt}\cdot\frac{1}{A}\right] = +\frac{E_A}{2.303RT} - \log C \quad \ldots\ldots\ldots(8)$$

in which E_A refers specifically to the energy of activation of the interfacial reaction. This last equation may be rearranged to give

$$+\log\frac{dH}{dt} = -\frac{E_A}{2.303RT}\left[\frac{1}{T}\right] + \log\left[C.A\right] \quad \ldots\ldots\ldots(9)$$

which shows that E_A may be evaluated for the α range over which a plot of log dH/dt against 1/T is linear. The value of log C may be calculated from the intercept on the log dH/dt axis.

The method of Thomas and Clarke is very simple and easy to apply, requiring only the measurement of pen-deflection as a function of temperature, and the value of the peak area. Each DSC trace yields one value for the activation energy of the interfacial reaction. Thomas and Clarke[171] obtained the value E_A = 16.5 ± 0.5 kcal mol^{-1} (α = 0.19 to 0.46) for the dehydration of $Mn(HCOO)_2.2H_2O$, which is in good agreement with other literature values.

The decomposition of $Mn(HCOO)_2.2H_2O$ has also been studied, by DSC, by Nolan and Lemay,[172] who used the more general equation (3) and the simple expression for $d\alpha/dt$ of Thomas and Clarke, i.e. $d\alpha/dt = dH/dt \cdot 1/A$. Systematic variation of the parameters m, n and p, of equation (3), and a least squares analysis of the Arrhenius plots resulting from each equation were accomplished with a computer programme to ascertain which values of m, n and p gave good data-fits. It was found that a wide range of equations and activation energies, corresponding to different stages of the reaction, could be obtained if data-fit were the only criterion used. For the particular values m = n = p = 0, they obtained a value E_A = 17.3 ± 0.1 kcal mol^{-1} (α 0 to 0.7) for the interfacial reaction, which agrees well with the result of Thomas and Clarke.[171] A number of techniques have been used by other workers[173-175] to obtain an activation energy for interfacial advance in the dehydration of $Mn(HCOO)_2.2H_2O$ as 17 ± 1 kcal mol^{-1}.

Other,[176-182] quite independent methods have been described

(and criticised) by which DSC thermograms may be analysed to yield kinetic data. Draper[183] has developed a theory of heterogeneous reactions which is independent of the Arrhenius equation. He assumes that such reactions have zero activation energy and that the rate determining step is the heat exchange between the reacting material and the environment. The theory has been successfully applied[183,184] to the decomposition of $CaCO_3$ and of $BaCl_2.2H_2O$. However, this approach has not been widely adopted.

It would seem that the application by Nolan and Lemay[172] of the theory by Šesták and Berggren[161] is the best general approach to the calculation of kinetic data from DSC traces. For work confined to the interfacial reaction, the method of Thomas and Clarke[171] would appear to be satisfactory, provided that the range of α, to which the calculated activation energy refers, is small and defined.

The method of Thomas and Clarke[171] has been used by House et al.[185-188] in the kinetic interpretation of DSC data for some palladium(II) complexes, PdX_2L_2, where L is a (substituted) pyrazine or (substituted) pyridine. A very recent (1974) report by House and Lau[189] has given the activation energy values for two benzoxazole complexes and one benzothiazole complex of the palladium dihalides. However, House et al.[185-189] have not reported the α ranges to which any of their E_A values refer, nor have they emphasised that E_A represents the energy of activation for the interfacial reaction. No log C values were calculated.

9.2 Kinetic data for the interfacial reaction of some solid-state decompositions

Since the full analysis of the DSC data to obtain E_A values following the method of Nolan and Lemay[172] was not practicable, the method of Thomas and Clarke[171] was applied to the decomposition of some of the transition-metal complexes for which enthalpy data are reported in this thesis. In all cases the E_A data reported (and log C and α range values) are the mean of at least four determinations and the error associated with E_A is the standard deviation of the mean. The error on log C is of the order of ±0.5.* The values of the pen-deflection, dH/dt, were measured by ruler. The agreement of these simple measurements with those obtained using a Leytool Micro-divider Setter, British Patent No. 685106, which is capable of measuring distances between 0.25 and 6.00 inches in magnitude to the nearest one thousandth of an inch, is shown in Table 9.1. The error in the ruler data is seen to be rarely more than 1%. The ruler measurement method was used throughout, since the use of the Micro-divider Setter is rather tedious.

Figure 9.1 shows the Thomas and Clarke[171] plot for the second decomposition peak of $CoCl_2(2MeBT)_2$, using the initial set of data, Trace A, in Table 9.1. The error on the lower limit of the ranges quoted in this thesis is likely to be of the order of 5 to 10%, since large errors will be incurred in the measurement of the very small dH/dt values. Also, the partial area, from which the lower limit of the α range is calculated, is the small difference between two large areas measured by a planimeter. Only those DSC

Table 9.1 The measurement of the pen deflection values, dH/dt $CoCl_2(2MeBT)_2$: second decomposition peak

Temperature °K	Pen deflection x 10 (in) ruler	Pen deflection x 10 (in) setter*	~% Error
TRACE A			
560	8.3	8.38	1
555	8.0	7.88	1
550	6.9	7.00	1
545	5.7	5.90	3
540	4.9	4.88	-
535	3.8	3.84	1
530	3.0	2.89	3
525	2.2	----[a]	-
520	1.6	----[a]	-
TRACE B			
565	11.1	11.10	-
560	11.1	11.25	1
555	10.0	10.00	-
550	8.4	8.37	-
545	6.6	6.64	1
540	5.3	5.30	-
535	4.0	4.02	-
530	2.9	2.90	-
525	2.0	----[a]	-
520	1.3	----[a]	-

* Leytool Micro-divider Setter. British Patent No. 685106

a These very small dH/dt values were not measurable by the setter.

Figure 9.1. Thomas and Clarke[171] plot for the second decomposition peak of $CoCl_2(2MeBT)_2$

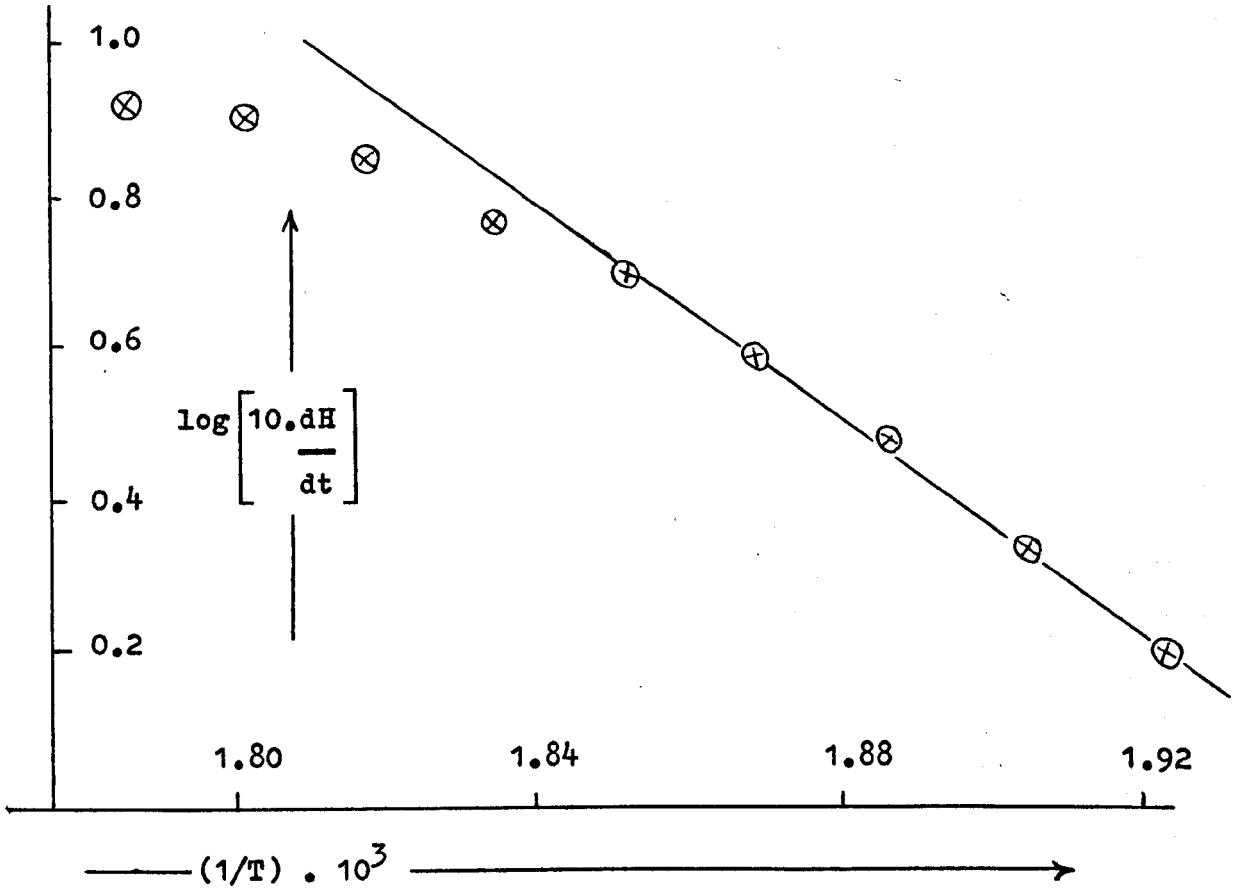

T = temperature ^{o}K

dH/dt = pen deflection in inches

E_A = 32.5 kcal mol^{-1}

DSC peak area = 1.35 sq ins

log C = 12.8

plot is linear over the temperature range 521 - 540 ^{o}K

peaks which were well-shaped were used to obtain kinetic information.

The kinetic data for the decomposition of sodium bicarbonate were evaluated by the Thomas and Clarke[171] method, as a check on the validity of the procedure. The data obtained are given in Table 9.2 along with other literature values. Good agreement is observed between the data calculated by the Thomas and Clarke method and the data from other techniques.

Table 9.3 and 9.4 report the kinetic data obtained for the decomposition of some $PtXMeZ_2.L$ and $IrX(CO)(PPh_3)_2.L$ complexes, respectively, where L is C_2F_4 or C_4F_6. Table 9.5 reports the data for the decomposition of some CoX_2L_2 complexes, where L is a halogenopyridine. Kinetic data for the decomposition of MX_2L_2 complexes, where L is benzothiazole, 2-methylbenzothiazole, benzoxazole or 2,4-dimethylthiazole, are reported in Table 9.6.

The interpretation of all these kinetic data is not simple. The discussion of the values in Tables 9.3 to 9.6 has been restricted to qualitative observations and general ideas concerning the kinetic process under observation.

Brennan et al.[35] and Heuvel and Lind[196] have pointed out that although the drawing in of the scanning baseline for each DSC peak incurs little error on the enthalpy measurement, kinetic data are likely to be in error. This is because the values for pen-deflection should strictly be taken between the traced peak and a baseline which has allowed for the change in specific heat of the material during the decomposition. However, the errors involved are likely to be greatest at very low α values near the beginning of the peak, in the region where the Thomas and Clarke method[171] for

Table 9.2 Kinetic data for the decomposition of sodium bicarbonate

$NaHCO_3$ (c) $\longrightarrow$ $\frac{1}{2}Na_2CO_3$ (c) + $\frac{1}{2}CO_2$ (g) + $\frac{1}{2}H_2O$ (g)

technique	E_A kcal mol^{-1}	log C	α-range	n*	reference
DSC[a]	20.7 ± 0.7	10.4	0.07 - 0.38	0	this work
DSC[b]	24.1	10.9	0.49 - 0.94	1.1	165
↕	26.9	12.9	0.01 - 0.96	1.1	165
↕	27.0	14.9	0.03 - 0.72	1.0	165
DSC[b]	33.3	14.8	0.01 - 0.49	0.23	165
TGA	20 ± 2	----	- - - - - -	1.0	190
DTA	20 ± 2	----	- - - - - -	1.0	191,192
TGA	25	----	- - - - - -	0.79	193
DTA	22 - 24	----	- - - - - -	0.83	193
DTA	20	----	- - - - - -	1.0	194
DTA	22.6	----	- - - - - -	1.0	195

* The quantity "n" is not strictly analogous to the order of reaction of ideal gas kinetics.

a Calculated from equation 8.

b Calculated from equation 7.

the evaluation of kinetic data is inoperable. Errors will still persist at slightly greater α values which come within the range of the quoted α values.

9.2.1 $PtXMeZ_2.L$

The salient features that emerge from the data of Table 9.3 are the following.

(a) For complexes (4) and (6), the E_A values are very similar. The E_A value for compound (4), where Z is $AsMe_3$, is only slightly greater than that for complex (6), where Z is $AsPhMe_2$.

(b) For complexes (3) and (4), where L is C_4F_6, the E_A values are also very similar, although that for the bromo complex is a little greater than that for the chloro complex.

(c) For complexes (1) and (2), where L is C_2F_4, the E_A values are much greater than those for the complexes (3), (4) and (6), where L is C_4F_6.

(d) Whereas for the C_4F_6 complexes, (3) and (4), halogen change has little effect on E_A, for the complexes (1) and (2), where L is C_2F_4, the change of halogen from Cl to Br has a marked effect on the E_A value.

(e) Complex (5) has a different decomposition path from the others and cannot be included in the comparisons.

(f) In all cases, the activation energy is much greater than the enthalpy of decomposition, by a factor of 2 or 3 for the C_4F_6

Table 9.3 Activation parameters for the interfacial reaction in the thermal decomposition of $PtXMeZ_2.L$

$$PtXMeZ_2.L\ (c) \longrightarrow PtXMeZ_2\ (c) + L\ (g)$$

Complex				ΔH_{dec} [a]	E_A	log C	α range
No.	Z	X	L	← kcal mol^{-1} →			
1	$AsMe_3$	Cl	C_2F_4	12	86.2 ± 0.9	50.2	0.06 - 0.24
2	$AsMe_3$	Br	C_2F_4	12	67.5 ± 1.2	38.4	0.06 - 0.51
3	$AsMe_3$	Cl	C_4F_6	16	39.0 ± 0.5	22.4	0.01 - 0.21
4	$AsMe_3$	Br	C_4F_6	15	41.6 ± 0.7	23.9	0.03 - 0.32
5	$AsMe_2Ph$	Cl	C_4F_6	18	*27.2 ± 0.5	17.2	0.05 - 0.30
					*22.3 ± 0.5	13.3	0.50 - 0.74
6	$AsMe_2Ph$	Br	C_4F_6	19	38.6 ± 1.2	23.9	0.07 - 0.49

a Only approximate ΔH_{dec} values are given here; more detailed data are given in Table 7.2.

* These are the E_A values for the two distinct, although not completely separated, peaks.

complexes, and a factor of 6 or 7 for the C_2F_4 complexes. For complex (3) the activation energy of 39.0 kcal mol^{-1} is virtually the mean of the observed enthalpy of decomposition, 16.4 ± 0.2 kcal mol^{-1}, and the calculated bond energy, E(Pt - C_4F_6), of 67.4 kcal mol^{-1}.

The most interesting of these points is the much higher E_A values noted for the C_2F_4 complexes. It would appear then that the energy "hump" to be surmounted for decomposition to occur is much less for the C_4F_6 complexes than for the C_2F_4 complexes, although the enthalpy data (Table 8.2) indicate that the C_4F_6 complexes are the more thermodynamically stable complexes. A possible reason for the observed E_A order is that in platinum(II) - acetylene complexes only one of the π-orbitals of the acetylene is used in bonding to the platinum atom. The other π-orbital may be synergically destabilised[109,197] allowing it to act as a Lewis base and so take part in reactions which the free acetylene could not do. It may be that this destabilisation leads to a decomposition process of lower E_A.

To the extent that the stability of the complexes depends on the kinetic trans effect of the ligand Z, in the transition state for decomposition, one might expect the complex, where Z is $AsMe_2Ph$, to have a lower E_A value than that where Z is $AsMe_3$. The electron-withdrawing phenyl group will increase the $d\pi - d\pi$ back-coordination, Pt → As, which will in turn tend to decrease the $d - \pi^*$ component of the platinum-acetylene bond, thereby enhancing the dissociation of the C_4F_6 molecule. This effect does not appear to be very important here, however.

The reason for the dependence of the E_A values for the C_2F_4 complexes on the nature of the ligand X as compared with the results for the C_4F_6 complexes is not apparent.

9.2.2 $\underline{IrX(CO)(PPh_3)_2.L}$

The kinetic data for some of these complexes are reported in Table 9.4. Although a great deal of data for activation energies for the formation and dissociation of other oxidative adducts of $IrX(CO)(PPh_3)_2$ with simple molecules such as oxygen has been obtained, such data refer mainly to the complexes in solution. However, a recent report by Ball and Pope[9] refers to a study of the kinetics of addition of hydrogen chloride gas to the solid complex, $IrCl(CO)(PPh_3)_2$, to give the trans-octahedral species. The kinetics of dehydrochlorination of both the cis and trans chloro isomers has also been studied. Their results will be referred to later.

A consideration of the data in Table 9.4 shows that no general trends in the value of E_A with variation of X or L can be observed. Unlike the $PtXMeZ_2.L$ complexes, there is no clear distinction between the E_A values for the C_2F_4 and C_4F_6 complexes. The E_A values for both $IrF(CO)(PPh_3)_2.C_4F_6$ and $IrCl(CO)(PPh_3)_2.C_2F_4$ are significantly higher than the other E_A values in Table 9.4. The E_A values in this Table are between 1.5 and 2.5 times the enthalpy of decomposition values, except for $IrCl(CO)(PPh_3)_2.C_4F_6$, where E_A and ΔH_{dec} are very similar. The comparison of values in Table 9.4 with each other is complicated by the recognition that the C_2F_4 and C_4F_6 complexes do not have the same stereochemistry, unlike the case

Table 9.4 Activation parameters for the interfacial reaction in the thermal decomposition of $IrX(CO)(PPh_3)_2 \cdot L$

$$IrX(CO)(PPh_3)_2 \cdot L\ (c) \longrightarrow IrX(CO)(PPh_3)_2\ (c) + L\ (g)$$

Complex		ΔH_{dec} [a]	E_A	log C	α range
X	L	kcal mol^{-1}	kcal mol^{-1}		
F	C_4F_6	24	53.6 ± 0.5	24.4	0.21 - 0.48
Cl	C_4F_6	23	20.1 ± 0.5	10.0	0.35 - 0.65
Br	C_4F_6	19	31.5 ± 0.7	15.3	0.07 - 0.42
F	C_2F_4	19	34.0 ± 0.6	15.4	0.09 - 0.57
Cl	C_2F_4	17	42.4 ± 1.4	18.5	0.51 - 0.75

a Only approximate ΔH_{dec} values are given here; more detailed data are given in Table 7.1.

of the $PtXMeZ_2.L$ complexes.

However, a general comparison of the data in Table 9.4 with those in Table 9.3 may be made. It is seen that the E_A values for the $PtXMeZ_2.L$ complexes are, on the whole, rather higher than those for the $IrX(CO)(PPh_3)_2.L$ complexes. Kinetic stability is generally thought to depend on the size of the energy gap between the highest filled ligand orbital and the lowest unfilled ligand orbital.[198] The results indicate that the orbital separation referred to is smaller in the iridium(I) complexes than in the platinum(II) complexes.

Ball and Pope[9] have obtained values for the activation energy, E_A, and enthalpy of decomposition, ΔH_{dec}, of the complex, cis-$Ir(H)Cl_2(CO)(PPh_3)_2$. These E_A and ΔH_{dec} values are of the same order of magnitude as the E_A and ΔH_{dec} values of the $IrX(CO)(PPh_3)_2.L$ complexes of Table 9.4. Ball and Pope propose that the transition-state is a five-coordinate species of the type shown below, rather than a distorted six-coordinate one.

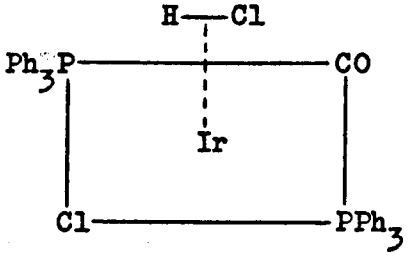

9.2.3 Halogenopyridine complexes of cobalt(II), CoX_2L_2

The activation parameters for the interfacial reaction in the thermal decomposition of some CoX_2L_2 complexes, where X is Cl or Br; L is 2-chloro, 2-bromo, 3-chloro or 3-bromopyridine, are reported in Table 9.5. Unlike the $PtXMeZ_2.L$ and $IrX(CO)(PPh_3)_2.L$ complexes, these complexes do not necessarily decompose in a single stage. The decomposition stage, to which the E_A data refer, is indicated in Table 9.5.

For complexes of the 2-halogenopyridines, there is great similarity in E_A values, the mean being 31.2 kcal mol^{-1}. For these complexes the E_A value refers to decomposition in one stage to the cobalt(II) halide. The E_A values are very similar to the corresponding ΔH_{dec} values.

For complexes of the 3-halogenopyridines, kinetic data are given for both the first and second steps of the decomposition. The E_A values for the loss of the first ligand are rather higher for the 3-bromopyridine complexes, whilst all the E_A values for the loss of the second ligand are very similar. For all the 3-halogenopyridine complexes, the E_A value is approximately twice the ΔH_{dec} value.

The most interesting feature of the results in Table 9.5, taken as a whole, is the remarkable similarity in E_A values. However, the complexes of the 2-halogenopyridines are tetrahedral, whilst the complexes of the 3-halogenopyridines, CoX_2L_2, and the intermediates, CoX_2(3-halogenopyridine), are octahedral. This structural difference precludes any further comparison of the data.

Table 9.5. Activation parameters for the interfacial reaction in the thermal decomposition of the complexes, CoX_2L_2, where L is a halogenopyridine and X is Cl or Br

$$CoX_2L_x\ (c) \longrightarrow CoX_2L_y\ (c) + (x - y)L\ (g)$$

Complex	Reaction x	Reaction y	ΔH [a] kcal mol^{-1}	E_A kcal mol^{-1}	log C	α range
L = 2-chloropyridine						
$CoCl_2L_2$	2	0	28	32.3 ± 0.4	14.4	0.01 - 0.38
$CoBr_2L_2$	2	0	30	30.3 ± 0.8	13.3	0.01 - 0.38
L = 2-bromopyridine						
$CoCl_2L_2$	2	0	30	32.5 ± 1.0	14.4	0.04 - 0.41
$CoBr_2L_2$	2	0	31	29.5 ± 0.3	12.6	0.04 - 0.58
L = 3-chloropyridine						
$CoCl_2L_2$	2	1	15	26.3 ± 0.3	11.9	0 - 0.57
	1	0	18	33.9 ± 2.9	12.7	0.05 - 0.28
$CoBr_2L_2$	2	1	17	28.8 ± 0.4	12.6	0.03 - 0.54
	1	0	17	30.7 ± 2.3	11.7	0.02 - 0.49
L = 3-bromopyridine						
$CoCl_2L_2$	2	0	14	33.2 ± 0.9	14.1	0.10 - 0.48
	1	0	18	30.9 ± 0.7	11.2	0.07 - 0.50
$CoBr_2L_2$	2	0	16	33.8 ± 1.4	14.4	0.04 - 0.45
	1	0	18	31.8 ± 1.9	11.9	0.09 - 0.58

a Only approximate ΔH values are given here; more detailed data for the stepwise heats of decomposition are given in Table 5.1.

9.2.3 Azole complexes, $MX_2(azole)_2$

Kinetic data for these complexes are reported in Table 9.6. The benzothiazole complexes show a remarkable complexity of decomposition pathways. Hence, E_A data for $MX_2(benzothiazole)_2$ are not very amenable to comparison, since the data refer to different decomposition stages. The E_A values for the decomposition stages of $MX_2(BT)_2$ are, in general, rather higher than those observed for the halogenopyridine complexes. Ratios of E_A : ΔH_{dec} for the benzothiazole complexes vary from 5 : 1 to 1 : 1.

House and Lau[189] quote a few data for some palladium(II) complexes of benzothiazole and benzoxazole, obtained also by the same Thomas and Clarke[171] method. Their results are summarised below,

Complex	ΔH_{dec} kcal mol^{-1}	E_A kcal mol^{-1}	E_A : ΔH_{dec}
$PdCl_2(BO)_2$	36 ± 2	34 ± 1	$\simeq$ 1 : 1
$PdI_2(BO)_2$	31 ± 1	20 ± 2	$\simeq$ 1 : 1.5
$PdI_2(BT)_2$	39 ± 1	24 ± 1	$\simeq$ 1 : 1.5

where E_A and ΔH_{dec} refer to the single stage decomposition to PdX_2. For two of these palladium complexes, $\Delta H_{dec} > E_A$. For an endothermic reaction, the propagation of the reactant-product interface has an energy of activation approximately the same as, or greater than, the enthalpy of decomposition.[199,200] This has been the case for the complexes for which E_A and ΔH_{dec} data are reported in this thesis.

Table 9.6. Activation parameters for the interfacial reaction in the thermal decomposition of the complexes, MX_2L_2, where L is an azole ligand

$$MX_2L_x\ (c) \longrightarrow MX_2L_y\ (c) + (x - y)L\ (g)$$

Complex	Reaction x	Reaction y	ΔH [a] kcal mol^{-1}	E_A kcal mol^{-1}	log C	α range
L = benzothiazole						
$MnCl_2L_2$	2	$\frac{1}{3}$	23	35.8 ± 0.7	15.7	0.03 - 0.50
	$\frac{1}{3}$	0	12	39.6 ± 2.8	14.8	0.09 - 0.43
$CoCl_2L_2$	2	-*	--*	28.7 ± 1.6	11.6	0.03 - 0.53
$NiCl_2L_2$	2	$\frac{1}{3}$	22	39.1 ± 2.1	16.6	0.02 - 0.50
	$\frac{1}{3}$	0	11	58.0 ± 1.0	22.3	0 - 0.39
$CdCl_2L_2$**	2	1	17	37.5 ± 1.4	18.0	0.05 - 0.37
$CdBr_2L_2$	2	$\frac{3}{4}$	16[b]	47.0 ± 0.9	24.4	0.03 - 0.19
	$\frac{3}{4}$	0	20	21.9 ± 0.8	9.0	0.10 - 0.79
L = 2-methylbenzothiazole						
$CoCl_2L_2$	2	1	19[b]	90.3 ± 2.5	44.7	0.04 - 0.19
	1	0	21	34.9 ± 1.6	13.7	0.03 - 0.36
$CoBr_2L_2$	2	1	18[b]	37.1 ± 1.2	17.3	0.06 - 0.39
	1	0	21	35.2 ± 0.6	13.2	0.04 - 0.62

a Only approximate ΔH values are given here; more detailed data for the stepwise heats of decomposition are given in Table 5.1.

* The DSC traces for this complex show two peaks, but these are not separated. No stepwise enthalpy data were calculated.

** The second peak was not suitable for kinetic analysis.

b These peaks were composite; the peak is followed by a plateau before the pen returns to the baseline.

Table 9.6. (cont.) Activation parameters for the interfacial reaction in the thermal decomposition of the complexes, MX_2L_2, where L is an azole ligand

$$MX_2L_x\ (c) \longrightarrow MX_2L_y\ (c) + (x - y)L\ (g)$$

Complex	Reaction x	Reaction y	ΔH [a] kcal mol^{-1}	E_A kcal mol^{-1}	log C	α range
L = benzoxazole						
$CoCl_2L_2$**	2	1	16	28.7 ± 0.4	13.8	0 - 0.37
$CoBr_2L_2$	2	1	16	22.2 ± 0.6	9.8	0.17 - 0.74
	1	0	18	28.9 ± 0.6	11.3	0.05 - 0.63
L = 2,4-dimethylthiazole						
$CoCl_2L_2$	2	1	14	19.3 ± 0.5	9.5	0.03 - 0.31
	1	0	16	28.7 ± 0.4	12.4	0.11 - 0.60

a Only approximate ΔH values are given here; more detailed data for the stepwise heats of decomposition are given in Table 5.1.

** The second peak was not suitable for kinetic analysis.

Table 9.6 contains data for three complexes, $CdBr_2(BT)_2$, $CoCl_2(2MeBT)_2$ and $CoBr_2(2MeBT)_2$ which give DSC peaks of a composite nature. The very high E_A values for the first decomposition stages of $CdBr_2(BT)_2$ and $CoCl_2(2MeBT)_2$ suggest that a very different type of transition-state is involved in these decompositions. The E_A value for the second decomposition stage of $NiCl_2(BT)_2$ would also appear to be anomalously high. It is possible that the higher E_A values correspond to decomposition stages where both decomposition and fusion are proceeding.

The calculation of kinetic data from DSC traces is, therefore, relatively simple. The difficulty with the halogenopyridine and azole complexes lies in interpreting these data, since the nature of the decompositions ensures that comparisons are not meaningful. House et al.[185-189] have interpreted their data for PdX_2L_2 complexes, where L is a substituted pyridine, in terms of the basicity of the ligands. However, the limited number of heterocyclic ligands, L, in the complexes MX_2L_2, for which E_A data are reported here, precludes this type of interpretation.

(Due to a calculation error, the log C values reported in this thesis are too large by a factor of two units, and the uncertainty associated with them should be increased to ± 1.)

REFERENCES

1. Halpern, J. (1970). Accounts Chem. Res., 3, 386
2. Vaska, L. (1968). Accounts Chem. Res., 1, 335
3. La Placa, S.J. and Ibers, J.A. (1965). J.Amer. Chem. Soc., 87, 2581
4. Ibers, J.A. and La Placa, S.J. (1964). Science, 145, 920
5. McGinnety, J.A., Doedens, R.J. and Ibers, J.A. (1967). Inorg. Chem., 6, 2243
6. McGinnety, J.A. and Ibers, J.A. (1968). Chem. Comm., 235
7. Ashcroft, S.J. and Mortimer, C.T. (1971). Inorg. Chem., 10, 1326
8. Ashcroft, S.J. and Mortimer, C.T. (1970). J. Organometallic Chem., 24, 783
9. Ball, M.C. and Pope, J.M. (1973). J. Chem. Soc. Dalton., 1802
10. Cox, J.D. and Pilcher, G. (1970). Thermochemistry of Organic and Organometallic Compounds, (London : Academic Press)
11. Dascent, W.E. (1970) Inorganic Energetics,(Penguin Library of Physical Sciences : Chemistry)
12. Mortimer, C.T. (1962) Reaction Heats and Bond Strengths, (Oxford : Pergamon Press)
13. Watson, E.S., O'Neill, M.J., Justin, J. and Brenner, N. (1964) Anal. Chem., 36, 1233
14. O'Neill, M.J. (1964). Anal. Chem., 36, 1238
15. Thermal Analysis Newsletter (1970). No. 9 (Perkin-Elmer Corporation, Norwalk, Conn., U.S.A.)
16. Brennan, W.P. (1971). Ph.D. thesis : Theory and Practice of Thermoanalytical Calorimetry, Princeton Univ. N.J.

17. Stull, D.R. and Sinke, G.C. (1956). Thermodynamic Properties of the Elements, (Adv. in Chem. Series, 18 : Amer. Chem. Soc.)

18. Gardiner, K.W., Klaver, R.F., Baumann, F. and Johnson, J.F. (1962). Gas Chromatography, Chap. 24, 349 (N.Brenner, J.E.Callen and M.D.Weiss editors) (New York : Academic Press)

19. Barrall, E.M.(II) and Johnson, J.F. (1970). Tech. Methods Polym. Eval., 2, 1

20. Schwenker, R.F.Jr. and Whitwell, J.C. (1968). Proc. Amer. Chem. Soc. Symp. Analytical Calorimetry, 249 , (R.S.Porter and J.F.Johnson editors) (Plenum Press : New York)

21. Technical Note, 270 - 3, (1968). Nat. Bur. of Standards

22. Technical Note, 270 - 4, (1969). Nat. Bur. of Standards

23. Circular 500, (1952). Nat. Bur. of Standards

24. Wendlandt, W.W. (1964). Chem. Analyst, 53, 71 (pub. by J.T.Baker, Chem. Co., New Jersey, U.S.A.)

25. Beech, G., Mortimer, C.T. and Tyler, E.G. (1967). J. Chem. Soc. (A), 925

26. Allan, J.R., Brown, D.H., Nuttall, R.H. and Sharp, D.W.A. (1964). J. Inorg. Nucl. Chem., 26, 1895

27. Gray, A.P. (1968). Proc. Amer. Chem. Soc. Symp. Analytical Calorimetry, 209 (R.S.Porter and J.F.Johnson editors) (Plenum Press : New York)

28. Thermal Analysis Newsletter, (undated). No. 5 (Perkin-Elmer Corporation, Norwalk, Conn., U.S.A.)

29. Pella, E. and Nebuloni, M. (1971). J. Thermal Anal., 3, 229

30. O'Neill, M.J. (1966). Anal. Chem., 38, 1331

31. Thermal Analysis Newsletter (undated). No. 3 (Perkin-Elmer Corporation, Norwalk, Conn., U.S.A.)

32. Ginnings, D.C. and Furukawa, G.T. (1957). J. Amer. Chem. Soc., 75, 522

33. Kubaschewski, O. and Evans, E.LL. (1958). Metallurgical Thermochemistry, (London : Pergamon Press)

34. Beech, G. (1967). Ph.D. thesis : The Thermochemistry of some Transition Metal Complexes, Keele Univ. England

35. Brennan, W.P., Miller, B., and Whitwell, J.C. (1969). Ind. Eng. Chem. Fundam., 8, 314

36. Thermal Analysis Newsletter (1972). No. 10 (Perkin-Elmer Corporation, Norwalk, Conn., U.S.A.)

37. O'Neill, M.J. and Fyans, R.L. (1971). Eastern Analytical Symposium New York, Design of Differential Scanning Calorimeters and the Performance of a New System. (available from the Perkin-Elmer Corporation)

38. Instrument News. (1972). 22, No. 1E (Perkin-Elmer Corporation, Norwalk, Conn., U.S.A.)

39. O'Neill, M.J. and Gray, A.P. (1971). Thermal Analysis, 1, 279 Proc. Third I.C.T.A. Davos.

40. Rogers, R.N. and Morris, E.D.Jr. (1966). Anal. Chem., 38, 410

41. Brewer, L., Somayajulu, G.R. and Brackett, E. (1963). J.Amer.Chem.Soc., 63, 111

42. Kulkarni, M.P. and Dadape, V.V. (1971). High Temp. Sci., 3, 277

43. Beech, G. and Lintonbon, R. (1971). Thermochim. Acta, 2, 86

44. Ashcroft, S.J. (1971). Thermochim. Acta, 2, 512

45. Langmuir, I. (1913). Phys. Rev., 2, 329

46. Duff, E.J., Hughes, M.N. and Rutt, K.J. (1968). J. Chem. Soc. (A), 2354

47. Duff, E.J., Hughes, M.N. and Rutt, K.J. (1969). J. Chem. Soc. (A), 2101

48. Duff, E.J. and Hughes, M.N. (1968). J. Chem. Soc. (A), 2144

49. Duff, E.J. (1970). J. Inorg. Nucl. Chem., 32, 3103

50. Nicholls, D. and Warburton, B.A. (1970). J. Inorg. Nucl. Chem., 32, 3871

51. Bagley, M.J., Nicholls, D. and Warburton, B.A. (1970). J. Chem. Soc. (A), 2694

52. Nicholls, D. and Warburton, B.A. (1971). J. Inorg. Nucl. Chem., 33, 1041

53. Reedjik, J. (1969). Recl. Trav. Chim. Pays-Bas, 88, 1451

54. Reedjik, J. (1970). Recl. Trav. Chim. Pays-Bas, 89, 605

55. Reedjik, J. (1970). Recl. Trav. Chim. Pays-Bas, 89, 993

56. Reedjik, J. (1971). Recl. Trav. Chim. Pays-Bas, 90, 117

57. Reedjik, J., Windhorst, J.C.A., Van Ham, N.H.M. and Groeneveld, W.L. (1971). Recl. Trav. Chim. Pays-Bas, 111, 235

58. Van Leeuwen, P.W.N.M. and Groeneveld, W.L. (1967). Inorg. Nucl. Chem. Letters, 3, 145

59. Billing, D.E. and Underhill, A.E. (1968). J. Chem. Soc. (A), 29

60. Beech, G., Mortimer, C.T. and Tyler, E.G. (1967). J. Chem. Soc. (A), 1111

61. Das, A.K. and Ramana Rao, D.V. (1970). J. Inst. Chemists (India), XLII, 127

62. Mohapatra, B.K. and Ramana Rao, D.V. (1971). Ind. J. Chem., 9, 715

63. Eilbeck, W.J., Holmes, F. and Underhill, A.E. (1967). J. Chem. Soc. (A), 757

64. Hughes, M.N. and Rutt, K.J. (1970). J. Chem. Soc. (A), 3015

65. Weaver, J.A., Hambright, P., Talbert, P.T., Kang, E. and Thorpe, A.N. (1970). Inorg. Chem., 9, 268

66. Duff, E.J., Hughes, M.N. and Rutt, K.J. (1969). J. Chem. Soc. (A), 2126

67. Duff, E.J. and Hughes, M.N. (1969). J. Chem. Soc. (A), 477

68. McWhinnie, W.R. (1965). J. Inorg. Nucl. Chem., 27, 2573

69. Gill, N.A. and Kingdon, H.J. (1966). Aust. J. Chem., 19, 2197

70. Ocone, L.R., Soulen, J.R. and Block, B.P. (1960). J. Inorg. Nucl. Chem., 15, 76

71. Brown, D.H., Nuttall, R.N. and Sharp, D.W.A. (1964). J. Inorg. Nucl. Chem., 26, 1151

72. Ahuja, I.S., Brown, D.H., Nuttall, R.H. and Sharp, D.W.A. (1965). J. Inorg. Nucl. Chem., 27, 1105

73. Hacker, M.J. (1972). Ph.D. thesis : Univ. of Leicester

74. Clarke, B., Green, M. and Stone, F.G.A. (1970). J. Chem. Soc. (A), 951

75. Baddley, W.H. (1968). J. Amer. Chem. Soc., 90, 3705

76. Vaska, L. and Peone, J. (1971). Chem. Comm., 418

77. Fitzgerald, R.J., Sakkab, N.Y., Strange, R.S. and Narutis, V. (1973). Inorg. Chem., 12, 1081

78. Clark, H.C. and Puddephatt, R.J. (1971). Inorg. Chem., 10, 18

79. Clark, H.C. and Puddephatt, R.J. (1970). Inorg. Chem., 9, 2670

80. Clark, H.C. and Puddephatt, R.J. (1970). Chem. Comm., 92

81. Allan, J.R., Brown, D.H., Nuttall, R.H. and Sharp, D.W.A. (1965). J. Inorg. Nucl. Chem., 27, 1529

82. Beech, G., Mortimer, C.T. (1967). J. Chem. Soc. (A), 1115

83. Beech, G. Mortimer, C.T. and Tyler, E.G. (1969). J. Chem. Soc. (A), 512

84. Ablov, A.V. and Konunova, Ts. B. (1963) Russ. J. Inorg. Chem., 8, 582

85. Albert, A., Goldacre, R. and Phillips, J. (1948). J. Chem. Soc., 2240

86. Katritzky, A.R. and Lagowski, J.M. (1960). Heterocyclic Chemistry, (London : Methuen & Co. Ltd.)

87. Pettit, L.D. (1971). Quart. Rev., 25, 1

88. Nelson, S.M. and Shepherd, T.M. (1965). Inorg. Chem., 4, 813

89. Lever, A.B.P., Nelson, S.M. and Shepherd, T.M. (1965). Inorg. Chem., 4, 810

90. King, H.C.A., Körös, E. and Nelson, S.M. (1963). J. Chem. Soc., 5449

91. King, H.C.A., Körös, E. and Nelson, S.M. (1964). J. Chem. Soc., 4832

92. Wong, P.T.T. and Brewer, D.G. (1968). Canad. J. Chem., 46, 131

93. Cabral, J. de O., King, H.C.A., Nelson, S.M., Shepherd, T.M. and (in part) Körös, E. (1966). J. Chem. Soc. (A), 1348

94. Gill, N.S., Nuttall, R.H., Scaife, D.E. and Sharp, D.W.A. (1961). J. Inorg. Nucl. Chem., 18, 79

95. Nyholm, R.S. (1951). J. Chem. Soc., 3245

96. Burstall, F. and Nyholm, R.S. (1952). J. Chem. Soc., 3570

97. Abel, E.W., Bennett, M.A. and Wilkinson, G. (1959). J. Chem. Soc., 2325

98. Elder, R.C. (1968). Inorg. Chem., 7, 1117

99. Elder, R.C. (1968). Inorg. Chem., 7, 2316

100. Roberts, J.D. and Caserio, M.C. (1965). Basic Principles of Organic Chemistry, (New York : W.A.Benjamin, Inc.)

101. Lever, A.B.P., Lewis, J. and Nyholm, R.S. (1964). J. Chem. Soc., 4761

102. Elderfield, R.C. (1957). Heterocyclic Chemistry, 6, (New York : John Wiley & Sons, Inc.)

103. Epstein, L.M., Straub, D.K. and Maricondi, C. (1967). Inorg. Chem., 6, 1720

104. Brown, H.C., Gintis, D. and Podall, H. (1956). J. Amer. Chem. Soc., 78, 5375

105. Orgel, L.E. (1960). Introduction to Transition Metal Chemistry, (London : Methuen)

106. Taylor, C.E. and Underhill, A.E. (1969). J. Chem. Soc.(A),368

107. Ferraro, J.R. (1971). Low Frequency Vibrations of Inorganic and Coordination Compounds, (New York : Plenum Press)

108. Parshall, G.W. and Jones, F.N. (1965) J. Amer. Chem. Soc., 87, 5356

109. Pettit, L.D. and Barnes, D.S. (1972). Topics in Current Chemistry, 28, 85 (Springer Verlag : Berlin)

110. Hartley, F.R. (1973). Chem. Rev., 73, 163

111. Hartley, F.R. (1969). Chem. Rev., 69, 799

112. Coulson, D.R. (1969). J. Amer. Chem. Soc., 91, 200

113. Chatt, J., Rowe, G.A. and Williams, A.A. (1957). Proc. Chem. Soc., 208

114. Chatt, J. (1961) Chimica Inorganica Accad. Nazl. Lincei, Roma. 113

115. Greaves, E.O., Lock, C.J.L. and Maitlis, P.M. (1968). Canad. J. Chem., 46, 3879

116. Pannatoni, C., Bombieri, G. and Belluco, V., and Baddley,W.H. (1968). J. Amer. Chem. Soc., 90, 798

117. Boston, J.L., Grim, S.O. and Wilkinson, G. (1963). J. Chem. Soc., 3468

118. Mays, M.J. and Wilkinson, G. (1965). J. Chem. Soc., 6629

119. Tsumura, R. and Hagihara, N. (1965). Bull. Chem. Soc. Japan, 38, 861

120. Miller, F.A. and Baumann, R.P. (1954). J. Chem. Phys., 22, 1544

121. Davies, B.N., Puddephatt, R.J. and Payne, N.C. (1972). Canad. J. Chem., 50, 2276

122. Sheehan, W.F. and Schomaker, V. (1952). J. Amer. Chem. Soc., 74, 4468

123. Dowlings, J.M. and Stoicheff, B.P. (1959). Canad. J. Chem., 37, 703

124. Mills, O.S. and Shaw, B.W. (1965). Acta Cryst., 18, 562

125. Francis, J.N., McAdam, A. and Ibers, J.A. (1971) J. Organometallic Chem., 29, 131

126. Mason, R. (1968). Nature, 217, 543

127. McWeeny, R., Mason, R. and Towl, A.D.C. (1969). Discuss. Faraday Soc., 47, 20

128. Kroto, H.W. and Santry, D.P. (1967). J. Chem. Phys., 47, 792

129. Glanville, J.O., Stewart, J.M. and Grim, S.O. (1967). J. Organometallic Chem., 7, 9

130. Clark, H.C. and Puddephatt, R.J. (1971). Inorg. Chem., 10, 416

131. Mason, R., Mingos, D.M.P., Rucci, G. and Connor, J.A. (1972). J. Chem. Soc. Dalton, 1729

132. Cook, C.D., Wan, K.Y., Gelius, U., Hamrin, K., Johansson, G., Olsson, E., Siegbahn, H., Nordling, C. and Siegbahn, K. (1971). J. Amer. Chem. Soc., 93, 1904

133. Mague, J.T. and Wilkinson, G. (1966). J.Chem. Soc. (A),1736

134. Collman, J.P., Vastine, R.D. and Roper, W.R. (1968). J. Amer. Chem. Soc., 90, 2282

135. Deeming, A.J. and Shaw, B.L. (1969). J. Chem. Soc. (A),1802

136. Park, P.J.D. and Hendra, P.J. (1969). Spectrochim. Acta, Part A, 25, 227

137. Adams, D.M., Chatt, J., Gerratt, J. and Westland, A.D. (1964). J. Chem. Soc., 734

138. Cottrell, T.L. (1958). The Strengths of Chemical Bonds, (London : Butterworths)

139. Ibers, J.A., McGinnety, J. and Kime, N. (1967). Abstracts Tenth Int. Conf. on Coordination Chemistry, Tokyo, 93

140. Camia, M., Lachi, M.P., Benzoni, L., Zanzottera, C. and Tacchi Venturi, M. (1970). Inorg. Chem., 9, 251

141. Muir, K.W. and Ibers, J.A. (1969). J. Organometallic Chem., 18, 175

142. McClure, G.L. and Baddley, W.H. (1971). J. Organometallic Chem., 27, 155

143. La Placa, S.J. and Ibers, J.A. (1966). Inorg. Chem., 5, 405

144. Vaska, L. (1966). Science, 152, 769

145. Ashley-Smith, J., Green, M. and Wood, D.C. (1970). J. Chem. Soc. (A), 1847

146. Clarke, B., Green, M., Osborn, R.B.L. and Stone, F.G.A. (1968). J. Chem. Soc. (A), 167

147. Baird, M.C. and Wilkinson, G. (1967). J. Chem. Soc. (A), 865

148. Green, M., Osborn, R.B.L. and Stone, F.G.A. (1970). J. Chem. Soc. (A), 944

149. Weinenger, M.S., Taylor, I.F. and Amma, E.L. (1971). Chem. Comm., 1172

150. Scott, R.N., Shriver, D.F. and Lehmann, D.D. (1970). Inorg. Chim. Acta, 4, 73

151. Vaska, L., Chen, L.S. and Senoff, C.V. (1971). Science, 174, 587

152. Holsboer, F., Beck, W. and Bartunik, H.D. (1973). J. Chem. Soc. Dalton, 1828

153. Griffth, W.P. (1967). The Chemistry of the Rarer Platinum Metals, (London : Interscience)

154. Vaska, L. (1971). Inorg. Chim. Acta, 5, 295

155. Peone, J.Jr. (1971). Ph.D. thesis : Clarkson College of Technology

156. Mortimer, C.T., McNaughton, J.L., Burgess, J., Hacker, M.J., Kemmitt, R.D.W., Bruce, M.I., Shaw, G. and Stone, F.G.A. (1973). J. Organometallic Chem., 47, 439

157. Strohmeier, W. and Fleischmann, R. (1969). Z. Naturforschg. 24b, 1217

158. Duswalt, A.A. (1968). Proc. Amer. Chem. Soc. Symp. Analytical Calorimetry, 313 (R.S.Porter and J.F.Johnson editors) (Plenum Press : New York)

159. Kambe, H., Mita, I. and Horie, K. (1968). Proc. 2nd. Int. Conf. Thermal Analysis, 2, 1071 (R.F.Schwenker Jr. and P.D.Garn editors) (Academic Press Inc. : London)

160. Rogers, R.N. (1972). Thermochim. Acta, 3, 437

161. Sestak, J. and Berggren, G. (1971). Thermochim. Acta, 3, 1

162. Hughes, M.A. (1965). Thermal Analysis 1965, 176 (J.P. Redfern editor) (Macmillan : London)

163. Brindley, G.W., Sharp, J.H. and Achar, B.N.N. (1965). Thermal Analysis 1965, 180 (J.P.Redfern editor) (Macmillan : London)

164. Kauffman, G.B. and Beech, G. (1970). Thermochim. Acta, 1, 99

165. Beech, G. (1969). J. Chem. Soc. (A), 1903

166. Beech, G. and Lintonbon, R.M. (1971). Thermochim. Acta, 3,97

167. Beech, G. and Thompson, F. (1971). Thermochim. Acta, 2, 195

168. Uricheck, M.J. (1966). Instrument News, 17, No. 2 (Perkin-Elmer Corporation, Norwalk, Conn., U.S.A.)

169. Rogers, R.N. and Smith, L.C. (1970). Thermochim. Acta, 1, 1

170. Rogers, R.N. and Morris, E.D.Jr. (1966). Anal. Chem., 38,412

171. Thomas, J.M. and Clarke, T.A. (1968). J. Chem. Soc. (A), 457

172. Nolan, P.S. and Lemay, H.E.Jr. (1973), Thermochim. Acta, 6, 179

173. Eckhardt, R.C. and Flanagan, T.B. (1964). Trans. Faraday Soc., 60, 1289

174. Clarke, T.A. and Thomas, J.M. (1969). J. Chem. Soc. (A), 227

175. Clarke, T.A. and Thomas, J.M. (1969). J. Chem. Soc. (A), 2230

176. Olafsson, P.G. and Bryan, A.M. (1971). J. Polym. Sci., Part B, 9, 521

177. Olafsson, P.G. and Bryan, A.M. (1971). Geochim. et Cosmochim. Acta, 35, 327

178. Kissinger, H.E. (1956). J. Res. Nat. Bur. Stand., 57, 217

179. Kissinger, H.E. (1957). Anal. Chem., 29, 1702

180. Reed, R.L., Weber, L. and Gottfried, B.S. (1965). Ind. Eng. Chem. Fundam., 4, 38

181. Akita, K. and Kase, M. (1968). J. Phys. Chem., 72, 906

182. Ozawa, T. (1965). Bull. Chem. Soc. Japan, 38, 1881

183. Draper, A.L. (1970). Proc. 3rd. Toronto Symp. Thermal Analysis, 63 (H.G.McAdie editor) (Chem. Inst. Canada : Ottawa)

184. Draper, A.L. and Sveum, L.K. (1970). Thermochim. Acta, 1,345

185. Farran, R. and House, J.E.Jr. (1972). J. Inorg. Nucl. Chem., 34, 2219

186. House, J.E.Jr. and Adams, M.J. (1970). J. Inorg. Nucl. Chem., 32, 345

187. House, J.E.Jr. and Farran, R. (1972). J. Inorg. Nucl. Chem., 34, 1466

188. Lau, P. and House, J.E.Jr. (1974). J. Inorg. Nucl. Chem., 36, 207

189. House, J.E.Jr. and Lau, P. (1974). J. Inorg. Nucl. Chem., 36, 223

190. Subramanian, K.S. and Radhakrishnan, T.P. (1971). Proc. Indian Acad. Sci., Sect. A, 73, 64

191. Subramanian, K.S., Radhakrishnan, T.P. and Sundaram, A.K. (1972). J. Thermal Anal., 4, 89

192. Subramanian, K.S. (1969). Government of India Atomic Energy Commission, B.A.R.C. - 429

193. Reich, L. (1966). J. Inorg. Nucl. Chem., 28, 1329

194. Wendlandt, W.W. (1961). J. Chem. Educ., 38, 571

195. Barrall, E.M.(II) and Rogers, L.B. (1966). J. Inorg. Nucl. Chem., 28, 41

196. Heuvel, H.M. and Lind, K.C.J.B. (1970). Anal. Chem., 42, 1044

197. Wheelock, K.S., Nelson, J.H., Cusachs, L.C. and Jonassen, H. (1970). J. Amer. Chem. Soc., 92, 5110

198. Chatt, J. and Shaw, B.L. (1960). J. Chem. Soc., 1718

199. Galwey, A.K. (1967). Chemistry of Solids, (London : Chapman and Hall)

200. Garner, W.E. (1955). Chemistry of the Solid State, (W.E. Garner editor) (Butterworths : London)

APPENDIX 1

PUBLICATIONS

The following four papers on the work reported in this thesis have already been published.

(1) Mortimer, C.T., McNaughton, J.L. and Puddephatt, R.J. (1972). J. Chem. Soc. Dalton, 1265

(2) Mortimer, C.T., McNaughton, J.L., Burgess, J., Hacker, M.J., Kemmitt, R.D.W., Bruce, M.I., Shaw, G. and Stone, F.G.A. (1973). J. Organometallic Chem., 47, 439

(3) Mortimer, C.T. and McNaughton, J.L. (1973). Thermochim. Acta, 6, 269

(4) Mortimer, C.T. and McNaughton, J.L. (1974). Thermochim. Acta, 8, 265

Three other papers, indicated below, have also been written.

(1) Mortimer, C.T., McNaughton, J.L., Burgess, J., Hacker, M.J. and Kemmitt, R.D.W. J. Organometallic Chem., in press

(2) Mortimer, C.T. and McNaughton, J.L. (submitted for publication in Thermochim. Acta.)

(3) Mortimer, C.T. and McNaughton, J.L. (submitted for publication in Thermochim. Acta.)

A review on the theory and applications of differential scanning calorimetry has also been written in conjunction with

Dr. C. T. Mortimer. This review is to appear in the M.T.P. International Review of Science, Series 2, Physical Chemistry, Thermochemistry and Thermodynamics (H.A.Skinner editor)

(Reprints of the four papers already in print are enclosed in a folder on the inside of the back cover of this thesis.)

APPENDIX 2

SUGGESTIONS FOR FURTHER WORK

The study of the decomposition of complexes of the type, MX_2L_n, could be extended in the following ways.

(1) Data for only one thiazole complex, $CoCl_2(thiazole)_2$, have been reported in this thesis. The series of thiazole complexes could be enlarged[1,2] and heat of sublimation data obtained to yield $\bar{D}$(M - thiazole) values.

(2) Isothiazole is also reported[3,4] to form metal complexes of the type MX_2L_n. It would be of interest to obtain the relevant data to calculate $\bar{D}$(M - isothiazole) values. The latter could then be compared with the $\bar{D}$(M - thiazole) values.

(3) Although there does not appear to be any literature report on the formation of complexes of isoxazole, there would seem to be no inherent reason why complexes of the type, $MX_2(isoxazole)_n$, should not be obtained. Several other derivatives of isoxazole are liquids are room temperature. These are the 3-methyl, 5-methyl and 3,5-dimethylisoxazoles. (All these are available from R.N.Emmanuel Ltd.)

Further topics of a similar nature to the work on the MX_2L_n complexes are indicated below.

(1) Malaviya et al.[5] report the very simple preparation of a series of copper(II) oxalate complexes with some amines,

$CuC_2O_4.L$ or $CuC_2O_4.L_2$. The ligands, L, include pyridine, aniline, isoquinoline, methylamine and ethylamine. Although no indication of thermal decomposition temperatures is cited, it is possible that heats of decomposition for the reaction given below could be

$$CuC_2O_4.L_n\ (c) \longrightarrow CuC_2O_4\ (c) + n\ L\ (g)$$

(n = 1 or 2)

obtained.

(2) Ambe and Ambe[6] report the preparation of some metal acetylacetonate complexes with 4,4'-bipyridine or pyrazine, $M(AA)_2L_n$, where AA is the acetylacetonate anion and M is Mn, Fe, Co, Ni or Zn. The pyrazine complexes lose pyrazine around 470°K to give the acetylacetonate. These complexes might be of use, therefore, to obtain heats of decomposition.

Similarly, Paul and Rao[7] have prepared the complexes, $Co(AA)_2L_2$, where L is quinoline, isoquinoline and 4-aminopyridine. Syamal[8] has also reported complexes of this type, where L is pyridine, β-picoline and γ-picoline. These complexes may yield DSC data also.

The work on the $MXYZ_2.L$ complexes could be continued along the following lines.

(1) Differential scanning calorimetric work on the sulphur dioxide adducts of $IrX(CO)(PPh_3)_2$, where X is F, Br or I, would indicate whether the observed stability order[9], as determined by decomposition temperatures, of F > Cl > Br > I, is in fact correct.

The DSC data for $IrCl(CO)(PPh_3)_2.SO_2$ have already been obtained by Ashcroft and Mortimer.[10]

(2) It is possible that, whereas the acrylonitrile complexes of $IrX(CO)(PPh_3)_2$, where X is Cl or Br, are unstable at room temperature, the adducts of 2-chloroacrylonitrile might be rather more stable and allow DSC data to be obtained.

(3) The work on the stable acrylonitrile complex of $IrF(CO)(PPh_3)_2$ needs to be repeated to obtain a pure sample and, hence, the heat of decomposition.

(4) Fitzgerald et al.[11] have reported the preparation of $IrF(CO)(PPh_3)_2.CH(CH_3)CH(CN)$, whereas cinnamonitrile, $CH(CH_3)CH(CN)$, does not give an adduct with $IrCl(CO)(PPh_3)_2$. This complex also could yield useful DSC data.

(5) The DSC heat of decomposition of $IrCl(CO)_2(PPh_3)_2$ would be of value. However, Vaska[12] suggests that this adduct decomposes slowly at room temperature. This would imply that the same difficulties might occur with the DSC study as have been found for the acrylonitrile complexes.

A related topic, which may be amenable to DSC study, is the evaluation of the heat of decomposition of the hexamethyl-Dewarbenzene complex of $PdCl_2$. This complex is reported to decompose at around 350°K.[13] The analogous complex of $PtCl_2$ has also been prepared.[14]

REFERENCES

1. Eilbeck, W.J., Holmes, F. and Underhill, A.E. (1967). J. Chem. Soc. (A), 757

2. Hughes, M.N. and Rutt, K.J. (1970). J. Chem. Soc. (A), 3015

3. Rivest, R. and Weisz, A. (1971). Canad. J. Chem., 49, 1750

4. Peach, M.E. and Ramaswamy, K.K. (1971). Inorg. Chim. Acta, 5, 445

5. Malaviya, J., Shukla, P.R. and Srivastava, L.N. (1973). J. Inorg. Nucl. Chem., 35, 1706

6. Ambe, S. and Ambe, F. (1973). J. Inorg. Nucl. Chem., 35, 1109

7. Paul, B. and Ramana Rao, D.V. (1969). J. Inst. Chemists (India), XLI, 223

8. Syamal, A. (1968). J. Ind. Chem. Soc., 45, 719

9. Peone, J. Jr. (1971). Ph.D. thesis : Clarkson College of Technology

10. Ashcroft, S.J. and Mortimer, C.T. (1970). J. Organometallic Chem., 24, 783

11. Fitzgerald, R.J., Sakkab, N.Y., Strange, R.S. and Narutis, V.P. (1973). Inorg. Chem., 12, 1081

12. Vaska, L. (1966). Science, 152, 769

13. Dietl, H. and Maitlis, P.M. (1967). Chem. Comm., 759

14. Shaw, B.L. and Shaw, G. (1973). J. Chem. Soc. Dalton, 264